ANALYSIS OF MIMO SYSTEM OVER A COMPOSITE FADING CHANNEL

a thesis submitted in fulfillment of the requirements

for the degree of

Doctor of Philosophy

by

Keerti Tiwari

(Enrollment No: 136001)

Under the supervision of

Prof. Sunil V. Bhooshan

Prof. Davinder S. Saini

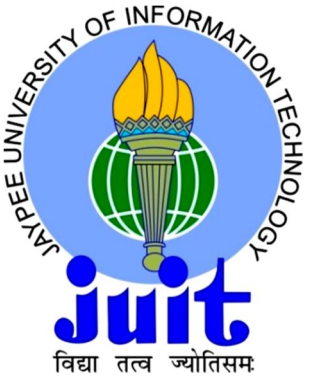

DEPARTMENT OF ELECTRONICS AND COMMUNICATION ENGINEERING

JAYPEE UNIVERSITY OF INFORMATION TECHNOLOGY

WAKNAGHAT, SOLAN – 173234, INDIA

FEBRUARY 2017

DECLARATION

I declare that the written submission signifies my ideas in my own work and where others ideas have been included. I have adequately cited and referenced the original sources. I have followed all the principles of academic honesty and integrity. I understand that any violation of the above will be the cause of disciplinary action by the Institute and can also induce penal action from the sources which have thus not been correctly cited or from whom proper permission has not been taken when required.

Keerti Tiwari

Keerti Tiwari

(Enrollment No. 136001)

Date: 24/11/2017

JAYPEE UNIVERSITY OF INFORMATION TECHNOLOGY
(Established by H.P. State Legislature vide Act No. 14 of 2002)
P.O. Waknaghat, Teh. Kandaghat, Distt. Solan - 173234 (H.P.) INDIA
Website : www.juit.ac.in
Phone No. +91-01792-257999 (30 Lines)
Fax : +91-01792-245362

Date: 24/.11../.2017

CERTIFICATE

This is to certify that the work presented in the thesis "**Analysis of MIMO System over a Composite Fading Channel**" which is being submitted by **Keerti Tiwari** in fulfillment of the requirement for the award of the degree of **Doctor of Philosophy** in the department of Electronics and Communication Engineering of Jaypee University of Information Technology, Waknaghat (H.P), India is an authentic record of candidate's own work carried out by her under our supervision.

The matter presented in this thesis has not been submitted by her for the award of any other degree in this Institute or any other Institute/University.

Professor and Head
Jaypee University of Information Technology,
Waknaghat, Distt. Solan (HP) 173234

Prof. Sunil V. Bhooshan
Professor and HoD,
Department of Electronics and Communication Engineering
Jaypee University of Information Technology, Waknaghat, (H.P.)

Prof. Davinder S. Saini
Professor and HoD,
Department of Electronics and Communication Engineering
Chandigarh College of Engineering and Technology, Chandigarh

Dedicated to my Parents, Sisters and Brother.

ACKNOWLEDGMENT

"Work until you no longer have to introduce yourself."

First of all, I express my sincere gratitude to my supervisors, Prof. Sunil V. Bhooshan, Jaypee University of Information Technology (JUIT) Waknaghat, Solan and Prof. Davinder S. Saini, Chandigah College of Engineering and Technology, Chandigarh for their guidance and encouragement. Their vast experience and deep understanding of the subject proved to be an immense help to me.

My sincere thanks to Vice-Chancellor, Director and Dean (Academic and Research), and Head Electronics and Communication (ECE) department, JUIT, Solan for providing me all the needed support to complete the research work. I am sincerely thankful to my committee members Prof. P.B. Barman, Dr. Shruti Jain and Dr. Ashwani Sharma for their constructive feedback and comments that have helped me in improving my thesis. I am grateful to Prof. Ghanshyam Singh, for his valuable suggestions and moral support. His profound view-points and motivation enlightened me in many ways. I pay regard to Dr. Neeru Sharma for providing me strength and motivation during the tough phase of the work. I also sincerely thank every member of the ECE Department and Administration of the JUIT Solan for their kind support.

I give my greatest gratitude to my parents, who have been offering all around support during the period of my studies and research. It is the tremendous blessings and endless sacrifice of my parents. They have shown immense patience and supported me in every possible way. I owe everything to them. I express the deepest gratitude to my sisters Neeti Tiwari Nayak, Preeti Tiwari and my brother Ashutosh Tiwari for their unconditional love, encouragement, appreciation, support during my studies as well as research and lifting me uphill this phase of life. I would like to pay regard to my brother-in-laws Atul Nayak and Dr. Pavan Tiwari for their motivation throughout my research work. I would like to extend warm thanks to my niece Adya and nephew Ayansh, their innocent smile and chats always bring a smile on my face and bring cheerfulness even in the odd time.

I express my profound thanks to my husband, Dr. Anukool Rajoriya for his concern, care, support and suggestions during the final stages of my research work. The writing of this thesis could not be possible without his kind assistance, suggestions and corrections. I am heartily thankful to my parents-in-laws and sister-in-law, Apeksha Rajoriya for their firm support during the final stages of Ph.D.

I am thankful to my friend Dr. Shweta Pandit for her valuable suggestions, motivation and prolific editing in my thesis. I am pleased to thank my friend Shraddha Tiwari for always listening me and finding time to have fun with the instances of stress and boredom throughout these years. I also thank my friends and lab-mates including (but not limited to), Dr. Shweta Pandit, Dr. Garima Bharti, Prabhat Thakur, Bindu Bharti, Aakanksha Sharma, Ashutosh Sharma and Isha Malhotra for their encouragement and maintaining research atmosphere in the lab. They always showed concern and discussed the things whenever required. I would like to thank all those people from the core of my heart who made this thesis possible.

In the last but not least, I thank the ultimate source of energy of every particle in the universe, the Almighty, for giving me enough energy and strength to complete the work.

(Keerti Tiwari)

TABLE OF CONTENTS

LIST OF FIGURES

LIST OF TABLES

LIST OF ABBREVIATIONS AND SYMBOLS

List of abbreviations used in alphabetical order

Abbreviation	Full Name
4G	Fourth generation
5G	Fifth generation
AF	Amount of fading
AoA	Angle of arrival
AoD	Angle of departure
ASEP	Average symbol error probability
AS	Antenna selection
AWGGN	Additive white generalized Gaussian noise
AWGN	Additive white Gaussian noise
BFHF	Bivariate Fox H-function
BEP	Bit error probability
BER	Bit error rate
CDF	Cumulative distribution function
CSI	Channel state information
DBPSK	Differential binary phase-shift keying
D-MIMO	Distributed multiple-input multiple-output
DPSK	Differential phase-shift keying
DQPSK	Differential quaternary phase-shift keying
EGC	Equal gain combing
FDD	Frequency division duplexing
FHF	Fox-H Function
GGD	Generalized Gaussian distribution
i.i.d.	Independent and identically distributed
i.n.d.	Independent and non-identically distributed

LLR	Log likelihood ratio
LoS	Line of sight
MAP	Maximum a posteriori
MCS	Modulation code scheme
MGF	Moment generating function
MIMO	Multiple-input multiple-output
MISO	Multiple-input single-output
ML	Maximum likelihood
MMSE	Minimum mean square error
MMSE-OSIC^2	MMSE-OSIC with candidates
M-QAM	M ary-quadrature amplitude modulation
MRC	Maximal ratio combining
MSE	Minimized mean-square error
NLoS	Non-line of sight
OSIC	Ordered successive interference cancellation
OSTBC	Orthogonal space time block code
PAM	Phase pulse amplitude modulation
PDF	Probability density function
PSK	Phase shift keying
QAM	Quadrature amplitude modulation
QRD	QR decomposition
QRM-MLD	QR decomposition and M-algorithm maximum likelihood detection
RF	Radio frequency
SC	Selection combining
SD	Sphere decoder
SER	Symbol error rate
SIC	Successive interference cancellation
SIMO	Single-input multiple-output
SINR	Signal to interference plus noise ratio

SISO	Single-input single-output
SM	Spatial multiplexing
SNR	Signal-to-noise ratio
STC	Space-time coding
STTC	Space time trellis code
SVD	Singular value decomposition
TAS	Transmit antenna selection
TDD	Time division duplexing
ToA	Time of arrival
V-BLAST	Vertical-Bell laboratories layered space-time
WG	Weibull-gamma
ZF	Zero forcing

List of symbols used in order as they appear first

Symbol	**Full Name**
λ	Wavelength in meters
N_r	Number of receive antennas
N_t	Number of transmit antennas
T	Symbol period
H	Channel vector
N_0	Variance
Y	Received signal vector
X	Transmitted signal vector
$\mathcal{N}$	Noise vector
C	Channel capacity
$p(x)$	Probability density function of x
$I(.;.)$	Mutual information
$\bar{\gamma}$	Average received SNR
E_s	Energy of the transmitted signals

$\Re_{xx}$	Autocorrelation function of transmit signal vector x
r	Rank of channel H
ς	Fixed total channel gain
μ_i	Singular values of channel H
C_{SIMO}	Channel capacity of SIMO
C_{MISO}	Channel capacity of MISO
$C_{ergodic}$	Ergodic channel capacity
$\bar{C}_{ol}$	Ergodic channel capacity for the open-loop system
$\bar{C}_{cl}$	Ergodic channel capacity for the closed-loop system
γ_i	Power transmitted by i-th antenna
γ_i^{opt}	Optimal power
P_e	Probability of error
$P_e\ (\gamma)$	Probability of error at a specific value of SNR γ,
$p(\gamma)$	PDF of γ
E_b	Bit energy
h	Amplitude values of the fading channel
$\overline{P_s}$	Average probability of error
$h_i(t)$	Attenuation of the i-th path at time t
$\tau_i(t)$	Path delay of i-th path w.r.t. time t
$\mathfrak{L}$	Number of resolvable paths at the receiver
h_{ij}	Complex channel gain
σ	Standard deviation/ shape parameter for lognormal shadowing
H_{LOS}	Rank-one matrix corresponding to the LoS component,
H_{NLOS}	Rank-one matrix corresponds to the NLoS components.
P_{LOS}	Power due to the LoS component
P_{NLOS}	Power due to the NLoS component
K	Specular amplitude
$I_0(.)$	Modified Bessel function of the first kind and zero order

m	Nakagami-*m* fading or shape parameter
β	Weibull shape parameter
Ω	Average fading power
$E[.]$	Expectation operator
m_n	Mean
m	Gamma shape parameter
d	Distance between transmitter and receiver
P_r	Received signal power
P_t	Transmitted power
G_t	Transmitter antenna gain
G_r	Receiver antenna gain
$\mathcal{L}$	System loss factor not related to propagation
ϑ	Path loss exponent
$F_{\gamma_{ij}}(\gamma)$	Cumulative distribution function of SNR
K_0	Modified Bessel function of second kind and zero-th order.
$G_{p,q}^{m,n}(.\|.)$	Meijer-G function
γ_o	Effective SNR for OSTBC MIMO system
$\|\|.\|\|$	Frobenius norm
R_c	Code rate of OSTBC
b	Number of bits
α_{ij}^2	Squared magnitude of the channel gain h_{ij}
Y_{MRC}	Received signals combined by MRC technique
W_{MRC}	Weight vector
$\mathcal{P}_s$	Average power of the instantaneous signal
$\mathcal{P}_{N_0}$	Average power of the noise signal
γ_{MRC}	Output SNR
P_s	Probability of symbol error
P_b	Probability of bit error

M	Modulation order
$Q(.)$	Gaussian Q-function
ρ	Symbol energy to noise ratio
a_m, b_m	Modulation specific constants
ℓ, k	Positive integers
d_g	Diversity gain
r	Transmission rate
g	i.i.d. gamma random variable
$\mathrm{Var}[.]$	Variance
W_{MMSE}	MMSE weight matrix
$w_{i,MMSE}$	i^{th} row vector of W_{MMSE}
$\hat{x}_{(i)}$	A sliced value of symbol $x_{(i)}$
$\hat{X}_{ML}$	Estimated transmit signal with ML detection
C_P	A set of symbol constellation signal points
$\mathcal{M}$	Candidate vector
E_b/N_0	Normalized energy per information bit to noise ratio
$E_b/N_{0_{min}}$	Minimum energy per information bit to noise ratio
S_0	Wideband slope
φ	Weibull scale parameter
$\gamma_{optimal}$	SNR for optimal detector
γ_k^{MMSE}	Post-processing SNR at the k^{th} receiver output
$\mathcal{R}^{MMSE}(\rho)$	Achievable sum rate for MMSE
E_b^{Rx}/N_0	Normalized received energy per information bit
$C'(.)$	First order derivative of ergodic capacity
$C"(.)$	Second order derivative of ergodic capacity
L	Selected antennas from N_t transmit antennas
A_L	A set of all promising antenna arrangements with L selected antennas
$\mathbb{i}_n$	Antenna indices in the n^{th} iteration

$\mathcal{E}_{ij}$	Error matrix
η	Shaping parameter
$\mathbb{R}^+$	Real and positive
ψ_0	Normalizing coefficient with respect to η
$\Gamma(.,.,.,.)$	Extended incomplete gamma function
κ	Weibull fading figure
$H_{p,q}^{m,n}(.)$	Fox H-Function
$\mathcal{D}_I$	Decision distance for in-phase components
$\mathcal{D}_Q$	Decision distance for quadrature phase components
$\mathcal{Q}_\eta\ (.)$	Generalized-$\mathcal{Q}$ function
R_{ddr}	In-phase-to-quadrature phase decision distance ratio
E_T	Average total energy per symbol

ABSTRACT

Multiple-input and multiple-output (MIMO) system has been recommended to enable future requirements of wireless communications. The efficient system designing demands an appropriate channel model, which should consider all the dominating effects of wireless scenario. Previously studied channel models like Multipath fading models only consider the small-scale fading effects, however, as it turns out that shadowing also degrades the system performance. Thus, some complex or less analytically submissive composite channel models have been proposed typically for single-input single-output (SISO) systems. These models are specifically used for mobile applications, however, a specific study of a model for MIMO system is required which can consider the radar clutters and different indoor/outdoor and mobile communication environments. Consequently, under such scenario, the performance improvement of MIMO system is also needed. The MIMO system performance improvement can be judged in terms of low error rate and high capacity using spatial diversity and spatial multiplexing respectively. Spatial diversity is further categorized into transmit and receive diversity techniques. Maximal ratio combining (MRC) and orthogonal space time block codes (OSTBCs) have been recommended as receiver and transmitter diversity.

In the beginning of this work, we have evaluated BER performance using OSTBC and MRC for distinct modulation techniques such as binary phase shift keying (BPSK), quadrature phase shift keying (QPSK), and 16-quadrature amplitude modulation (16-QAM) over different multipath fading channels viz. Rayleigh, Rician and Nakagami-*m* fading channels. Also, the same diversity techniques are used to evaluate error rate performance of MIMO system operating over single and double-Weibull fading channels, where, double scattering induces double fading in the wireless radio environment. For the first time, novel analytical expressions for cumulative distribution function (CDF) of double-Weibull distribution is computed in terms of Meijer-G function. Also, probability density function (PDF) and CDF for single and double-Weibull random variables are evaluated. CDF based closed form expressions of symbol error rate (SER) are computed for the proposed systems design. Simulation and analytical results show that double-Weibull fading gives significantly inferior SER performance compared to that of single-Weibull fading.

Further, we have selected Weibull-gamma (WG) composite fading that captures multipath fading and shadowing effects. For the same, we have presented an analytical expression for the amount of fading (AF) of WG which measures the severity of fading. Also, exact analytical expressions for SER are computed for MIMO systems using OSTBC and MRC. Our results show

that MRC gives approximately 3 dB enhanced SER performance than OSTBC, irrespective of antenna used. There is a tradeoff between computational complexity and optimal performance in most of the detection techniques. Ordered successive interference cancellation (OSIC) with minimum mean square error (MMSE) gives acceptable performance and complexity while maximum likelihood (ML) detection offers optimal performance at a higher complexity. Finally, MMSE-OSIC with candidates ($OSIC^2$) detection finds a balance between both. Thus, we used all these techniques for spatially multiplexed MIMO system. Simulation results illustrate that MMSE-$OSIC^2$ detection technique gives the improved SER performance which is similar to ML performance and its complexity level approaches to MMSE-OSIC.

After that, we present capacity analysis in detail for MIMO system under a low signal-to-noise ratio (SNR) regime as many users frequently operate in SNR below 0dB. For the analysis, we used spatial multiplexing (SM) with optimal detection, SM with MMSE detection and OSTBC. Novel closed-form expressions are evaluated for the capacity of MIMO systems at low SNR under WG fading channels which facilitate performance comparison for proposed techniques.

Then, we evaluated antenna selection (AS) techniques for the same channel conditions because it improves both error rate and capacity. We have shown that though optimal AS improves the system performance at the cost of enhanced complexity, sub-optimal AS technique should be used.

In the end, we considered a generalized noise i.e. additive white generalized Gaussian noise (AWGGN) along with composite fading conditions. A generalized Q-function is used to model various noise forms like impulsive, Gamma, Laplacian, Gaussian and uniform. The average symbol error probability (ASEP) of MIMO system is calculated for 16-QAM using MMSE-OSIC, ML and MMSE-$OSIC^2$ detection in WG fading subjected to AWGGN. Analytical expressions are presented in the form of Fox-H function (FHF). Since FHF is a generalized function from which other functions could be derived. These expressions confirm the validation of simulation results.

The results of this work offer, for the first time, methods to enhance MIMO system performance in less and severe fading as well as shadowing environment. The enhancement is the cumulative effects of choosing the appropriate channel models, spatial multiplexing/detection and spatial diversity techniques both at the transmitter and the receivers separately under the presence of arbitrary noise.

CHAPTER 1

Introduction

1.1 Introduction

The growing demands of wireless communications due to new emerging applications, pose many technical challenges in developing the modern wireless communication systems. The main two challenges are the capacity, how much maximum information can convey through the channel between the clients of the system, and the probability of error, the probability of mistaking the transmitted signal with another one. One of the major underlying causes of the poor performance of wireless channel is the multiple-path propagation phenomena. Therefore, we require a system that is less prone to the issue of multiple-path propagation albeit meeting the ever-growing demand for high data rate and quality of communications. From the past few years, the multiple-input multiple-output (MIMO) communication system has been providing a feasible solution to overcome these challenges. MIMO system comprises of multiple antennas both at transmitter and receiver to turn multiple-path propagation into a useful signal. Much of the framework to utilize multiple antennas has been laid down by Foschini and Telatar. They proved in [1] and [2] that communication systems with multiple antennas have a much higher capacity than single antenna systems. Also, multiple antennas can be used to improve the bit error rate (BER) of the wireless system. However, there is a tradeoff between these two objectives. These systems enormously enhance the system performance without adding overhead to bandwidth and transmit power over flat fading channels with a tolerable amount of complexity compared to conventional single antenna systems [3-5].

MIMO systems are one of the viable approaches towards fourth generation (4G) development. 4G systems must provide data rate close to 100 Mbps for users on the mobile network and around 1 Gbps for users with wireless access [6]. Apart from high data rates, 4G must be able to provide a high quality of service that is needed to enable improved multimedia experience, smooth streaming video, universal access and mobility across all communication systems.

1.1.1 Benefits

The multiple antenna techniques mainly provide the benefits of antenna diversity or simply known as spatial diversity and spatial multiplexing [5, 7]. Also, such techniques offer spatial diversity gain, spatial multiplexing gain and array gain. Array gain is the signal-to-noise (SNR) ratio at the receiver

that occurs as a result of the coherent combining of multiple antennas at the transmitter, receiver or both. However, the spatial diversity gain and spatial multiplexing gain can be achieved by the following organization.

A) Antenna Diversity

The basic idea behind antenna diversity is to transmit the same information over many independent fading paths and then combine these paths in such a way to reduce the fading of the resultant signal, thereby improving the error rate performance. In other words, the signal with its multiple copies are transmitted to achieve the benefit from multiple independent fading paths which assure that all the links will not go in deep fade simultaneously. Thus, the possibility of obtaining reliable data from receiver increases significantly. Diversity offers a number of replicas of a transmitted signal over time, frequency or space [8, 9].

- *Time Diversity:* same data is repeatedly transmitted at suitably separated (more than coherence time) time instances.
- *Frequency Diversity:* the same data is repeatedly transmitted at suitably separated (more than coherence bandwidth) frequency bands.
- *Spatial Diversity:* A number of antennas are separated by approximately λ/2 (λ is wavelength) distance to implement independent fading channels.

To further increase diversity, the spatial diversity can be applied in two following forms

- *Polarization diversity:* independent channels are employed by considering that the vertically and horizontally polarized paths are independent.
- *Angle diversity:* multiple receive antennas having different directivity are employed to receive the same information-carrying signal at different angles.

Fig. 1.1 illustrates the different antenna arrangements namely SISO, SIMO, MISO and MIMO systems for antenna diversity.

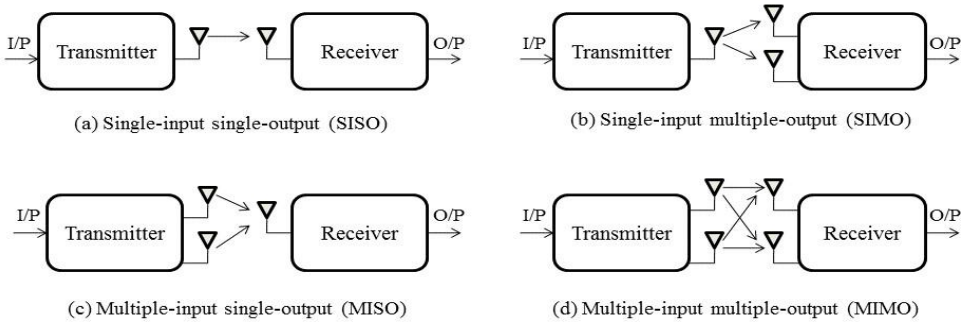

Fig. 1.1 Different antenna arrangements (a) SISO (b) SIMO (c) MISO (d) MIMO

- *Single-input single-output (SISO) system* consists single transmit and single receive antenna. Although, it is simple and does not require additional processing and diversity. However, interference and fading limit its performance.
- *Single-input multiple-output (SIMO) system* has single transmit and multiple receive antennas (N_r). The multiple receive antennas support to get a stronger signal through diversity. These systems require most of the processing at the receiver and also termed as receive diversity.
- *Multiple-input single-output (MISO) system* comprises of multiple transmit antennas (N_t) and single receive antenna. The receiver processing is shifting to transmitter side so it requires less complex receiver processing. It has positive impact on size, cost, and battery consumption and also termed as transmit diversity
- *Multiple-input multiple-output (MIMO) system* employs N_t number of antennas at the transmitter and N_r number of antennas at the receiver side. MIMO is used to provide improvements in both channel robustness as well as channel capacity which is unable to achieve from MISO and SIMO systems. [10].

The spatial diversity can be merged with the time and frequency diversity regarding space-time and space-frequency diversity without any extra time and frequency resource respectively. Spatial diversity is further categorized into receive and transmit diversity.

a) Receive Diversity

In receive diversity, different combining techniques are used to improve the system performance. The most common forms of combining techniques consist of selection combining (SC), maximal ratio combining (MRC), and equal gain combing (EGC) [11].

- *Selection combining (SC):* In SC, the received signal with the maximum SNR among N_r branches is selected for decoding.
- *Maximal ratio combining (MRC):* In MRC, all N_r branches are combined according to their weighted sum.
- *Equal gain combing (EGC):* EGC is a special case of MRC for which all the signals from multiple branches are combined with equal weights.

In the above combining techniques, MRC offers the best performance in terms of error rate, but it becomes costly and bulky to assemble in cell phones. Thus, transmit diversity come into existence.

b) Transmit Diversity

The receive diversity has a serious drawback of extreme computational load that occurs on the receiver side, which may experience high power consumption in mobile units for the downlink. Thus, the transmit diversity has been taken into account which requires a complete channel state information (CSI) at the transmitter. To achieve transmit diversity, space-time coding has been recommended that supports to achieve the diversity gain at the transmitter side and involves only a simple linear processing on the receiver side for decoding. For further reduction in the computational complexity of mobile units, differential space-time code is recommended, which does not require CSI estimation at the receiver side [9, 12, 13]. Alamouti has given a simple space-time code (STC) [3], which is as follows

- *Space-time code (STC):* STCs have been proposed to take the advantages of spatial and time diversity. In space time coding, the maximum possible diversity is equal to the product of number of transmit and receive antennas i.e. $N_t N_r$. Alamouti [3] has given the simplest form of orthogonal STC which consists two transmit antennas and one receive antenna. Note that, to maintain orthogonality, the inner product of two vectors should be zero or product of two functions over a specified symbol time should be zero and denoted by

  $$\int_0^T x_1(t)x_2(t)dt = 0 \tag{1.1}$$

  where $x_1(t)$ and $x_2(t)$ are two functions defined at the same time t over a symbol period T.

The Alamouti code contains two significant properties.

- Simple decoding: Simple linear processing is used to decode each symbol distinctly.
- Maximum diversity: This code fulfills the rank criterion and offers the maximum achievable diversity [14].

These are very desirable properties that can be achieved for two transmit antennas. Spatial diversity increases the error rate performance, however, it cannot improve the capacity significantly.

B) Spatial Multiplexing

The different data is transmitted through various links to improve the data rate of the system using spatial multiplexing (SM). MIMO SM must follow the condition of $N_r \geq N_t$. Consequently, it offers the multiplexing gain of $\min(N_r, N_t)$. The improved capacity performance can be achieved through SM by transmitting number of data streams from number of antennas. Transmitted signals go through different paths and each of these path is represented by channel gain. For recovering the transmitted data at the receiver, a substantial signal processing is required and MIMO system

decoder must perform the estimation of channel gain. Once the estimation has performed, then a channel matrix H has produced and the transmitted data streams is reconstructed by multiplying the received vector with the inverse of H. However, in real scenario, the propagation is not straightforward which creates the difficulty in appropriate detection. Therefore, spatial de-multiplexing which requires an efficient detection, is a challenging task. The current rigorous research includes the development of signal identification techniques. Furthermore, we discuss the different detection techniques in Section 1.2.

1.1.2 MIMO System Framework

The MIMO frame structure is shown in Fig. 1.2 [15].

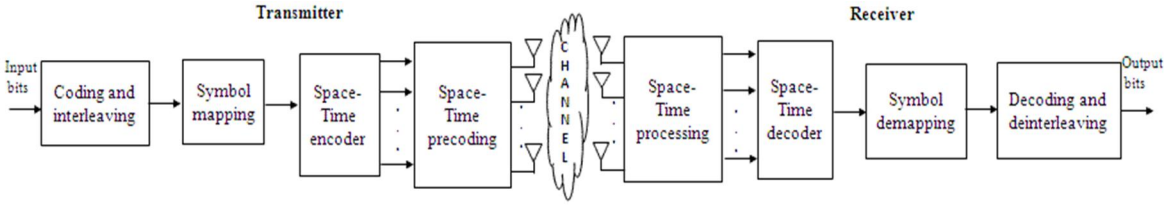

Fig. 1.2 MIMO Framework

The transmitted message bits are encoded and then interleaved. Interleaving is performed to protect the transmission against burst errors. In interleaving, different code words are mixed to form a code word and then transmitted over a channel. Therefore, error bursts are spread across multiple codes. Thus, the burst error affects only a correctable number of bits in each codeword that leads to the correct decoding of the codeword. Then, interleaved codeword is mapped to data symbols using different modulation techniques such as binary phase shift keying (BPSK), quadrature phase shift keying (QPSK), and M ary-quadrature amplitude modulation (M-QAM). The mapped symbols are treated as input to space-time encoder that gives one or more spatial data streams as output. The spatial data streams are mapped to transmit antennas using space-time precoding. The signals generated from the transmit antennas propagate over the channel and reach at the receiver antenna array. The receiver collects the signals at the output of each receive antenna element and converses the transmitter operations for decoding the data. A number of variations can occur in the relative placement of blocks, the functionality and the interaction between the blocks.

1.1.3 Channel Model

MIMO systems consist of three main components, the transmitter, the channel (H), and the receiver. In Fig. 1.3, N_t and N_r represent number of transmit and receive antenna elements respectively.

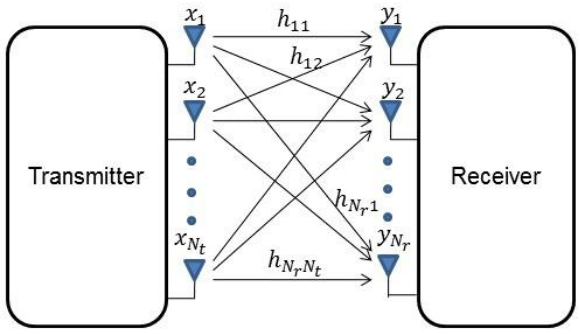

Fig. 1.3 MIMO system with $N_r \times N_t$ antennas

Each element of channel H is independent and identically distributed (i.i.d.) Gaussian random variables with zero mean and N_0variance. The channel element h_{ij} characterizes the complex channel gain between the i-th transmitter and the j-th receiver,

$$H = \begin{bmatrix} h_{11} & h_{12} & \cdots & h_{1N_t} \\ h_{21} & h_{22} & \cdots & h_{2N_t} \\ \vdots & \vdots & \ddots & \vdots \\ h_{N_r1} & h_{N_r2} & \cdots & h_{N_rN_t} \end{bmatrix} \tag{1.2}$$

The transmitted bandwidth is too narrow. Thus, it gives considerably flat frequency response (i.e., the channel is memoryless). For a deterministic channel, we find the normalization constraint for the elements of H as

$$\sum_{i=1}^{N_t} |h_{i,j}|^2 = N_t, j = 1,2, \ldots . N_r \tag{1.3}$$

The MIMO system model is given as

$$Y = HX + \mathcal{N} \tag{1.4}$$

where Y is the received signal vector of size $N_r \times 1$, X is the transmit signal vector of size $N_t \times 1$ and $\mathcal{N}$ is the noise vector of size $N_r \times 1$, each noise element is taken as i.i.d. white Gaussian noise with variance N_0 [16]

Equation (1.4) can be expended as

$$\begin{bmatrix} y_1 \\ y_2 \\ \vdots \\ y_{N_r} \end{bmatrix} = \begin{bmatrix} h_{11} & h_{12} & \cdots & h_{1N_t} \\ h_{21} & h_{22} & \cdots & h_{2N_t} \\ \vdots & \vdots & \ddots & \vdots \\ h_{N_r1} & h_{N_r2} & \cdots & h_{N_rN_t} \end{bmatrix} \begin{bmatrix} x_1 \\ x_2 \\ \vdots \\ x_{N_t} \end{bmatrix} + \begin{bmatrix} n_1 \\ n_2 \\ \vdots \\ n_{N_r} \end{bmatrix} \tag{1.5}$$

It is assumed that there is fixed channel within a transmission but a random channel variation arises between burst to burst [17].

1.1.4 Channel capacity

Channel capacity is well-defined by Shannon as the maximum rate of information transmission through a channel with negligible error [18]. Considering transmit signal vector X and received signal vector Y as a random variable, the channel capacity C is represented by the maximum mutual information $I(.;.)$ between them and is given by

$$C = \max_{p(x)} I(X;Y) \tag{1.6}$$

The maximization is applied over all possible probability density functions $p(x)$ of X. The transmit data should be Gaussian distributed to achieve data rate close to capacity. Shannon derived the normalized capacity i.e. capacity per unit bandwidth for band-limited white Gaussian noise channel and given by

$$C = \log_2(1 + \bar{\gamma}) \tag{1.7}$$

where $\bar{\gamma}$ is average received SNR.

A) Deterministic MIMO Channel Capacity

A MIMO system consists N_t transmit and N_r receive antennas with narrowband time-invariant channel H having matrix size $N_r \times N_t$. X is the transmitted symbol vector ($X \in \mathbb{C}^{N_t \times 1}$) that consists N_t independent input symbols. Equation (1.4) can be rewritten as

$$Y = \sqrt{\frac{E_s}{N_t}} HX + \mathcal{N} \tag{1.8}$$

The mutual information using (1.6) can be represented as

$$I(X;Y) = \log_2 \det\left(I_{N_r} + \frac{E_s}{N_t N_0} H \Re_{xx} H^{\dagger}\right) \tag{1.9}$$

where $(.)^{\dagger}$ represents Hermitian transposition and $\Re_{xx}$ is autocorrelation function of transmit signal vector X which is defined as

$$\Re_{xx} = E\left[XX^{\dagger}\right] \tag{1.10}$$

Also, the channel capacity for deterministic MIMO channel is given as [10]

$$C = \max_{\mathrm{Trace}(\Re_{xx}) = N_r} \log_2 \det\left(I_{N_r} + \frac{E_s}{N_t N_0} H \Re_{xx} H^{\dagger}\right) \tag{1.11}$$

If H is not known to transmitter, signal can be spread equally among all the antennas. Thus, $\Re_{xx} = I_{N_t}$ and capacity of (1. 11) can be represented as

$$C = \log_2 \det\left(I_{N_r} + \frac{E_s}{N_t N_0} HH^{\dagger}\right) \tag{1.12}$$

Assuming the fixed total channel gain $\|H\|^2 = \sum_{i=1}^{r} \delta_i = \varsigma$, here, $\curlyvee$ denotes the rank of H $\left(i.e., \curlyvee = \min(N_r, N_t)\right)$. H has a full rank when $N_r = N_t = N$ and $\curlyvee = N$. The maximum channel capacity is achieved by considering the same singular values of H for all (SISO) parallel channels, i.e.,

$$\mu_i = \frac{\varsigma}{N}, i = 1,2, \ldots\ldots N \tag{1.13}$$

MIMO capacity is maximized for the orthogonal channel condition, thus, $HH^{\dagger} = H^{\dagger}H = \frac{\varsigma}{N} I_N$, for this case, capacity increases N times than that of each parallel channel, which is given as

$$C = N\log_2\left(1 + \frac{\varsigma E_s}{N_t N_0}\right) \tag{1.14}$$

For a SIMO channel, the channel gain is denoted as $h \in \mathbb{C}^{N_r \times 1}$ and hence $\curlyvee = 1$ and $\delta_1 = \|H\|^2$. Accordingly, the channel capacity is defined irrespective of the CSI availability at the transmitter side and given as

$$C_{SIMO} = \log_2\left(1 + \frac{E_s}{N_0}\|H\|^2\right) \tag{1.15}$$

When $|h_i|^2 = 1, i = 1,2, \ldots\ldots N_r$ and $\|h\|^2 = N_r$, the capacity is given as

$$C = \log_2\left(1 + \frac{E_s}{N_0} N_r\right) \tag{1.16}$$

We can see from (1.16) that a logarithmic improvement can be seen in channel capacity with the number of antennas. Also, we can transmit only a single data stream and the CSI availability at the transmitter side does not enhance the channel capacity.

For the case of a MISO channel, the channel gain is given as $h \in \mathbb{C}^{1 \times N_t}$ thus $\curlyvee = 1$ and $\delta_1 = \|h\|^2$. If CSI is unavailable at the transmitter side, the channel capacity is expressed as

$$C_{MISO} = \log_2\left(1 + \frac{E_s}{N_t N_0}\|h\|^2\right) \tag{1.17}$$

when $|h_i|^2 = 1, i = 1, 2, \ldots\ldots N_t$ and $\|h\|^2 = N_t$, the capacity is given as

$$C_{MISO} = \log_2\left(1 + \frac{E_s}{N_0}\right) \tag{1.18}$$

B) Random MIMO Channel Capacity

In the previous section, MIMO channels are assumed to be deterministic, however, MIMO channels change randomly. Therefore, H is a random matrix and its channel capacity is randomly time-varying. Assume the random channel as an ergodic process, MIMO channel capacity also known as ergodic channel capacity is represented by

$$C_{ergodic} = E[C(H)] = E\left[\max_{\text{Trace}(\Re_{xx})=N_t} \log_2 \det\left(I_{N_r} + \frac{E_s}{N_t N_0} H \Re_{xx} H^{\dagger}\right)\right] \tag{1.19}$$

The open-loop system detemines the ergodic channel capacity without using CSI at the transmitter side as

$$\bar{C}_{ol} = E\left[\sum_{i=1}^{r} \log_2\left(1 + \frac{E_s}{N_t N_0}\delta_i\right)\right] \tag{1.20}$$

Similarly, the closed-loop system offers the ergodic channel capacity using CSI at the transmitter side as

$$\bar{C}_{cl} = E\left[\max_{\sum_{i=1}^{r}\gamma_i = N_t} \sum_{i=1}^{r} \log_2\left(1 + \frac{E_s}{N_t N_0}\gamma_i\delta_i\right)\right] = E\left[\sum_{i=1}^{r} \log_2\left(1 + \frac{E_s}{N_t N_0}\gamma_i^{opt}\delta_i\right)\right] \tag{1.21}$$

where γ_i is power transmitted by i-th antenna and γ_i^{opt} is optimal power.

1.1.5 Probability of Error

The probability of error is evaluated by averaging it for a particular modulation in AWGN channels over the possible ranges of signal strength due to fading in a slow flat fading channel. Considering fixed channel gain, the probability of error in AWGN channels is observed as a conditional error probability. Hence, one can obtain the probability of error in slow flat fading channels by averaging the error in AWGN channels over the fading probability density function (PDF). Accordingly, the probability of error in a slow flat fading channel can be computed in terms of SNR as

$$P_e = \int_0^{\infty} P_e(\gamma) p(\gamma) d\gamma \tag{1.22}$$

where $P_e(\gamma)$ is the probability of error for an arbitrary modulation at a particular value of SNR γ, $\gamma = h^2 E_b/N_0$, and $p(\gamma)$ is PDF of γ due to the fading channel. E_b is bit energy and h represents amplitude values of the fading channel with respect to E_b/N_0. This section defines the PDF based probability of error, although cumulative distribution function (CDF) and moment generating function (MGF) can also be used to evaluate error rate [19, 20].

When the fading environment superimposes shadowing on multipath fading, a common performance metric i.e. average error probability is obtained by averaging over the distribution of the shadowing conditioned on the mean SNR [21]

$$\overline{P_s} = \int_0^\infty P_s(\gamma)\, p(\gamma|\bar{\gamma}) d\gamma \tag{1.23}$$

where γ denote the random SNR due to path loss, shadowing, and multipath.

1.1.6 Channel Estimation on the Transmitter Side

Generally, the channel state information (CSI) is not directly available at the transmitter. Thus, some indirect resources are needed to make it available at the transmitter. The time division duplexing (TDD) system can exploit the channel reciprocity among opposite links (downlink and uplink). It permits for indirect channel estimation which relies on the signal received from the opposite direction. The frequency division duplexing (FDD) system does not have reciprocity between opposite directions and the transmitter depends on the channel feedback information from the receiver. Specifically, CSI must be estimated at the receiver side and then, fed back to the transmitter side. Exploitation of channel information permits for increasing the channel capacity, improving error performance while reducing hardware complexity [22]. Precoding and antenna selection are the conventional methods that exploit CSI on the transmitter side.

- *Precoding:* The MIMO system may not be able to adequately recover the transmitted data streams (layers) depending on the resulting channel conditions if the signal to interference plus noise ratio (SINR) is too less at any of the receive antennas. With the addition of precoding, the transmitter which is having knowledge of the present channel conditions can effectively combine the layers before transmission with the aim of equalizing the signal reception across the multiple receive antennas.
- *Antenna Selection:* Antenna selection techniques provide a smaller number of RF modules than the number of transmit antennas to decrease the cost related to the multiple RF modules.

1.1.7 Wireless Fading Channels

The wireless channel environment governs the performance of wireless communication systems. The interpretation of wireless fading channels will lay the foundation for developing high performance and bandwidth-efficient wireless communication technology. In wireless communication, radio propagation ensures the behaviour of radio waves that are propagated from

the transmitter to receiver. In the radio propagation, electromagnetic waves are primarily affected by the physical phenomena such as reflection, diffraction, and scattering [11, 23].

Reflection is caused by electromagnetic wave propagation which impinges upon an object with huge dimensions in comparision to the wavelength, e.g., the surface of the earth and building. *Diffraction* arises when a surface obstructs the radio path between the transmitter and receiver with sharp irregularities or small beginnings. *Scattering* impels the electromagnetic wave radiation to deviate from a direct path through one or more local obstacles, with small dimensions compared to the wavelength. The obstacles viz. foliage, street signs, and lamp posts carry scattering, are termed as scatters. Fig. 1.4 organizes the types of fading channels.

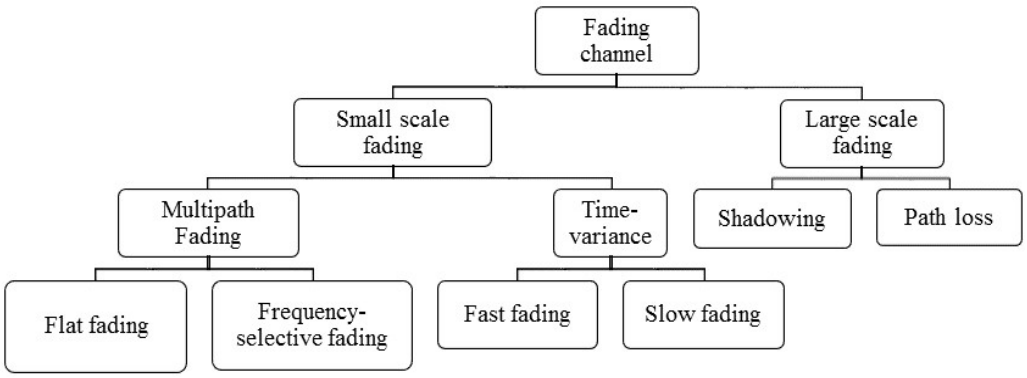

Fig. 1.4 Types of fading [24]

A distinctive characteristic of a wireless channel is determined by *fading,* which produces due to varying signal amplitude over time and frequency. Although the additive noise is the most common source of signal degradation, fading is another cause of signal degradation that is distinguished by a non-additive signal interference in the wireless channel. Fading that occurs may due to multipath propagation, is called *multipath fading*, or to *shadowing* from obstacles that affect the radio wave propagation, called *shadow fading*.

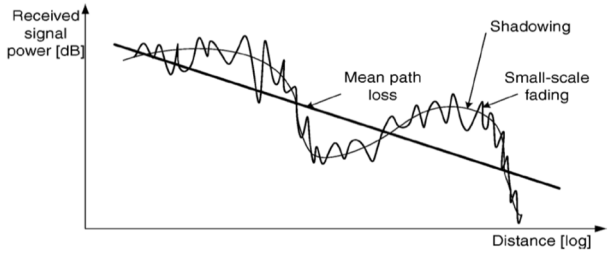

Fig. 1.5 Small scale and Large scale fading [24]

Presently, the most common wireless channel models have been established for 800 MHz to 2.5 GHz by widespread channel analysis in the ground. Concurrently, spatial MIMO channel models are recently establised by the numerous study and standardization actions such as IEEE 802, METRA Project, 3GPP/3GPP2, and WINNER Projects, targeting at speedy wireless communication and diversity gain.

Large-scale fading is produced by the mean path loss that reduces with distance and shadowing that differs along the mean path loss. Due to the shadowing produced by obstacles on the path, the signal strength at the receiver may be different even at the same distance from a transmitter. Moreover, the scattering elements suffer small-scale fading, which produces a short-term variation of the signal that has earlier practised shadowing. The simple or complex channel model for MIMO systems are subjected to the essential correctness and environment modeled.

A) Small Scale Fading

Small-scale fading, or simply fading defines the rapid fluctuation of the amplitude of a radio signal over a short period of time or travel distance. It is produced by interference between two or more forms of the transmitted signal which reach at the receiver at slightly different times. The amount of multipath is responsible for small-scale fading condition which is catogerized as either as frequency-selective or frequency flat. The mobile speed (characterized by the Doppler spread) which is dependent on the time varying nature of a channel, is called short term fading and categorized as either fast fading or slow fading. The multipath fading channel can be modeled as follows when we denote the transmitted signal by $x(t)$ and the received signal by $y(t)$

$$y(t) = \sum_{i=1}^{\Omega} h_i(t)\, x\,(\tau - \tau_i(t)) \tag{1.24}$$

where $h_i(t)$ is the attenuation of the i-th path at time t, $\tau_i(t)$ is the corresponding path delay, and Ω denotes the number of resolvable paths at the receiver. Different PDFs for small-scale fading are as follows

i) Rayleigh PDF

The Rayleigh PDF considers a non-line of sight (NLoS) path with multiple scatterers. Rayleigh fading is observed as a realistic model for tropospheric and ionospheric signal propagation as well as the result of heavily developed urban environments on radio signals. This model comprises i.i.d. complex, zero mean, and unit variance channel elements and is represented by [25]

$$h_{ij} = \frac{1}{\sqrt{2}}\,(normal\,(0,1) + \sqrt{-1}\,.normal\,(0,1)) \tag{1.25}$$

This model clearly estimates the environment in better way by taking large antenna spacing compared to the wavelength. The PDF of Rayleigh fading is given by

$$p(x) = \frac{2x}{\Omega}\exp\left(-\frac{x^2}{\Omega}\right),\ 0 \le x \le \infty \tag{1.26}$$

where $\Omega = E[x^2]$ is average fading power.

ii) Rician PDF

Rician fading considers both the line of sight (LoS) and NLoS paths. The MIMO channel matrix for the LoS environment is expressed as [26]

$$H = \sqrt{\frac{K}{K+1}}H_{LOS} + \sqrt{\frac{K}{K+1}}H_{NLOS} \tag{1.27}$$

$$\text{where } K\ (dB) = 10\log_{10}\frac{P_{LOS}}{P_{NLOS}} \tag{1.28}$$

In (1.27), H_{LOS} corresponds to the LoS component with rank-one matrix, and H_{NLOS} corresponds to the NLoS components. In (1.28), P_{LOS} and P_{NLOS} are the power due to the LoS component, and NLoS component respectively [27]. The H_{NLOS} component is typically modeled as (1.25). SISO system requires the smaller fade margin for large *K* factor. In MIMO systems, rank-one H_{LOS} component is more dominant for high *K* factor, and the H_{NLOS} component is less dominant. Nevertheless, simulations and measurements in rich multipath scenario ensures the less dominant nature of LoS component [17]. The PDF of Rician fading is given by

$$p(x) = \frac{2(K+1)x}{\Omega}\exp\left(\frac{-(K+1)x^2}{\Omega} - K\right)I_0\left(2\sqrt{\frac{K(K+1)}{\Omega}}x\right),\ K \ge 0, x \ge 0 \tag{1.29}$$

where x is the Rician amplitude and Ω is the total power from both paths, and turns as a scaling factor to the distribution. *K* is the specular amplitude, $I_0(.)$ is the modified Bessel function of the first kind and zero-th order.

iii) Nakagami-m PDF

Nakagami-*m* fading generates due to multipath scattering with relatively larger time-delay spreads, and different clusters of reflected waves, where envelope of each cluster signal follow Rayleigh distribution. It provides the best fit to land mobile and indoor mobile multipath propagation as well as scintillating ionospheres radio links [19]. The Nakagami-*m* channel matrix is created as

$$H = sqrt\{gammarand(m, \Omega/m, N_t, N_r)\} \tag{1.30}$$

where m is shape parameter also called fading parameter and $\Omega = E[x^2]$. The Nakagami-m PDF is given as

$$p(x) = \frac{2m^m}{\Gamma m\, \Omega^m} x^{2m-1} \exp\left(\frac{-m}{\Omega} x^2\right), x \geq 0, m \geq 1/2, \Omega > 0 \quad (1.31)$$

where $\Gamma(.)$ denotes gamma function.

iv) Weibull PDF

In the Weibull channel model, h_{ij} is represented in terms of Gaussian in-phase elements (U_{ij}) and quadrature phase elements (V_{ij}) of the multipath components [28] as

$$h_{ij} = (U_{ij} + jV_{ij})^{2/\beta_{ij}} \quad (1.32)$$

The amplitude of channel coefficient can be taken as $X_{ij} = |h_{ij}|$. H is represented in terms of scale parameter φ and shape parameter β as

$$H = wblrand(\varphi, \beta, N_t, N_r) \quad (1.33)$$

PDF of Weibull random variable x is expressed in [29] as

$$p_{X_{ij}}(x) = \frac{\beta_{ij}}{\Omega_{ij}} x^{\beta_{ij}-1} \exp\left(-\frac{x^{\beta_{ij}}}{\Omega_{ij}}\right),\ \beta_{ij} > 0, \Omega_{ij} \geq 0, x \geq 0 \quad (1.34)$$

where Ω_{ij} is average fading power which is represented as $\Omega_{ij} = E[X_{ij}^{\beta_{ij}}]$ or $\Omega_{ij} = \varphi^{\beta_{ij}}$ and $E[.]$ denotes expectation operator. For $\beta_{ij} = 1$ and $\beta_{ij} = 2$, Weibull distribution is reduced to exponential and Rayleigh distribution respectively. All the entries are denoted from i-th transmit antenna to j-th receive antenna.

A) Large Scale Fading

Large-scale fading occurs as the mobile moves through a large distance (several hundred or thousands of meters), or a distance of the order of cell size [11]. It is categorized as shadowing and average path loss.

a) Shadowing

Shadowing is produced by obstacles between the transmitter and receiver that absorb power. Once the obstacle absorbs complete power, the signal remains blocked. A variation due to shadowing occurs over distances relative to the length of the obstructing object (10-100 meters in outdoor and less in indoor).

i) Lognormal PDF

The lognormal PDF is formed by applying central limit theorem for the products of random variables [30] that models the effects of long-term fading or shadowing observed in wireless systems [31-33]. In particular cases, it is applicable to model short-term fading as well [32]. PDF of the lognormal random variable is defined in [34] with parameters $m_n \in \mathbb{R}$ and $\sigma \in (0, \infty)$, where m_n is mean and σ is standard deviation, given by

$$p(x) = \frac{1}{\sqrt{2\pi\sigma^2 x}} \exp\left\{-\frac{(\log_e(x) - m_n)^2}{2\sigma^2}\right\}, 0 < x < \infty \quad (1.35)$$

where σ is shape parameter.

ii) Gamma PDF

The gamma distribution is widely preferred in wireless communications to model the power in fading channels [35, 36]. Due to less complex statistical behaviour compared to log-normal distribution, it is widely used to model shadowing effects [31]. The PDF is given by

$$p(g) = \frac{1}{\Gamma m\, \Omega^m}\, g^{m-1} \exp\left(\frac{-g}{\Omega}\right), \; x, \Omega, m \geq 0 \quad (1.36)$$

where m is shape parameter and $\Omega = E[g^2]$.

b) Path loss

Path loss occurs due to the dissipation of power radiated by the transmitter as well as effects of the propagation channel. A variation due to path loss obtains over very large distances (100-1000 meters). In path loss models, it is assumed that path loss is the identical at a given transmit-receive (T-R) distance. As with the proposed large-scale radio wave propagation models, the free space model forecasts that received power declines as a function of the T-R separation distance raised to some power. The free space power received by a receiver antenna is represented by the Friis free space equation that is separated from a radiating transmitter antenna by a distance *d,*

$$P_r(d) = \frac{P_t G_t G_r \lambda^2}{(4\pi)^2 d^2 \mathcal{L}} \quad (1.37)$$

where P_t is the transmitted power, $P_r(d)$ is the received power which is a function of the T-R separation, G_t and G_r are the transmitter and receiver antenna gain respectively, d is the T-R separation distance in meters, $\mathcal{L}$ denotes the system loss factor not associated to propagation ($\mathcal{L} \geq 1$), and λ is the wavelength in meters. When antenna gains are involved, the path loss for the free space model is represented by

$$PL(\text{dB}) = 10\log\frac{P_t}{P_r} \tag{1.38}$$

In this case, $PL \propto \frac{1}{d^2}$, however, for a large-scale propagation model, $PL \propto 1/d^{\vartheta}$, where the value of path loss exponent ϑ depends on the specific propagation environment, e.g., ϑ is equal to 2 in free space and ϑ will have a larger value when obstructions are present [11, 21].

We can observe both the effects of small-scale and large-scale fading at the same time caused by rapid change in wireless environment. Thus, the composite channel modeling is required that includes multipath as well as shadowing effects. Consequently, the powerful solutions are required to solve some real-world problems having interference effects in MIMO communication systems [21].

1.2 Related Work

MIMO systems are applied to enhance the wireless system performance even in the severe fading environment. Thus, the following sections present the techniques to improve MIMO system performance in multipath fading, shadowing and composite fading subjected to AWGN as well as generalized Gaussian noise.

1.2.1 Spatial Diversity Techniques

MIMO systems have been employed to improve the wireless system performance using different receiver combining techniques. As we have already discussed that error rate and capacity are important measures to identify the system performance, therefore EGC, SC and MRC have been exploited with MIMO system according to the requirement of the system designer. In [37], Falujah and Prabhu have evaluated the average bit error probability (BEP) of MIMO systems for the differential binary and quadrature phase-shift keying (DBPSK and DQPSK respectively) employing post-detection EGC diversity over Rayleigh fading channels. They considered a less complex and inexpensive MIMO receiver in comparison to the coherent phase-shift keying system (PSK) for MIMO using MRC diversity reception. In [38], the non-coherent EGC technique has been employed to analyze the error performance of M-ary orthogonal signals over generalized multipath fading channels. Also, the generalized fading distribution envelopes have been measured to show the arbitrary non-identical values which are possibly supported by received average SNR and/or the fading parameters and the impact of arbitrary correlation among diversity branches have been obtained efficiently to estimate average error rate performance of the system.

MRC diversity has been used to maximize the output SNR in multiple antenna systems [39]. Also, it gives better performance than SC and EGC techniques. MIMO-MRC systems have been employed to improve the system error rate and capacity performance under different fading conditions. Ref. [40] presents the bit error rate (BER) analysis using rectangular-QAM. However, the result is only applicable for Gray code mapping. In [41], the average symbol error rate (SER) performance of MIMO-MRC systems is estimated in noise limited and interference-limited scenario. The significance of MIMO-MRC is defined by the fact that it consists the optimal point-to-point (i.e., single transmitter-receiver) linear transceiver design which maximizes the receive SNR [42] when one data stream is transmitted and perfect channel knowledge is available at both the transmitter and the receiver. In [43], a novel insight is offered into how the mutual connections of LoS and spatial correlation components impact the performance of MIMO-MRC systems.

In the recent work, authors [44] evaluated the performance of the MIMO-MRC system with the feedback delay and channel estimation error. Taking the feedback delay and channel estimation error, practical imperfect factors into account, they derived the analytical expressions of average SERs of the MIMO-MRC system, which was used to examine the performance loss in terms of the array gain and diversity order. We have already discussed in Section 1.1.1 that the receive diversity compels most of the computational burden on the receiver side, which may experience high power consumption for mobile units in the case of the downlink. Therefore, transmit diversity techniques i.e. STC have been implemented to improve the MIMO system performance in a severely faded environment with adaptable complexity level to achieve transmitter diversity gain [9, 12, 13]. Consequently, STC has been categorized into orthogonal space-time block codes (OSTBCs) and space-time trellis code (STTC) which have been recommended for achieving full diversity gain [9]. In STTC, an information stream is encoded via N_t convolution encoders (or via one convolutional encoder with N_t outputs) to find N_t streams of symbols that are transmitted from N_t antennas simultaneously. Delay diversity [45] is based on STTC, where first antenna transmits the data stream as $\left[x_{n,}x_{n+1,\ldots\ldots}\right]$, while second antenna transmits same stream but delayed by d_0 symbol intervals and hence, the data stream is $\left[x_{n-d_0,}x_{n+1-d_0,\ldots\ldots}\right]$. Due to added delay, resulting codes achieve spatial diversity instead of full diversity with higher decoding complexity. However, the decoding complexity increases exponentially by increasing number of transmit, receive antennas and transmission rate [46]. Thus, Alamouti [3] provided OSTBCs to overcome this problem. OSTBC provides full diversity of 2 and code rate 1 using 2 transmit antennas. Due to the orthogonal nature of codeword matrix, Alamouti code has fast ML decoding properties that simplify single symbol

ML detection. Thus, OSTBC can be achieved along with the provision of a very simple ML decoding algorithm, based only on linear processing of the received signals [4, 10]. These codes can be generalized for more than two transmit antennas using the orthogonal design theory [4]. However, talking on short coming, authors [47] have shown that OSTBC neither provides coding gain nor achieve a rate larger than ¾ for more than two transmit antennas.

In [48], capacity performance has been evaluated under Rayleigh, Rician, Nakagami-*m* and Weibull fading channels. In [49], two new selection techniques, space-time sum-of-squares combining selection diversity and space-time sum-of-magnitudes selection diversity, were employed with Alamouti STBC and established to offer nearly the identical performance as SNR selection, but with quite simpler operations. Later on, authors have employed OSTBC/MRC in MIMO system to analyze the distribution of the sum of squared random variables for estimating the improved error performance with reduced computation complexity [50]. Consequently, MRC has been proven its importance to achieve the better error performance than SC, however, at the cost of more computational complexity compared to that of SC and applying OSTBC along with MRC at the transmitter improves the MIMO system significantly.

1.2.2 Signal Detection Techniques

In MIMO systems, spatial multiplexing (SM) and spatial diversity play a key role to support high data rate services and reliable communication respectively. However, there is a tradeoff between spatial multiplexing and diversity for multiple access channels [15, 51]. The requirement of high data rate is increasing for next generation communication systems. Diversity requires the usage of a simple detection technique at an expense of capacity reduction, however, a significant capacity gain can be achieved through spatial multiplexing with improved transmission rate [4]. Although, a suitable detection technique for de-multiplexing is a research issue for an efficient system design.

The reported literature of [52-59] displays various detection techniques to enhance the system performance. Initially, zero forcing (ZF) and ZF-successive interference cancellation (SIC) were introduced [60-62], which are computationally efficient but suffer from noise enhancement problem. Noise enhancement problem in ZF is known to be resolved by minimum mean square error (MMSE) technique. For system performance improvement, the MMSE-SIC technique has been recommended with fast and computationally efficient algorithms [56, 63, 64]. In conventional SIC, the receiver arbitrarily takes one of the estimated symbols and subtract its effect from the received symbols, so it does not give the best performance. The ordered successive interference cancellation (OSIC) technique has been proposed with MMSE to further improve the system performance. It has

been analyzed by Hoefel [65] that the relative performance gain achieved through MMSE-OSIC receiver is firmly dependent on a number of transmit and receive antennas, modulation code scheme (MCS) and order of spatial stream. The order of detection has a substantial impact on the complete performance of OSIC detection due to the error propagation caused by incorrect decision in the previous stages. Consequently, the different detection ordering methods such as SNR based, column norm based and SINR based ordering have been investigated in the past [24]. The post detection SINR based ordering offers the best performance among all three ordering techniques [24]. After that, an optimal selection technique for vertical-Bell laboratories layered space-time (V-BLAST) technique using OSIC detection with respect to error rate is developed which has less complexity. Due to error propagation, these techniques show limited performance improvement in error rate since they use an equal number of transmit and receive antennas [66]. A complete review of algorithms proposed for the new and severe signal identification efforts for MIMO systems is given in [67] with the detection of the multiple transmit antennas.

Maximum likelihood (ML) signal detection technique has been employed to achieve the optimal error rate performance. In ML detection, all transmit signal vectors are used to produce corresponding ML metrics. Nevertheless, the computational complexity increases exponentially with the increase in a number of transmit antennas and constellation points, although MMSE is simpler than ML detection [68]. Recently, there has been a lot of efforts made to achieve the ML performance with a reduced level of complexity. The maximum likelihood detection with QR decomposition and M-algorithm (QRM-MLD) and sphere decoder (SD) have also been implemented to reduce the complexity [69]. The QRM-MLD algorithm reduces the receiver complexity, however, it results in erroneous log likelihood ratio (LLR) values due to a finite number of candidate symbol vectors [70-72]. Therefore, a competent LLR computation algorithm has been described. Instead of calculating LLR values only at the last stage, this algorithm calculates the updated estimated values at each stage. Later on, authors have given the LLR based essential properties that simplify the sorting step included in successive cancellation list decoding. Consequently, it reveals the requirement of the knowledge of statistical channel model in the accurate LLR calculation [73, 74]. SD uses depth-first search which approaches the complexity of ML, and QRM-MLD uses breadth-first search which gives fixed level of computational complexity. Moreover, in QRM-MLD, performance improves and approaches ML by increasing candidate vector but with the increased complexity. A new technique has been proposed that selects a number of candidates at each layer unlike MMSE-OSIC, which is called MMSE-OSIC with candidates

(MMSE-OSIC^2) [75]. This technique gives a near-ML performance with a complexity level similar to that of traditional MMSE-OSIC and efficiently generates the LLR values.

1.2.3 Precoding and Antenna Selection Techniques

In reality, full CSI may not be directly available due to feedback overhead and feedback delay. Specifically, CSI for the time-varying channel cannot be followed completely by the transmitter, and hence, only partial information (e.g., the statistical information) can be exploited. The precoding techniques and antenna selection techniques are the conventional procedures that use CSI on the transmitter side. It is noted that the pre-equalization scheme on the transmitter side performs better than the receiver-side equalization. It is associated with the fact that the receiver-side equalization faces noise enhancement problem. In [22], it has been described that the exploitation of CSIT (partial or perfect knowledge) improves the capacity and error rate performance of MIMO system with less complexity. Also, in SM-MIMO systems, simultaneous transmission of data requires parallel radio frequency (RF) chains which contain low noise amplifier, frequency down-converter, and an analog-to-digital converter. The parallel RF chains at the transmitter and/or receiver of MIMO system adds overhead to hardware complexity, power and size [76]. It becomes difficult to integrate such complex hardware in the mobile units simultaneously while retaining their ease of handling and compactness. Moreover, simultaneous transmission from multiple antennas has inherent drawbacks of inter-antenna interference, the requirement of synchronization, etc. [77]. These difficulties can be overcome by the MIMO systems with single RF chain at the transmitter which in turn activates single antenna at a time for transmission. The reduced cost of multiple RF modules can be achieved by using antenna selection (AS) techniques. It is more effective technique than precoding. These techniques can be considered to practice a reduced number of RF modules than the number of transmit antennas.

Many linear precoding techniques require each antenna to transmit its own data. Authors [78] have analyzed the latest technology of MIMO with the theoretical background. They made a comparison of capacity obtained after using two precoding methods based on the spatially multiplexed system. They have applied two precoding techniques to multiple antennas, considering multiuser-MIMO downlink. Ref. [79] explains a differential system employing OSTBC with PSK, PAM, and QAM constellations, over arbitrarily correlated Rician fading channels. The SER performance of such a differential system is analyzed by a memory-less precoding matrix at the transmitter. Recently in [80], the security performance obtained by employing a practical precoded OSTBC in MISO wireless networks has been investigated. In particular, space time codewords are

precoded with an optimum matrix that minimizes the error rate. In [76], AS algorithms is applied at the transmitter and receiver side using less complex selection diversity.

Authors [81] offered a QR decomposition (QRD)-based selection technique that maximizes the lower bound. With some matrix properties, it has been theoretically proven that the lower bound generated by the QRD is tighter than that by the singular value decomposition (SVD). Note that, a lower bound of the free distance was established to avoid the exhaustive search in ML detection that was derived with the SVD. Then, a basis transformation scheme is proposed so that the lower bound generated by the QRD can further be tightened. As a result, the QRD-based selection method achieves near optimum performance. Finally, the use of the proposed approaches to other applications, such as receive antenna selection, joint transmit/receive antenna selection, and antenna selection has been extended in MIMO relay systems [82]. In the V-BLAST technique, OSIC technique was proposed as an available competent detection technique regarding performance and complexity. Though, MIMO system suffers from high complexity and implementation cost. As a practical solution, antenna selection technique has been presented. Since the existing literature considered only the capacity-based selection, authors [59] developed an optimal selection technique for a V-BLAST technique using OSIC detection with respect to error rate performance. Its complexity is illustrated to be proportional to the fourth power of the number of transmit antennas. Then, a near-optimal selection technique has been exploited to reduce the complexity without considerable performance degradation compared to the optimal selection technique.

Afterward, the energy efficient MIMO system is used and AS has been employed to enhance the performance of point-to-point MIMO, cooperative MIMO, multiuser MIMO and large scale MIMO systems [83]. In [84], maximal ratio combining and OSTBC are recommended with AS technique to improve the MIMO system performance. Also, distributed-MIMO system performance has been analyzed in [85] over Rayleigh fading channel, however, the shadowing impact has not been considered.

1.2.4 Channel Modeling

Channel modeling is a paramount issue for efficient wireless system design. Several multipath fading scenarios such as Rayleigh, Rician and Nakagami-*m* fading have been considered in the past to evaluate the system performance with various detection techniques. Consequently, system performance has been well analyzed under these scenarios [86-89]. One other multipath channel model called Weibull channel model is taken into consideration due to its flexible and practical nature to describe multipath fading in various radar clutters, indoor and outdoor scenario. This

model has been considered for evaluating the system performance in diversity scenario. The effect of Weibull fading severity and correlation on overall system performance has been explored with receiver combining techniques in [90-93]. In [94, 95], SC is used to evaluate system performance over Weibull fading channel. The results of error rate demonstrate that for the same average channel gains, the performance on independent and non-identically distributed (i.n.d.) channels may be better or inferior to on i.i.d. channels. Further, the theory of effective rate has been shown much attention, since it yields the delay aspect into account when performing channel capacity analysis [96].

The keyhole effects deteriorate the channel matrix by limiting both rank deficient and spatial correlation effects, which severely degrades the MIMO system capacity. The channel capacity performance can be improved by cascading multiple channel models. Therefore, many multiplicative stochastic models have been used to analyze the fading collectively instead of separating it from several parts. The received signals can explain the physical significance of these models. The received signals consist of the product of a large number of rays reflected through statistically independent scatterers [97]. For example, double-Rayleigh (i.e., Rayleigh × Rayleigh) amplitude distribution obtained by diffracting wedges. Such distribution is induced through double scattering in the wireless radio channel. Moreover, the high-SNR slope of double-Rayleigh fading shows inferior performance than that of single-Rayleigh fading [98]. In [99-102], double-Rayleigh and double-Nakagami-*m* models have been recommended for keyhole channel modeling of MIMO systems and for capacity analysis in low power regime. The work presented in [103] enumerates that the receiver performance degrades with disruptive effects of cascaded fading however these effects can be compensated by increasing diversity branches. In [29], a cascaded Weibull channel model produced by the product of independent but not essentially identically distributed Weibull random variables is presented. Double-Weibull channel model can achieve the improved capacity in comparison to the capacity of the single-Weibull channel model.

In several practical wireless environments, multipath fading and shadowing appear at the same time which creates a composite fading. The shadowing effects caused by the slow variations are superimposed on multipath propagation arising from rapid fluctuations [104]. Subsequently, various models have been proposed for analyzing the performance of the wireless system. The composite channel models such as Rayleigh-LN, shadowed-Rician, Gamma-Gamma, *K*, generalized-*K* [36, 48, 105-108] and more recent Weibull-gamma (WG) [109] are extensively employed to see the combined effects of both small scale fading and shadowing. Ref. [105] has shown that gamma

distribution is numerically more appropriate than lognormal distribution to model shadowing effects and hence preferred in recent approaches. Table 1.1 [110] presents the existing models which define both the multipath fading and shadowing conditions.

Table 1.1 Composite Channel models

Proposed models	Channel modeling /Generation	Remarks
Suzuki model [111]	A product of Rayleigh processes with the lognormal process	For non-direct line of sight communication. However, it is not suitable for direct line of sight communication.
Extended Suzuki models [112]	A product of a Rice process and a lognormal process	Suitable to describe the nature of large classes of frequency non-selective land mobile satellite channels. However, it is unable to model non-uniform scattering
Generalized modified Suzuki model [113]	A product of Weibull process and lognormal process	To model shadow fading along with inhomogeneous and anisotropic diffuse scattering.
K- fading model [105, 114, 115]	A product of Rayleigh process and lognormal process	To model non-line of sight and shadowing.
Weibull-lognormal fading model [116-119]	A product of Weibull process and lognormal process	Composite model, but due to lognormal distribution it faces mathematical complexity
Generalized-*K* Fading model [106, 120, 121]	A product of a gamma random variable and a channel matrix with i.i.d. Nakagami-*m* entries	An accurate approximation of most of the fading and shadowing effects.
Extended Generalized-*K* fading model [122-124]	The combination of two independent Rayleigh distributed RVs with the average unit powers such that each pair of these RVs are independent, and one RV represents shadowing, and another one represents multipath fading components. Both the components are distributed according to generalized Nakagami-*m* PDFs	For modeling wireless and optical communication channels. Superior model but mathematically complex.
Weibull-Gamma fading model [109, 125-127]	A product of Weibull and gamma random process	Simpler and relatively new one which is used for outdoor, indoor, communication and radar clutters including shadowing effects.

Due to extensive adaptability, experimental fitness and analytical compliance, the composite WG distribution is suitable for analyzing MIMO system in the present wireless environment. As discussed before that the Weibull fading is flexible to model severe and non-severe multipath fading environments, it considers the radar clutters and different mobile fading effects, however, Gamma model is preferred to model shadowing effects and jointly WG composite fading model is designed to measure both the effects. WG channel model is a generalized model that comprises Rayleigh-Gamma and exponential-Gamma distributions as its special cases. Subsequently, this model approaches some other fading models [36, 109].

In [128], WG has been described in the hypergeometric form, and subsequently, an alternative has been given in [109] where WG distribution is denoted in the form of Meijer-G function. In [129], outage probability has been obtained through a joint distribution using selection combining. Also, arbitrary input branches have been considered over exponentially correlated composite WG fading channels. Thereafter, representations of bivariate WG distribution and outage probability with dual-branch selection diversity have been measured over bivariate WG fading channel [130].

1.2.5 Low SNR Analysis

Since many sites in the geometry lie on the edge of their cells. Therefore, apart from operating at high SNR, users frequently operate at low SNR. According to [131], 40% of the geographical area receives signal as low as 0dB and less than 10% area has an SNR greater than 10dB. In such conditions, the system performance evaluation at low SNR is imperative to the designers. MIMO systems namely SM with the optimal detector, SM with the MMSE detector and OSTBC have been implemented to evaluate performance at low SNR over Weibull fading channel [132].

1.2.6 Noise Modeling

To the best of our knowledge, most of the reported work [133-135] included both the higher and lower modulation orders in multipath fading perturbed by AWGN, however, noise can deviate from its Gaussianity both in terms of asymmetry and sharpness. Therefore, the requirement of a generic noise model has come into existence. The additive and multiplicative power line noises affect the system performance extensively in power line communication (PLC). Further, the additive noise is categorized into background noise and impulsive noise. The background noise and impulsive noise models follow Nakagami-*m* and Middleton class A distribution respectively, while the multiplicative PLC noise produces fading in the received signal power [136, 137]. The different fields of communication such as sonar applications and a compressed sensing created a growing interest of additive white generalized Gaussian noise (AWGGN) and thus, the same noise scenario

is considered to evaluate the error rate performance of system [138, 139]. Many noise forms such as impulsive, gamma, Gaussian, Laplacian are produced by the generic noise model [140, 141]. Most popular is AWGN, which normally used to model background noise in the channel as well as noise introduced at the receiver front end and it is the most common noise model in communication systems. In many real life communication links, such as urban, indoor and underwater acoustic channels, the dominant ambient disturbances affecting radio channels are atmospheric and man-made electromagnetic noises which deviate strongly from the prevalent Gaussian model [142]. The generalized Gaussian distribution (GGD) is the growing research interest for modeling different noise effects.

A novel unified performance analysis of STBCs operating in MIMO network and AWGGN scenario is presented in [143]. The system performance is analyzed in terms of the average BER of a multi-hop wireless communication system perturbed by an AWGGN [144]. The rectangular-QAM has been given attention to calculate average symbol error probability (ASEP) using Gaussian Q-function under a composite fading scenario in the presence of AWGGN [145]. Consequently, rectangular-QAM is a combination of in-phase and quadrature-phase pulse amplitude modulation (PAM) signals. There is significant scope to model a MIMO system by exploiting the diversity and efficient detection in a composite fading scenario that considers a real practical environment. To evaluate the performance of MIMO composite channel in generic noise scenario is an open area of research and will be of interest to both the industry and academia as it improves the wireless radio system performance even in severe fading and noise scenario.

1.3 Problem Formulation

The potential challenge in MIMO systems is to improve the capacity and error rate performance in highly severe environment. There are significant channel models which can model the real wireless scenario, however, they are complex in nature. Also, further enhancement in data rate and reliability is also an issue in such composite fading scenario.

The improved capacity can be achieved at high SNR, but the key task is to achieve the capacity in low SNR under severely faded environment. ML is optimum detection technique but it suffers from computational complexity, and there have been linear detection techniques which are simple but result in sub-optimal performance. The research has been mainly focused on achieving the ML performance with a reduced level of complexity. Thus, to choose an efficient detection technique

which approaches the ML performance with less complexity and significant performance improvement is imperative to the system designer.

If channel state information is known (full or partial) at transmitter side, the capacity and error rate performance improve significantly. Antenna selection techniques play an important role to improve the system performance. Although antenna selection techniques have been used in MIMO system under different multipath and some other composite fading environment [146], they have not been used in WG fading scenario.

The effect of additive noise has been seen over MIMO composite channel, however, the deviation of noise can be possible from AWGN. Thus, generalized noise model is useful in such condition. Error rate performance SISO systems have been evaluated under composite fading and generalized noise scenario. The analysis of MIMO system with simple and efficient detection under such practical scenario is a significant problem.

Based on the above discussions, we have framed the primary objectives of our thesis as follows:

- To analyze and improve the MIMO system performance in spatial diversity and spatially multiplexed scenario under multipath, cascaded and composite fading channel.
- To derive and develop performance criteria for MIMO system in low SNR regime over composite WG fading channel.
- To analyze the MIMO system performance using antenna selection.
- To use efficient detection for MIMO system performance analysis in composite fading and generic noise scenario.

1.4 Contribution of Thesis

The contribution of the thesis is enlisted below

1. Performance analysis of MIMO system over different multipath and a cascaded fading channel
    i) OSTBC and MRC diversity are used to analyze the error performance of MIMO system performance over Rayleigh, Rician, Nakagami-*m* and Weibull and double Weibull fading channel.
    ii) PDF and CDF are evaluated in the double-Weibull fading scenario.
    iii) SER expressions are derived with OSTBC and MRC in Weibull and double-Weibull Fading.

2. Performance analysis of MIMO system over a composite Weibull-gamma (WG) fading channel
    i) The amount of fading (AF) is evaluated.
    ii) OSTBC and MRC diversity techniques are considered to analyze error performance of MIMO system.
    iii) Three detection techniques, namely, MMSE-OSIC, ML and MMSE-OSIC^2 are used to evaluate the system error performance.
3. Low SNR analysis of MIMO system over WG fading channel
    i) MMSE and optimal detection techniques are used to evaluate the capacity performance
    ii) OSTBC diversity technique is considered to evaluate the capacity performance.
    iii) The derived linear expressions are validated through computer simulation.
4. Antenna selection for MIMO performance improvement over WG fading channel.
    i) Optimal and suboptimal detection is used to enhance the system capacity performance.
    ii) OSTBC is used to evaluate error rate performance.
5. Performance analysis of MIMO system in WG fading and AWGGN scenario
    i) MMSE-OSIC, ML and MMSE-OSIC^2 detection techniques are used to evaluate the error performance.
    ii) Simplified expressions for ASEP are given for WG fading and also for its special cases

1.5 Thesis Organization

This thesis work provides the detailed analysis of MIMO system using the most appropriate OSTBC and effective MRC diversity techniques. In addition, SM-MIMO has also been considered using different detection techniques.

The reminder of this thesis is organized as follows. In Chapter 2, we have analyzed the MIMO system performance using OSTBC and MRC diversity techniques in multipath fading such as Rayleigh, Rician, Nakagami-*m* and Weibull fading. Also, the effect of double-scattering in terms of double-Weibull fading has also been seen in MIMO system. The analytical expressions for PDF and CDF are derived for single and double Weibull fading channel. Also, SER expressions are computed by CDF.

In Chapter 3, a composite WG fading channel model is used with the same system set-up. Again, CDF based SER expressions are computed but in WG fading for the validation of simulation results. AF has also been computed and analyzed for WG fading. Further, error rate performance of SM-MIMO system has been evaluated using different detection techniques. The error rate has been compared to that of optimal ML detection and simpler MMSE-OSIC detection.

Chapter 4 presents the MIMO system capacity performance in low SNR regime in WG fading scenario. Optimal detector provides the maximum capacity of MIMO system, MMSE detector is less complex than optimal detector and offers improved capacity performance. In addition, OSTBC is diversity oriented technique. Thus, we have explored these three techniques in WG fading scenario in our work. We have evaluated the capacity of MIMO system at low SNR under WG fading channel.

Chapter 5 evaluates the optimal and sub-optimal AS based capacity of MIMO system over WG fading channel. AS is used to analyze BER performance using OSTBC for M-QAM under same WG fading scenario. The improved error rate performance can be achieved in diversity scenario, however, improved capacity performance can be achieved through SM.

In Chapter 6, SM is employed to improve the error rate performance of MIMO system using MMSE-OSIC which is fairly simpler than ML detection. Also, an efficient MMSE-OSIC^2 detection is used to achieve near-ML performance with reduced complexity. Fox-H function (FHF) based exact analytical expressions are calculated to represent error rate probability for 16-QAM over WG fading channel in the presence of AWGGN. AWGN and Laplacian noise are taken into account as special cases of AWGGN. Also, the fading and shadowing parameter variations are demonstrated.

Finally, Chapter 7 concludes the thesis work and presents the future direction in MIMO channel modeling.

CHAPTER 2

MIMO Multipath and Cascaded Fading Channels in Diversity Scenario

2.1 Introduction

In MIMO systems, reliability is achieved by spatial diversity which is categorized into transmit and receive diversity. To achieve full transmit diversity, STBC and to achieve receiver diversity, MRC techniques are mostly recommended to improve the wireless link performance [10, 147] in less faded and severely faded wireless environment. Thus, it is required to use suitable channel models which can operate in such environments. The ease or complexity to design a MIMO channel model depends on the essential accuracy and nature of the environment to be modeled. As it is given in [27] that the channel matrix of a physical model is followed by some physical parameters such as the angle of arrival (AoA), the angle of departure (AoD) and the time of arrival (ToA) of a signal. Once the channel is modeled analytically in MIMO system, all the channels behave as SISO channels between each transmit and receive antenna. In addition, the channels are assumed as i.i.d. MIMO channels [27]. In the wireless fading environment, the error rate of MIMO system can be decreased by implementing appropriate diversity technique. Thus, this chapter focuses on OSTBC and MRC diversity techniques employed to improve the MIMO system performance over multipath and cascaded fading channels.

In Chapter 1, the channel models in less fading and severe fading multipath environment have been described, and hence Rayleigh, Rician and Nakagami-*m*, Weibull fading PDF have been presented. To evaluate the MIMO system performance under these practical scenarios is imperative to the system designer. In [48, 148-150], capacity performance is evaluated in diversity scenario over such multipath fading channels, however, error performance is also an important measure. Furthermore, a tightly estimated results of MRC receivers for BER and capacity have shown over independent Weibull fading channels [151], however, MIMO system has not taken into account. Thus, under different fading scenarios, we have analyzed the error rate performance using STBC and MRC diversity for distinct modulation techniques such as BPSK, QPSK, and 16-QAM [152]. In addition, along with Weibull or single-Weibull, a double-Weibull fading scenario has been used to analyze the error rate of MIMO system. As discussed earlier, a double-Weibull fading is the result of multiple scatterers in the environment and its channel model is produced by the product of two independent but not essentially identically distributed Weibull random variables [29]. The double-

Weibull fading has gained the remarkable attention to model the propagation scenario [153]. This chapter also incorporates a comparative analysis of MIMO system under single and double-Weibull fading in diversity scenario [154]. Moreover, double-Weibull fading represents cascading of two Weibull random variables. We derived the expression of CDF for double-Weibull fading in Meijer-G form. Consequently, we have given the exact expressions for first order statistics such as PDF and CDF for proposed Weibull channel models. For mathematical analysis of proposed single and double-Weibull channel models, simple SER expressions are computed for OSTBC and MRC using CDF.

The remainder of the chapter is organized as follows. Section 2.2 describes the MIMO channel model with OSTBC and MRC along with single-Weibull and double-Weibull fading. Analytical expressions for SER under Weibull and double-Weibull fading are given in Section 2.3. Section 2.4 presents simulation results. Finally, Section 2.5 concludes the chapter.

2.2 System and Channel model

Consider the same MIMO system model as defined in (1.8) having N_t transmit and N_r receive antennas with channel H having matrix size $N_r \times N_t$, X is the transmitted symbol vector ($X \in \mathbb{C}^{N_t \times 1}$) that consists N_t independent input symbols. Rayleigh, Rician and Nakagami-m channel coefficients h_{ij} have already been presented in Chapter 1 by (1.25), (1.27) and (1.30) respectively. These are commonly used channel models, therefore, simulation has been performed under these scenarios using diversity techniques. Further, we have given attention to Weibull fading, thus, the cascaded Weibull fading has also been considered.

Following (1.34), the average SNR for Weibull fading is $\bar{\gamma} = E\left[X_{ij}^2\right] E_s/N_0 = \Omega_{ij}^{\frac{2}{\beta}} \Gamma\left(1+\frac{2}{\beta}\right) E_s/N_0$. Also, Weibull distribution is represented in terms of effective SNR by replacing β_{ij} with $\beta_{ij}/2$ and Ω_{ij} with $\left(\bar{\gamma}/\alpha_{ij}\right)^{\beta_{ij}/2}$ and is given by

$$p_{\gamma_{ij}}(\gamma) = \frac{\beta_{ij}}{2}\left(\frac{\alpha_{ij}}{\bar{\gamma}}\right)^{\beta_{ij}/2} \gamma^{\beta_{ij/2}-1} \exp\left[-\left(\frac{\gamma\alpha_{ij}}{\bar{\gamma}}\right)^{\beta_{ij}/2}\right] \tag{2.1}$$

where $\alpha_{ij} = \Gamma\left(1+\frac{2}{\beta_{ij}}\right)$. CDF can be expressed in terms of SNR as

$$F_{\gamma_{ij}}(\gamma) = 1 - \exp\left[-\left(\frac{\alpha_{ij}\gamma}{\bar{\gamma}}\right)^{\beta_{ij}/2}\right] \tag{2.2}$$

The product of two Weibull distributed random variables $X_{ij}(ij = 1,2)$ creates the double-Weibull fading distribution given in [29] as

$$p_{X_{ij}}(x) = \frac{2\beta_{ij}}{\Omega_{1_{ij}}\Omega_{2_{ij}}} x^{\beta_{ij}-1} K_0\left(2\sqrt{\frac{x^{\beta_{ij}}}{\Omega_{1_{ij}}\Omega_{2_{ij}}}}\right) \tag{2.3}$$

where K_0 is modified Bessel function of second kind and zero-th order. With $\beta_{ij} = 2$ and $\Omega_{1_{ij}} = \Omega_{2_{ij}} = \Omega_{ij}$, (2.3) can be modified in terms of PDF of double-Rayleigh fading model [155] and can be represented as a function of SNR given below

$$p_{\gamma_{ij}}(\gamma) = \frac{\beta_{ij}{\alpha_{ij}}^{\beta_{ij}}}{\left(\bar{\gamma}_{1_{ij}}\bar{\gamma}_{2_{ij}}\right)^{\beta_{ij/2}}} \gamma^{\beta_{ij/2}-1} K_0\left(2\sqrt{\frac{{\alpha_{ij}}^{\beta_{ij}}\gamma^{\beta_{ij/2}}}{\left(\bar{\gamma}_{1_{ij}}\bar{\gamma}_{2_{ij}}\right)^{\beta_{ij/2}}}}\right) \tag{2.4}$$

After some mathematical formulation, a simplified closed form expression for CDF is derived using [156, Equations (20) and (26)], which is given as

$$F_{\gamma_{ij}}(\gamma) = \frac{{\alpha_{ij}}^{\beta_{ij}}}{\left(\bar{\gamma}_{1_{ij}}\bar{\gamma}_{2_{ij}}\right)^{\beta_{ij/2}}} \gamma^{\beta_{ij}/2} G_{1,3}^{2,1}\left(\frac{(\alpha_{ij})^{\beta_{ij}}\gamma^{\beta_{ij/2}}}{\left(\bar{\gamma}_{1_{ij}}\bar{\gamma}_{2_{ij}}\right)^{\beta_{ij/2}}}\middle|_{0,0,-1}^{0}\right) \tag{2.5}$$

In Fig. 2.1 and Fig. 2.2, PDF and CDF are determined respectively under single and double-Weibull fading in terms of γ where $\bar{\gamma} = \bar{\gamma}_{1_{ij}}\bar{\gamma}_{2_{ij}}$ and $\bar{\gamma} = \bar{\gamma}_{1_{ij}} = \bar{\gamma}_{2_{ij}} = 0$ dB.

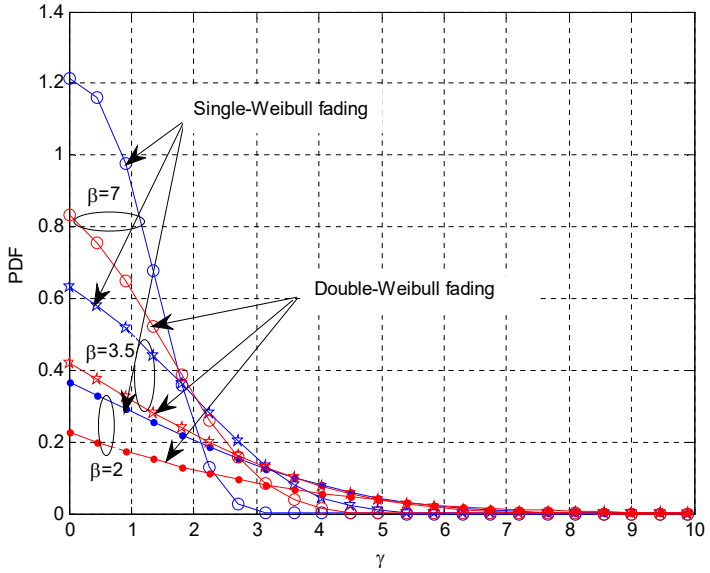

Fig. 2.1 PDF for single and double-Weibull fading at $\bar{\gamma} = \bar{\gamma}_{1_{ij}} = \bar{\gamma}_{2_{ij}} = 0dB$

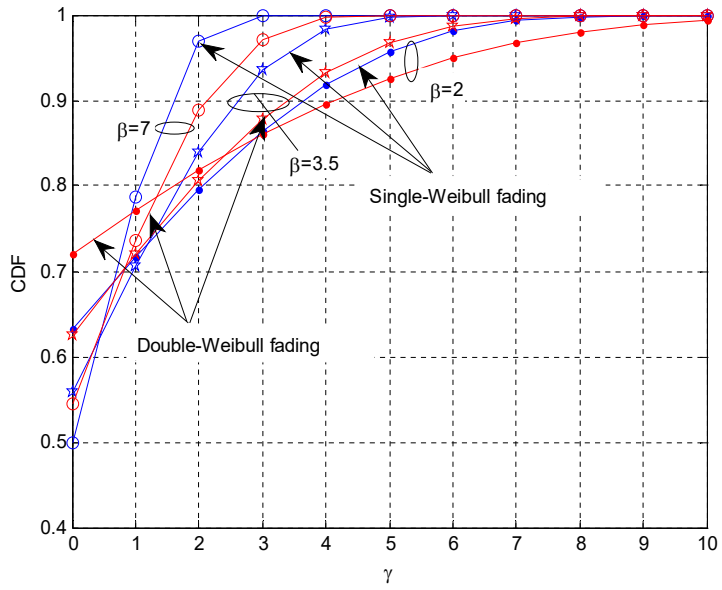

Fig. 2.2 CDF for single and double-Weibull fading at $\bar{\gamma} = \bar{\gamma}_{1_{ij}} = \bar{\gamma}_{2_{ij}} = 0\text{dB}$

Consequently, it is shown that PDF is decreasing and CDF is initially increasing under double-Weibull fading in comparison to that of single-Weibull fading. With the increase of β, large peak of PDF is achieved and CDF tends to unity at low SNR. At high values of γ, PDF is going to infinity and CDF is unity.

STBC and MRC have been shown their significance to improve the error rate performance. Hence, they are described as follows

A) Orthogonal Space Time Block Code

OSTBC is the most suitable transmit diversity technique which improves the error rate performance of MIMO system by opposing channel fading. Since each antenna transmits multiple replicas of the same information, the process improves performance significantly and hence, the chances of losing the information decrease exponentially. The effective SNR γ_o for OSTBC MIMO system is given as

$$\gamma_o = \frac{E_s}{N_0 R_c N_t} \|H\|^2 \tag{2.6}$$

where $\|H\|^2 = \sum_{i=1}^{N_r} \sum_{j=1}^{N_t} \left\|h_{ij}\right\|^2$, $\|.\|$ is the Frobenius norm of channel matrix H. When a codeword transmits N_s symbols over T symbol periods, the code rate of OSTBC R_c is equal to N_s/T symbols per channel use.

- *Alamouti STBC:* Alamouti STBC contains two transmit antennas irrespective of the number of receive antennas. In this scheme, b number of bits are transmitted by using a modulation technique that maps each of the b bits to one symbol from a constellation with $2b$ symbols. The constellation can be real or complex and commonly used constellation are PSK and QAM. Therefore, the transmitter takes x_1 and x_2 symbols from constellation using a block of $2b$ bits, that are transmitted from antenna one and two. The transmitted codeword of Alamouti scheme is represented as

$$\mathrm{X} = \begin{bmatrix} x_1 & x_2 \\ -x_2^* & x_1^* \end{bmatrix} \tag{2.7}$$

Equation (2.7) implements a two branch transmit diversity technique. In this coding technique, the rows serve as the different time instants, and the columns represent the transmitted symbol through each antenna. First and second row of (2.7) denotes the transmission at the first and second time instant respectively. At a time t, antenna 1 and antenna 2 transmit the symbols x_1 and x_2 respectively. At time $t + T$, antenna 1 and antenna 2 transmit the symbols $-x_2^*$ and x_1^* respectively, where '$(.)^*$ ' is the complex conjugate.

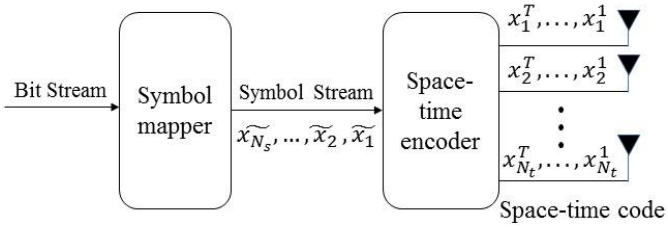

Fig. 2.3 Space-time encoder [24]

Fig. 2.3 illustrates the general design of space-time block encoder. The codeword matrix X having matrix size $N_t \times T$ is defined as the output of the space-time block encoder. Let a row vector x_i denote the i-th row of the codeword matrix. Then, x_i is transmitted by the i-th transmit antenna over T symbol period. To simplify the ML detection at the receiver, the following property is required.

$$\begin{aligned} \mathrm{X}\,\mathrm{X}^{\dagger} &= c\left[\left|x_i^1\right|^2 + \left|x_i^2\right|^2 + \cdots \left|x_i^T\right|^2\right] I_{N_t} \\ &= c\|x_i\|^2 I_{N_t} \end{aligned} \tag{2.8}$$

where c is a constant. The above property infers that the row vectors of the codeword matrix are orthogonal to each other, that is,

$$x_i x_j^{\dagger} = \sum_{t=1}^{T} x_i^t \left(x_j^t\right)^* = 0, i \neq j, \quad i, j \epsilon (1,2, \ldots N_t) \tag{2.9}$$

To check whether the code carries full diversity or not, we compute the rank of all possible difference matrices Diff(X, X′) [4]. If the rank is 2 for every X = X′, then the code offers full diversity. Considering another pair of symbols (x_1', x_2'), codeword matrix is denoted as

$$\mathrm{X}' = \begin{bmatrix} x_1^{'} & x_2^{'} \\ -x_2'^{*} & x_1'^{*} \end{bmatrix} \tag{2.10}$$

The difference matrix is represented as

$$\mathrm{Diff}(\mathrm{X}, \mathrm{X}') = \begin{bmatrix} x_1^{'} - x_1 & x_2^{'} - x_2 \\ x_2^{*} - x_2'^{*} & x_1'^{*} - x_1^{*} \end{bmatrix} \tag{2.11}$$

The determinant of difference matrix, det[Diff(X, X′)] is $\left|x_1^{'} - x_1\right|^2 + \left|x_2^{'} - x_2\right|^2$ and it is zero only, when $x_1^{'} = x_1$ and $x_2^{'} = x_2$. Thus, Diff(X, X′) is a full rank matrix when X ≠ X′ and Alamouti satisfies the determinant criteria. Consequently, it provides $2N_r$ diversity for N_r receive antennas. Hence, Alamouti is called full diversity code.

If we consider one receive antenna, then the signal reception and decoding both depend on the number of accessible receive antennas. The receive signals are characterized by taking one receive antenna as [3],

$$\begin{aligned} y_1^{(1)} &= \quad y_1(1) = h_{11} x_1 + h_{12} x_2 + n_1^{(1)} \\ y_1^{(2)} &= \quad y_1(t+T) = -h_{11} x_2^* + h_{12} x_1^* + n_1^{(2)} \end{aligned} \tag{2.12}$$

where y_1 is the received signal at antenna 1, h_{ij} represents complex channel gain from the i-th transmit antenna and the j-th receive antenna, n_1 is complex random variable showing AWGN noise at antenna 1, and y^k denotes y at a time instant k (at time t + (k-1) T). The received signals are joined as

$$\begin{aligned} \widetilde{x_1} &= \quad h_{11}^* y_1^{(1)} + h_{12}\, y_1^{*(2)} \\ \widetilde{x_2} &= \quad h_{12}^* y_1^{(1)} + h_{11} y_1^{*(2)} \end{aligned} \tag{2.13}$$

Substituting (2.12) into (2.13) yields

$$\widetilde{x_1} = (\alpha_{11}^2 + \alpha_{12}^2) x_1 + h_{11}^* n_1^{(1)} + h_{12} n_1^{*(2)}$$

$$\widetilde{x_2} = (\alpha_{11}^2 + \alpha_{12}^2)x_2 - h_{11}n_{11}^{*(2)} + h_{12}^* n_1^{(1)} \tag{2.14}$$

where α_{ij}^2 is the squared magnitude of the channel gain h_{ij}.

ML detection maximizes the following decision metric over all possible values of x_1 and x_2

$$|y_1 - \alpha_{11}x_1 - \alpha_{12}x_2|^2 + |y_2 - \alpha_{11}x_2^* - \alpha_{12}x_1^*|^2 \tag{2.15}$$

Equation (2.15) requires full search over all possible pairs of x_1 and x_2. Consequently, its complexity increases exponentially by increasing N_t. Deleting the terms those are independent of codewords, the above minimization problem can be decomposed into two parts for separate decoding of x_1 and x_2, given as

$$|x_1|^2\left[(y_1\alpha_{11}^* + y_2^*\alpha_{12} - x_1)^2 + (\alpha_{11}^2 + \alpha_{12}^2 - 1)\right] \tag{2.16}$$

$$|x_2|^2\left[(y_1\alpha_{12}^* - y_2^*\alpha_{11} - x_2)^2 + (\alpha_{11}^2 + \alpha_{12}^2 - 1)\right] \tag{2.17}$$

The above decomposition reduces the decoder complexity, however, the complexity increases linearly instead of exponentially by increasing the number of transmit antennas.

B) Maximal Ratio Combining (MRC)

In MRC, all the received signals coming from multiple diversity branches are combined constructively. A transmit weight vector is given to the symbol to be transmitted that forms the transmitted signal vector. This technique amplifies the strong signal of branches and attenuate the weak signals. However,

- Combining more than one branch needs co-phasing, if there is no co-phasing then the addition of branch signals would not be possible in coherent manner at the combiner. Accordingly, the resultant of the output could still display substantial fading due to the constructive and destructive addition of signals in all the branches.
- More weight should be given to branches having a high SNR than branches having a low SNR [21].

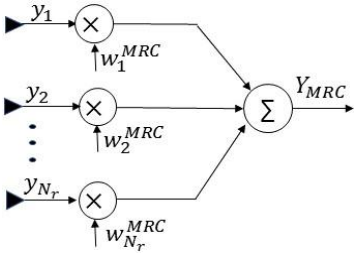

Fig. 2.4 Maximal ratio combiner

In a SIMO system, the signal vector $Y \in \mathbb{C}^{N_r \times 1}$ at the received N_r antennas is represented as

$$Y = \sqrt{\frac{E_s}{N_0}} HX + \mathcal{N} \tag{2.18}$$

The received signals in the different antennas are combined by MRC technique to achieve the best performance as shown in Fig. 2.4. MRC technique combines all the N_r branches by the following weighted sum

$$Y_{MRC} = \left(w_1^{MRC}, w_2^{MRC}, \ldots\ldots\ldots w_{N_r}^{MRC}\right) Y = \sum_{j=1}^{N_r} w_j^{MRC} y_j \tag{2.19}$$

where $\left(w_1^{MRC}, w_2^{MRC}, \ldots\ldots\ldots w_{N_r}^{MRC}\right) = W_{MRC}^T$ and W_{MRC} is a weight vector. The combined received signal can be decomposed into signal and noise part which is as follows

$$\begin{aligned} Y_{MRC} &= W_{MRC}^T \left(\sqrt{\frac{E_s}{N_0}} HX + \mathcal{N} \right) \\ &= \sqrt{\frac{E_s}{N_0}} W_{MRC}^T HX + W_{MRC}^T \mathcal{N} \end{aligned} \tag{2.20}$$

Equation (2.20) gives the average of the instantaneous signal power and that of the noise power respectively and given as

$$\mathcal{P}_s = E\left[\left| \sqrt{\frac{E_s}{N_0}} W_{MRC}^T HX \right|^2 \right] = \frac{E_s}{N_0} E\left[\left| W_{MRC}^T HX \right|^2 \right] = \frac{E_s}{N_0} \left| W_{MRC}^T H \right|^2 \tag{2.21}$$

$$\mathcal{P}_{N_0} = E\left[\left| W_{MRC}^T \mathcal{N} \right|^2 \right] = \left\| W_{MRC}^T \right\|^2 \tag{2.22}$$

From (2.21) and (2.22), the average SNR for the MRC is expressed as

$$\gamma_{MRC} = \frac{\mathcal{P}_s}{\mathcal{P}_{N_0}} = \frac{E_s \left| W_{MRC}^T H \right|^2}{N_0 \left\| W_{MRC}^T \right\|^2} \tag{2.23}$$

From the Cauchy-Schwartz inequality,

$$\left| W_{MRC}^T H \right|^2 \leq \left\| W_{MRC}^T \right\|^2 \|H\|^2 \tag{2.24}$$

Equation (2.23) is upper-bounded as (2.24), and the output SNR is determined by:

$$\gamma_{MRC} \leq \frac{E_s \left\| W_{MRC}^T \right\|^2 \|H\|^2}{N_0 \left\| W_{MRC}^T \right\|^2} = \frac{E_s}{N_0} \|H\|^2 \tag{2.25}$$

Note that the SNR in (2.25) is maximized at $W_{MRC} = H^*$, which produces $\gamma_{MRC} = E_s\|H\|^2/N_0$. In addition, the weight factor of each branch in (2.19) must be matched to the corresponding channel for MRC. EGC is a special case of MRC in which all the signals from multiple diversity branches are combined with equal weights. MRC offers the best performance, maximizing the post-combining SNR.

2.3 Symbol Error Rate Analysis in Weibull fading

The probability of symbol error (P_s) is obtained from probability of bit error (P_b) in a straightforward means if we assume Gray encoding (i.e. nearest neighbors change by only one bit), and if we assume that errors are only caused by confusion with nearest neighbors (which is a good assumption at moderate to high SNRs) [157]. In this case, a symbol error causes only one bit error and the P_b is approximated as

$$P_b \approx \frac{1}{\log_2 M} P_s \tag{2.26}$$

where M is modulation order. Average SER is an important measure to evaluate the wireless system performance and is given in [158] as

$$\text{SER}(\gamma) = E\left[a_m Q\left(\sqrt{2b_m\gamma}\right)\right] \tag{2.27}$$

where $Q(.)$ is the Gaussian Q-function, a_m and b_m are modulation constants which define specific modulation technique. The values of (a_m, b_m) for different modulation formats are given in Table 2.1 as

Table 2.1 Modulation techniques with modulation-explicit constants

Modulation Technique	**Modulation constants (a_m, b_m)**
BPSK	$(1, 1)$
QPSK	$(2, 1/2)$
M-PSK	$(2, \sin^2(\pi/\text{M}))$
M-QAM	$4(\sqrt{M}-1)/\sqrt{M}, 3/2(M-1)$

The SER expression can be rewritten as

$$\text{SER} = \frac{a_m\sqrt{b_m}}{2\sqrt{\pi}} \int_0^\infty \frac{e^{-b_m x}}{\sqrt{x}} F_\gamma(x)dx \tag{2.28}$$

In (2.28), $F_\gamma(x)$ is the CDF of γ. Substituting (2.2) into (2.28) and using [103, Equation (21)], SER for single-Weibull fading is written in simplified form as

$$\mathrm{SER}_{sw}(\gamma) = \sum_{i=1}^{N_r}\sum_{j=1}^{N_t}\frac{a_m}{2}\left(1 - \frac{\sqrt{2k}}{(2\pi)^{(\ell+k-1)/2}} G_{\ell,k}^{k,\ell}\left[\left(\frac{\alpha_{ij}}{\bar{\gamma}}\right)^{k\beta_{ij}/2}\frac{\ell^{\ell}}{{b_m}^{\ell}k^{k}}\Bigg|_{0,\Delta(\ell,1/2),0}^{\Delta(\ell,1/2)}\right]\right) \tag{2.29}$$

where $\frac{\ell}{k} = \frac{\beta}{2}$ and $\Delta(u,v) = \frac{v}{u}, \frac{v+1}{u}, \ldots, \frac{v+u-1}{u}$, ℓ and k are positive integers. Substituting (2.5) into (2.2) and representing $e^{-b_m x}$ in the form of Meijer-G function [156, Equation (11)], SER for double-Weibull fading channel is given by

$$\mathrm{SER}_{dw}(\gamma) = \sum_{i=1}^{N_r}\sum_{j=1}^{N_t}\frac{a_m\sqrt{b_m}\alpha^{\beta_{ij}}}{2\sqrt{\pi}\left(\bar{\gamma}_{1_{ij}}\bar{\gamma}_{2_{ij}}\right)^{\beta_{ij}/2}}\int_0^{\infty}\gamma^{(\beta_{ij}-1)/2}\,G_{0,1}^{1,0}(b_m\gamma|_0^-)G_{1,3}^{2,1}\left(\frac{(\alpha_j)^{\beta_{ij}}\gamma^{\beta_{ij}/2}}{\left(\bar{\gamma}_{1_{ij}}\bar{\gamma}_{2_{ij}}\right)^{\beta_{ij}/2}}\Bigg|_{0,0,-1}^{0}\right)d\gamma \tag{2.30}$$

Using [156, Equation (21)], (2.30) becomes

$$\mathrm{SER}_{dw}(\gamma) = \sum_{i=1}^{N_r}\sum_{j=1}^{N_t}\frac{a_m\alpha^{\beta_{ij}}}{\sqrt{2}k\left(\bar{\gamma}_{1_{ij}}\bar{\gamma}_{2_{ij}}\right)^{\frac{\beta_{ij}}{2}}(2\pi)^{\frac{\ell}{2}+k-1}}\left(\frac{\ell}{b_m}\right)^{\beta_{ij}/2}$$

$$\times G_{k+\ell,3k}^{2k,k+\ell}\left[\left(\frac{\alpha^{\beta_{ij}}}{\left(\bar{\gamma}_{1_{ij}}\bar{\gamma}_{2_{ij}}\right)^{\beta_{ij}/2}}\right)^{k}\frac{\ell^{\ell}}{k^{2k}{b_m}^{\ell}}\Bigg|_{0,0,\Delta\left(\ell,\frac{(1-\beta_{ij})}{2}\right),\Delta(k,-1)}^{0,\Delta\left(\ell,\frac{(1-\beta_{ij})}{2}\right)}\right] \tag{2.31}$$

The generic forms of SER are given by (2.29) and (2.31) for both the applied diversity techniques in single and double-Weibull fading respectively when β_{ij} is replaced by β_i for MRC. After substituting the values of $\bar{\gamma}$, $\bar{\gamma}_{1_{ij}}$ and $\bar{\gamma}_{2_{ij}}$ and into (2.29) and (2.31) for OSTBC and MRC MIMO systems, the desired results are finally obtained.

2.4 Simulation Results

In the previous sections, we have presented the underlying framework of our work in terms of closed form expressions and models for various quantities. Now in this section, we will utilize those models to evaluate error rate for different modulation techniques. Firstly, BER is evaluated for BPSK, QPSK and 16-QAM modulation techniques with STBC and MRC over different fading channels such as Rayleigh, Rician, Nakagami-*m* and Weibull channel. BER is computed for Rayleigh fading, two distinct values of rice factor K over Rician fading and different values of m over Nakagami-*m* fading channels with OSTBC ($N_t = 2, N_r = 1$) and MRC ($N_t = 1, N_r = 2,4$), where $m \geq 0.5$. BER for MIMO system using BPSK, QPSK and 16-QAM with Alamouti STBC are shown in Fig. 2.5, Fig. 2.6 and Fig. 2.7 under different channel conditions such as Rayleigh, Rician and Nakagami-*m*

respectively. Also, BER performance with MRC under same scenario as chosen in Alamouti STBC is depicted in Fig. 2.8, Fig. 2.9 and Fig. 2.10.

We have evaluated the BER performance at 6dB SNR and find that minimum error rate of 0.02385 is obtained for BPSK in Rayleigh fading with STBC ($N_t = 2, N_r = 1$). However, 65.5% less BER is achieved using receiver diversity i.e. MRC ($N_t = 1, N_r = 2$) compared to that of STBC, for the same modulation technique. For rice factor K=1 of Rician channel, BER of 0.01755 is obtained for BPSK with STBC and 70.6% reduced BER is achieved with MRC ($N_t = 1, N_r = 2$), than that of STBC. Increasing the value of K from 1 to 6, error rate performance also improves. When the number of receiver antennas are increased from 2 to 4, 0.00001 BER is obtained. For Nakagami-m channel, we get reduced BER at a higher value of m and vice versa. Therefore, 0.05262 BER for m=0.5 and 0.00729 BER for m=3 is obtained with STBC as well as 46% and 88.6% reduced BER is achieved with MRC ($N_t = 1, N_r = 2$) compared to STBC ($N_t = 2, N_r = 1$) using BPSK for m=0.5 and m=3 respectively. In MRC, less BER is obtained for K=6 than K=1 using lower order modulation (BPSK) compared to QPSK and 16-QAM. We observe from the simulation results that high values of m require low SNR and its severity decreases progressively as m increases and BER performance is same as Rayleigh fading for Nakagami-m shape parameter m=1. Consequently, MRC offers nearly 3dB improved BER performance than STBC.

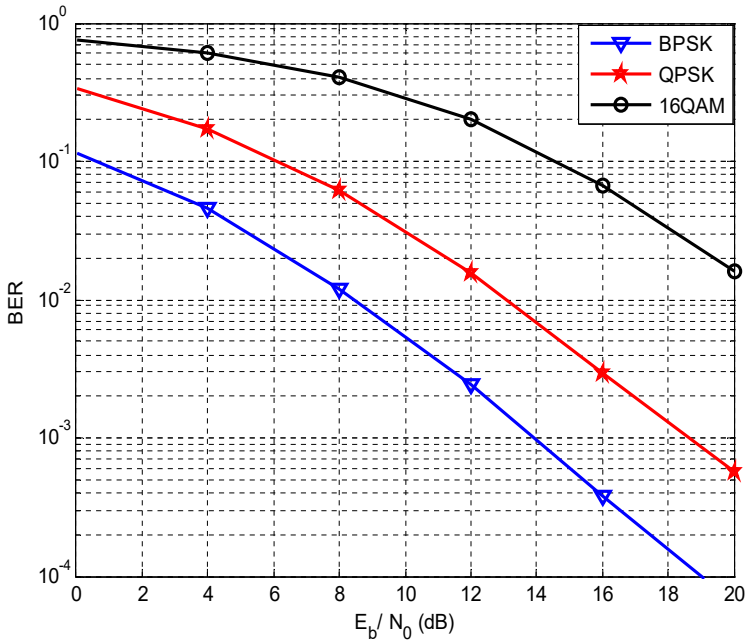

Fig. 2.5 BER for STBC using BPSK, QPSK and 16-QAM over Rayleigh Channel ($N_t = 2, N_r = 1$)

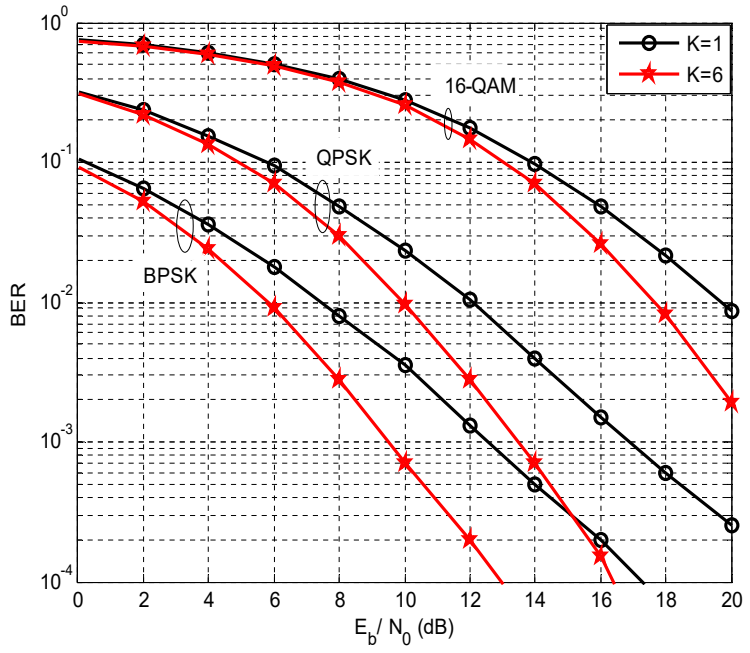

Fig. 2.6 BER for STBC using BPSK, QQPSK and 16-QAM over Rician Channel for K=1, 6 ($N_t = 2$, $N_r = 1$)

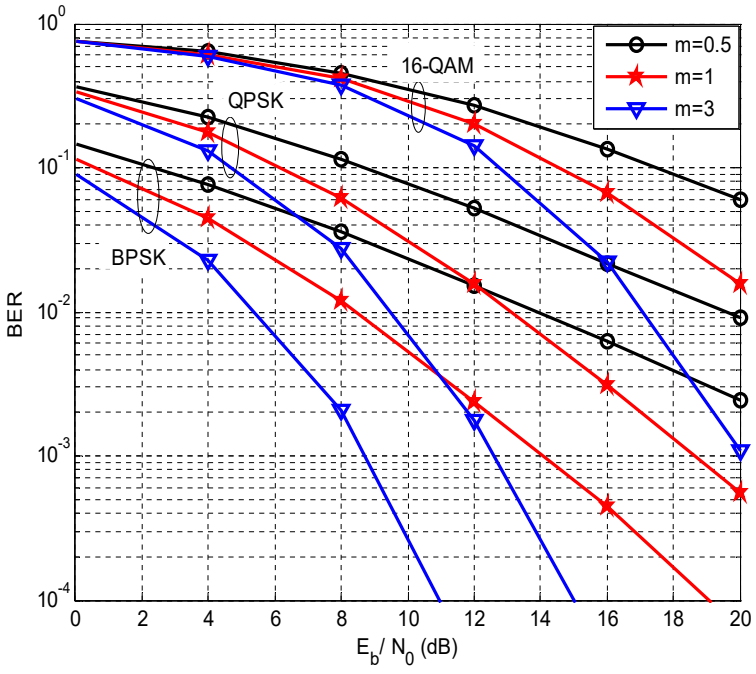

Fig. 2.7 BER for STBC using BPSK, QPSK and 16-QAM over Nakagami-m channel for m=0.5, 1, 3 and instantaneous power Ω =1dB, ($N_t = 2$, $N_r = 1$)

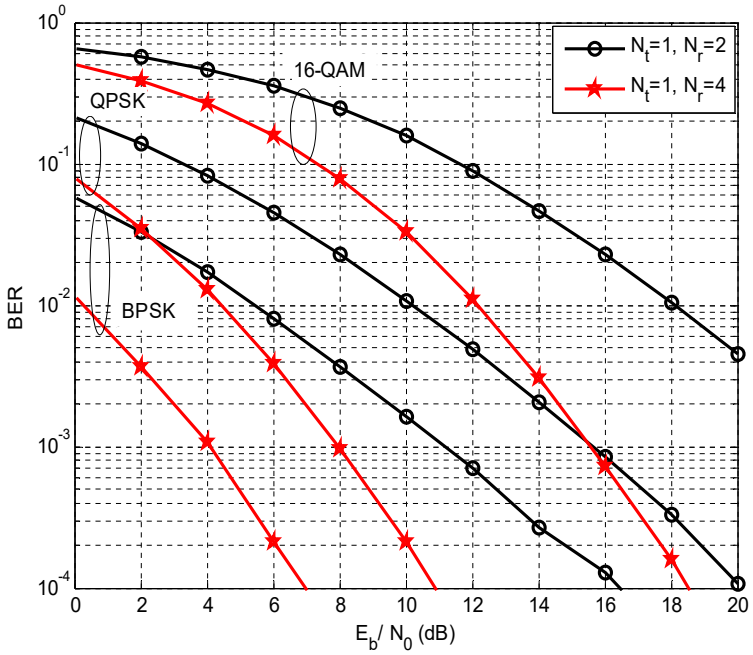

Fig. 2.8 BER for MRC using BPSK, QPSK and 16-QAM over Rayleigh Channel with ($N_t = 1$, $N_r = 2$) and ($N_t = 1$, $N_r = 4$)

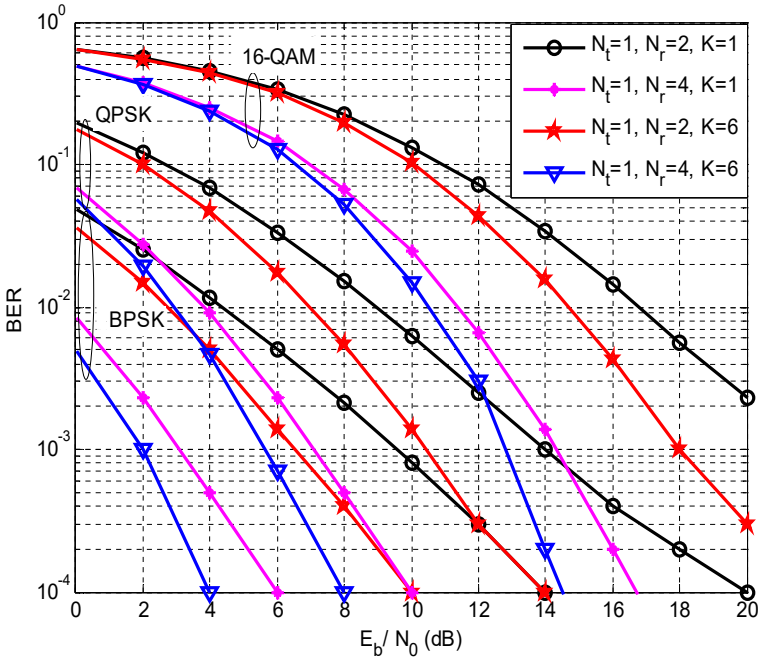

Fig. 2.9 BER for MRC using BPSK, QPSK and 16-QAM over Rician Channel for K=1, 6 with ($N_t = 1$, $N_r = 2$) and ($N_t = 1$, $N_r = 4$)

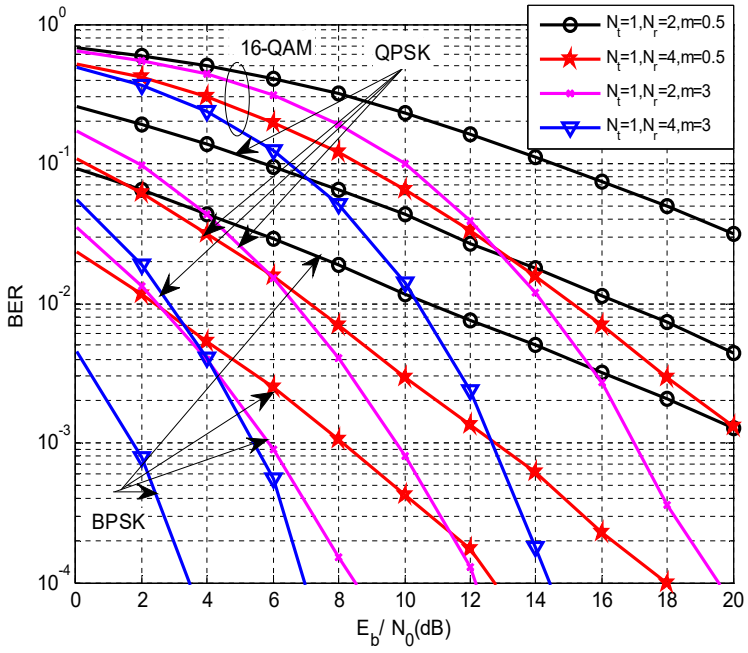

Fig. 2.10 BER for MRC using BPSK, QPSK and 16-QAM over Nakagami-m channel for m=0.5, 1, 3 and Ω =1dB with ($N_t = 1, N_r = 2$) and ($N_t = 1, N_r = 4$)

Considering $N_r = 4$ in MRC, less BER is obtained compared to $N_r = 2$. The higher order modulation techniques are significantly less flexible to noise and interference but the use of these modulation can obtain the high data rate of a link. Our simulation results show that for high modulation orders, BER performance is degraded. Thus, when channel conditions are worst, we use the energy efficient modulation techniques e.g., BPSK and QPSK. As channel conditions improve, we prefer spectrally efficient modulation techniques like 16-QAM. Also, we analyze that BER performance improves by increasing the number of antennas. Therefore, to maximize the different diversity gain, different combinations of number of antennas at the transmitter and receiver side are chosen.

The generic forms of SER are given by (2.28) and (2.30) for both the applied diversity techniques in single and double-Weibull fading respectively when β_{ij} is replaced by β_i for MRC. After substituting the values of $\bar{\gamma}$, $\bar{\gamma}_{1_{ij}}$ and $\bar{\gamma}_{2_{ij}}$ and into (2.28) and (2.30) for OSTBC and MRC MIMO systems, the desired results are finally obtained. Then, SER is determined for MIMO-OSTBC ($N_r = 1, N_t = 2$) and MIMO-MRC ($N_r = 2, N_t = 1$) systems using BPSK, QPSK and 16-QAM modulation techniques over single and double-Weibull fading channel. Again, it is clear from Fig. 2.11 and Fig. 2.12 that MRC gives 3dB better error performance than OSTBC. MIMO-OSTBC

gives the maximum possible diversity order of $N_r N_t \beta$ in the absence of double scattering; however, $2N_r N_t \beta$ diversity order is achieved due to double scattering. Also, MIMO-MRC achieves the maximum offered spatial diversity order in double-Weibull fading. The selected values of β are 2, 3.5 and 7 to determine the system performance. As the value of β increases, severity of fading reduces which improves the error rate performance. At $\beta = 2$, Weibull distribution is transformed into Rayleigh distribution and hence, at this value of β, (2.28) and (2.30) illustrate the SER under Rayleigh and double-Rayleigh fading respectively. In addition, $\beta = 1$ converts Weibull distribution into exponential distribution. For all simulation, double Weibull fading is produced by multiplying two Weibull random variables, for OSTBC $\Omega_{ij} = \Omega_{1_{ij}} = \Omega_{2_{ij}} = 1$, for MRC $\Omega_i = \Omega_{1_i} = \Omega_{2_i} = 1$ and $R_c = 1$ bps are assumed. Here, MATLAB is used to depict simulation results and MAPLE is used to compute analytical results.

Fig. 2.11 to Fig. 2.14 justify the previously mentioned behaviour of higher and lower modulation orders and that behaviour signifies that BPSK ($a_m = b_m = 1$) and QPSK ($a_m = 2,\ b_m = 0.5$) modulation techniques are preferred for poor channel conditions. Consequently, for improved channel conditions, we prefer spectrally efficient 16-QAM ($a_m = 3,\ b_m = 0.1$).

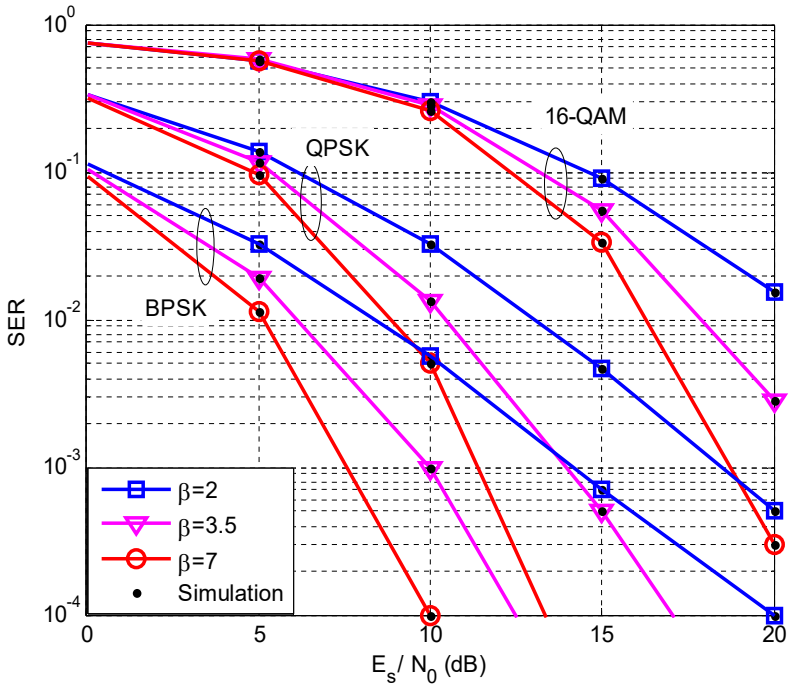

Fig. 2.11 SER for OSTBC ($N_r = 1, N_t = 2$) using BPSK, QPSK and 16-QAM over single-Weibull fading channel for β= 2, 3.5 and 7

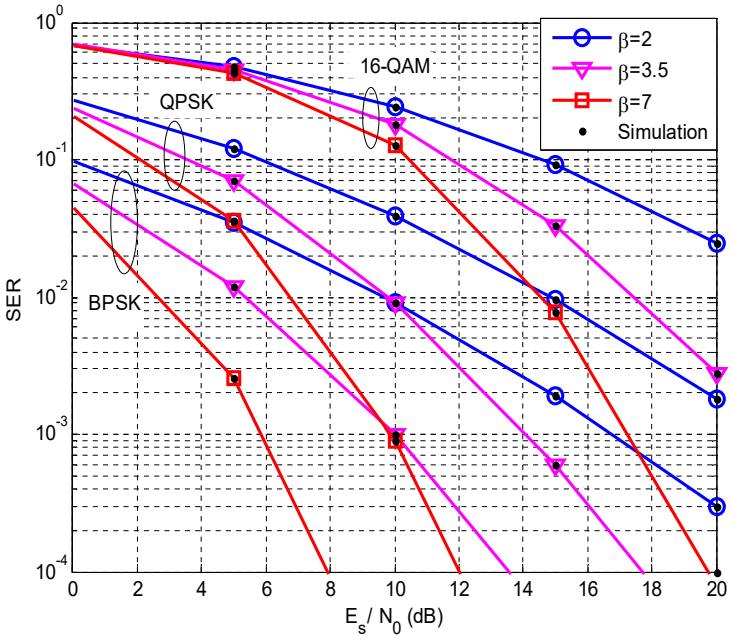

Fig. 2.12 SER for MRC ($N_r = 2, N_t = 1$) using BPSK, QPSK and 16-QAM over single-Weibull fading channel for β= 2, 3.5 and 7

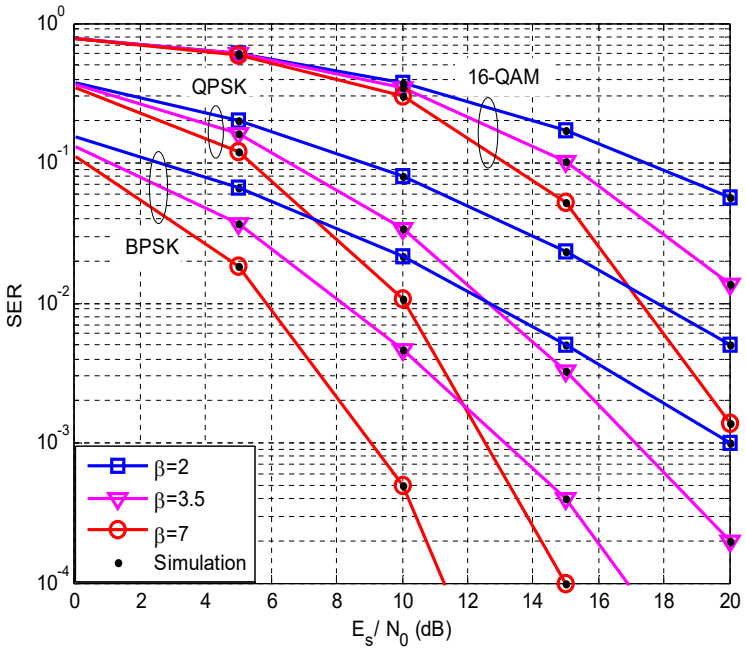

Fig. 2.13 SER for OSTBC ($N_r = 1, N_t = 2$) using BPSK, QPSK and 16-QAM over double-Weibull fading channel for β= 2, 3.5 and 7

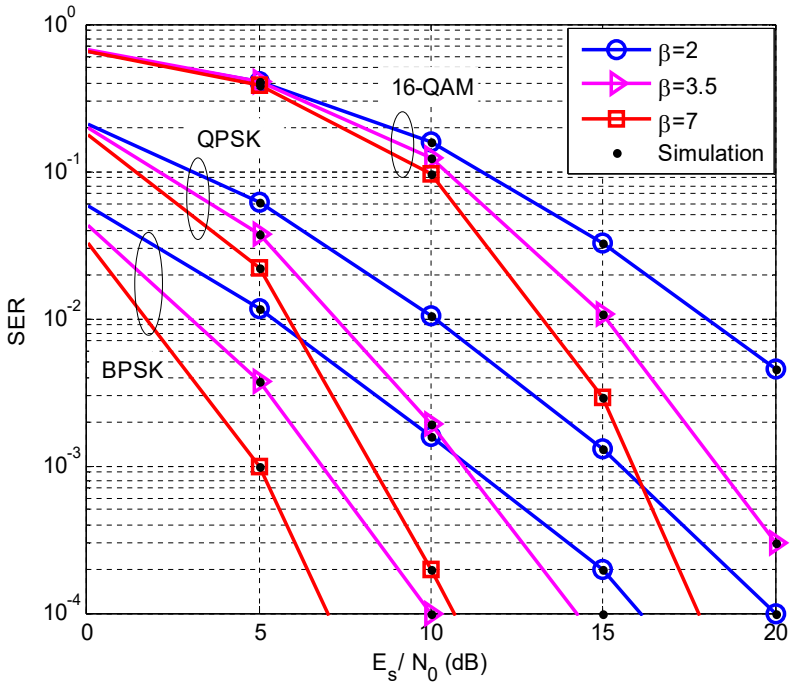

Fig. 2.14 SER for MRC ($N_r = 2, N_t = 1$) using BPSK, QPSK and 16-QAM over double-Weibull fading channel for β= 2, 3.5 and 7

We conclude from Fig. 2.11 to Fig. 2.13 that double-Weibull fading degrades the system error rate performance. The results illustrate that to obtain an error rate of 10^{-2} for BPSK at $\beta = 2$, additional 4.5dB SNR is required in double-weibull fading. Consequently, by increasing β from 2 to 7, additional 0.9dB SNR is required in double-Weibull fading. Using higher order modulation (i.e. 16-QAM), 4dB and 1dB less SNR is required at $\beta = 2$ and 7 respectively in single-Weibull fading as compared to double-Weibull fading. Hence, at higher order modulation, double-Weibull channel model performs better as compared to lower order modulation and at large value of β, additional required SNR is small. Finally, it is observed that the analytical results show good estimation to simulation results.

2.5 Conclusion

In this chapter, we evaluated the performance of employing STBC in the MIMO system over different fading channels such as Rayleigh, Rician, Nakagami-*m*, Weibull when receiver used MRC diversity. Then, Weibull channel model is used to analyze the MIMO system performance using the same diversity techniques. These systems are used to evaluate SER in single and double-Weibull fading environment. Due to energy efficient lower modulation order techniques (BPSK and QPSK),

our results demonstrate that MRC with lower modulation order always leads to low error rate. Consequently, for the same error rate, less SNR is required for BPSK and QPSK than 16-QAM. Thus, diversity techniques with digital modulation can be used in multiple antenna systems to improve the reliability and data rate. We conclude from the results that double-Weibull model degrades the error performance compared to that of the single-Weibull model. As the fading parameter increases for any modulation technique, the required SNR gap between single and double-Weibull fading decreases.

CHAPTER 3

MIMO Composite Weibull-Gamma Fading Channel Performance with Diversity and Different Detection Techniques

3.1 Introduction

In the previous chapter, we have analyzed MIMO system performance with OSTBC and MRC in various multipath fading and cascaded Weibull fading scenario. We have already discussed earlier that the shadowing also degrades the system performance. Thus, we have considered a composite channel model i.e. Weibull-gamma [109, 125] which takes into account the effects of both multipath fading and shadowing to evaluate the MIMO system performance using appropriate diversity and detection techniques. However, we have to keep in mind that there is a tradeoff between diversity and multiplexing as shown in Fig. 3.1. In NLoS MIMO systems, diversity gain d_g and transmission rate r has the relationship of $d_g(r) = (N_r - r)(N_t - r)$. According to this relation, transmission rate increases in bps/Hz over 3dB increase in SNR and correspondingly, BER reduces with $2 - d_g(r)$. Thus, it is impractical to increase the transmission rate with decreased BER [159]. Further, to determine the severity of fading in Weibull-gamma fading, it is necessary to define the amount of fading (AF) [160]. Thus, in this chapter, we have determined the AF in detail.

There is a trade-off between computational complexity and optimal performance in most of the detection techniques. One of the detection techniques which gives improved performance is OSIC with MMSE, however, it does not give optimal performance [161]. ML detection can achieve the optimal performance but at the expense of higher complexity level. Therefore, MMSE-OSIC with candidates ($OSIC^2$) detection is recommended as a solution in which a number of candidate vectors are selected for each layer [75]. MMSE- $OSIC^2$ gives a near ML performance with a complexity level comparable to that of traditional MMSE-OSIC. Therefore, we have considered this technique to enhance the error rate performance of MIMO system. We also presented a comparative analysis based on MMSE-OSIC and ML detection and measured the system complexity in terms of a number of mathematical operations.

The work proposed in [125] paved the way our work. Since the statistical characterization of MIMO-WG fading channel has not been completely explored in the reported literature. Therefore, WG channel model is taken into consideration for the system performance analysis.

In this chapter, WG channel is used with OSTBC and MRC for analyzing the MIMO system performance. Although MRC gives the superior error rate performance compared to that of other receiver combining techniques, OSTBC is less complex than MRC. Due to mathematical simplicity, we used CDF based approach to evaluate the SER performance for the proposed system design. Exact analytical expressions for SER are calculated in terms of Meijer-G function. As higher order modulation techniques offer high data rates, hence, 16-PSK and 16-QAM are used to analyze the system performance. This chapter also evaluates the error performance of spatial multiplexed (SM) MIMO systems with different detection techniques such as MMSE-OSIC, ML and MMSE-OSIC^2 in a composite Weibull-gamma (WG) fading environment [154]. Consequently, the dominating effects of fading and shadowing with their small parameters values as well as the mitigating effects by varying their parameters values are demonstrated.

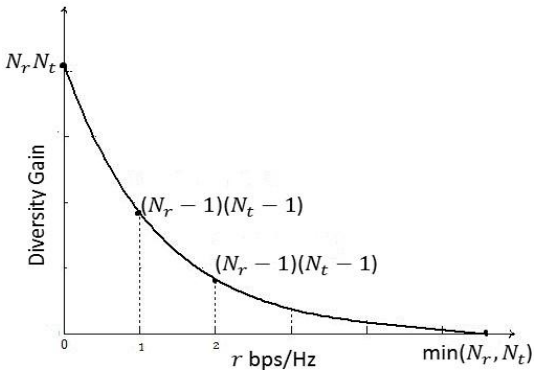

Fig. 3.1 Spatial diversity-spatial multiplexing tradeoff

This chapter has been organized as follows. Section 3.2 describes the MIMO system and channel model. AF for WG channel is explained in Section 3.3. We present analytical and simulation results for SER in Section 3.4. Finally, Section 3.5 concludes the chapter.

3.2 System and Channel Model

The same system configuration is considered in this chapter as mentioned in Chapter 2. Here, H is considered to model the effects of small-scale and large-scale fading known as the WG fading channel. This channel matrix is given by $H = \sqrt{g/d^{\vartheta}}H_w$. Here, g denotes i.i.d. gamma random variable ($g = E[x^2]$ in which x is Weibull random variable), d is the distance between transmitter and receiver and ϑ is the path loss exponent and each entry of matrix H_w follows an i.i.d Weibull PDF. In [109], WG composite PDF is calculated from (1.33) and (1.35) through conditional PDF

$$p(x) = \int_0^{\infty} p\,(x/y)p_y(y)dy \tag{3.1}$$

WG PDF is given in terms of Meijer-G function and given as [109]

$$p_X(x) = \frac{\beta x^{\beta-1}}{\Gamma m}\left[\frac{\left(1+\frac{2}{\beta}\right)}{\Omega}\right]^{\frac{\beta}{2}} \frac{k^{\frac{1}{2}}\ell^{k-\frac{\beta+1}{2}}}{(2\pi)^{\frac{\ell+k}{2}-1}} G_{0,k+\ell}^{k+\ell,0}\left(\frac{[x^2\Gamma(1+2/\beta)]^{\ell}}{\Omega^{\ell}\ell^{\ell}k^{k}}\Big|_{b_{k+\ell}}\right) \tag{3.2}$$

where $\Omega = E[g^2], b_{k+\ell} = 1-\Delta(k,1), 1-\Delta(\ell, 1-m+\beta/2), \frac{\ell}{k} = \frac{\beta}{2}, \Delta(u,v) = \frac{v}{u}, \frac{v+1}{u}, \ldots, \frac{v+u-1}{u}$, ℓ and k are positive integers.

The consequent power PDF of WG fading is given in [125] as

$$p(\gamma) = \frac{\beta^{m-\frac{\beta-1}{2}} m^{\beta/2}}{\sqrt{2}\sqrt{2\pi}^{\beta}\Gamma m}[\Gamma(1+2/\beta)]^{\beta/2} \frac{\gamma^{\frac{\beta}{2}-1}}{\overline{\gamma}^{\beta/2}} G_{0,\beta+2}^{\beta+2,0}\left[\left(\frac{1}{4}\left(\frac{m\Gamma(1+2/\beta)}{\beta\overline{\gamma}}\right)^{\beta}\gamma^{\beta}\Big|1/2,0,\Delta(\beta, m-\beta/2)\right)\right] \tag{3.3}$$

For $m\to\infty$, the WG distribution approximates Weibull distribution. Using [19, Equation (9.34.3)], for $\beta = 2$, it follows *K* or Rayleigh-lognormal distribution. For $\beta = 2$, $m\to\infty$, it approaches Rayleigh distribution and for $\beta\to\infty$, $m\to\infty$, it approaches AWGN distribution. Weibull and gamma random variables are independent of each other. Table 3.1 shows the special cases of WG fading channel distribution.

Table 3.1 WG Fading Distribution

Parameter Values	Channel Distribution
$m \to \infty$	Weibull
$\beta = 2$	*K* or Rayleigh-lognormal
$\beta = 2, m \to \infty$	Rayleigh
$\beta = \infty, m \to \infty$	AWGN

Substituting (3.2) in the expression of the n-th order moments of X, and using [162, Equation (7.811/4)], a closed form expression can be represented as

$$\mathrm{E}[x^n] = \frac{\beta}{2}\left[\frac{\Gamma(1+2/\beta)}{\Omega}\right]^{-n/2} \frac{k^{\frac{n}{\beta}+3/2}\ell^{k+\frac{n}{2}-3/2}}{(2\pi)^{\frac{\ell+k}{2}}\Gamma(m)} \prod_{j=1}^{k+\ell}\Gamma\left(b_j + \frac{\beta+n}{2\ell}\right) \tag{3.4}$$

Furthermore, after some mathematical formulations in (3.4), n-th moment is given as [109]

$$\mathrm{E}[x^n] = \frac{\Gamma\left(1+\frac{n}{\beta}\right)\Gamma\left(m+\frac{n}{2}\right)}{\Gamma m}\left[\frac{\Gamma\left(1+\frac{2}{\beta}\right)}{\Omega}\right]^{-\frac{n}{2}} \tag{3.5}$$

The SNR per received symbol is expressed as, $\gamma = X^2\rho$, where $\rho = E_s/N_0$ is symbol energy to noise ratio. The average SNR is given as $\bar{\gamma} = \rho\|H\|^2 = \Omega N_t N_r m\rho$, by taking n=2 in (3.5). Moreover, CDF of γ is also computed and given in [109] as

$$F_\gamma(\gamma) = \left(\frac{\Gamma\left(1+\frac{2}{\beta}\right)}{\frac{\bar{\gamma}}{m}}\right)^{\frac{\beta}{2}} \frac{\beta k^{\frac{1}{2}} \ell^{m-\frac{\beta+3}{2}} \gamma^{\frac{\beta}{2}}}{2\Gamma m\left(\sqrt{2\pi}\right)^{\ell+k-2}} G_{1,k+\ell+1}^{k+\ell,1}\left(\frac{\left[m\Gamma\left(1+\frac{2}{\beta}\right)\gamma\right]^{\ell}}{(\bar{\gamma}\ell)^{\ell} k^{k}}\middle|_{b_{k+\ell},-\frac{1}{k}}^{1-\frac{1}{k}}\right) \tag{3.6}$$

3.3 Amount of Fading (AF)

For a particular channel model, the severity of fading can be determined by AF [87, 163]. Authors [34, 164] defined AF for various multipath and shadow faded channels such as Rayleigh, Weibull, Nakagami-m, *GK* fading channel. We computed AF for WG that shows the degree of fading practiced at the output of a MIMO system and represented by

$$\text{AF} = \frac{\text{Var}[x^2]}{(\text{E}[x^2])^2} = \frac{(m+1)\Gamma(1+4/\beta)}{m\Gamma(1+2/\beta)^2} - 1 \tag{3.7}$$

where $\text{Var}[.]$ denotes variance.

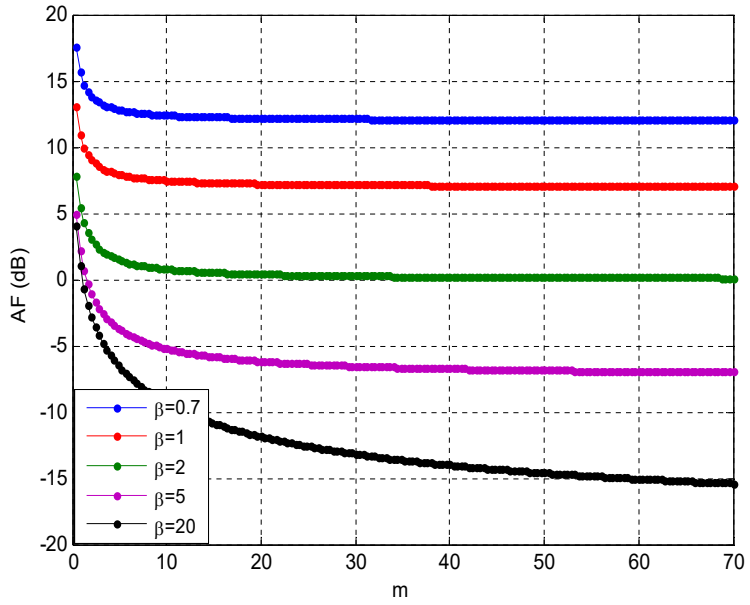

Fig. 3.2 The amount of fading for WG fading

In Fig. 3.2, AF is shown for different values of β in terms of m. AF decreases exponentially as the value of β and/or m increases. The channel performance is degraded for small values of m and β i.e., $m\in$ [0, 1] and $\beta\in$ [0, 1.5]. After a certain limit, AF does not change with both the fading

parameters (m,β) and attains a constant value. At m =1, AF is 15.13dB, and 0.124dB when β is 0.7 and 20 respectively. Numerically, 99.18 % reduction in AF is possible due to high β.

The OSTBC and MRC have already been discussed in Chapter 2, and they are employed to enhance the system performance in WG fading in next section.

3.4 Symbol Error Rate Analysis

3.4.1 MIMO OSTBC and -MRC System

Using (2.27) and substituting (3.2) into (2.27), setting the value of γ_o according to (2.6) and after some mathematical computation, the appropriate SER expression for proposed OSTBC-MIMO system is achieved using [162, Equation (7.813.1)]

$$\mathrm{SER_o}(\rho) = \sum_{i=1}^{N_t}\sum_{j=1}^{N_r}\frac{a_m b_m}{2\sqrt{\pi}}\frac{2^{\frac{1}{2}-\frac{1}{\ell}+\frac{1-\beta_{ij}}{2\ell}}}{\left(\frac{R_c d^{\vartheta} N_t \Gamma\left(1+\frac{2}{\beta_{ij}}\right)}{\Omega_{ij} m_{ij}\rho}\right)^{\frac{\beta_{ij}}{2}}}\frac{k^{\frac{1}{2}}\ell^{m_{ij}-\frac{\beta_{ij}+3}{2}-1}}{2\Gamma m_{ij}\left(\sqrt{2\pi}\right)^{\ell+k-2}}$$

$$\times G_{2,k+\ell+1}^{k+\ell,2}\left(\frac{\left[R_c\, d^{\vartheta} N_t m_{ij}\Gamma\left(1+{}^{2}/_{\beta_{ij}}\right)\right]^{\ell}}{\left(\Omega_{ij} m_{ij}\rho\ell\right)^{\ell} k^{k} b_m}\middle|_{b_{k+\ell},-\frac{1}{k}}^{1-\frac{1}{\ell}-\frac{\beta_{ij}-1}{2\ell},1-\frac{1}{m_{ij}}}\right) \quad (3.8)$$

Similarly, substituting the value of γ_{MRC} according to (2.23), SER for MIMO-MRC system over WG fading [165] is represented as

$$\mathrm{SER_M}(\rho) = \sum_{i=1}^{N_t}\sum_{j=1}^{N_r}\frac{a_m b_m}{2\sqrt{\pi}}\frac{2^{\frac{1}{2}-\frac{1}{\ell}+\frac{1-\beta_j}{2\ell}}}{\left(\frac{\Gamma\left(1+\frac{2}{\beta_j}\right)}{\Omega_{\mathrm{j}} m_j\rho}\right)^{\frac{\beta_j}{2}}}\frac{k^{\frac{1}{2}}\ell^{m_j-\frac{\beta_j+3}{2}-1}}{2\Gamma m_j\left(\sqrt{2\pi}\right)^{\ell+k-2}}$$

$$\times G_{2,k+\ell+1}^{k+\ell,2}\left(\frac{\left[m_j\Gamma\left(1+{}^{2}/_{\beta_j}\right)\right]^{\lambda}}{\left(\Omega_{\mathrm{j}} m_j\rho\ell\right)^{\ell} k^{k} b_m}\middle|_{b_{k+\ell},-\frac{1}{k}}^{1-\frac{1}{\ell}-\frac{\beta_j-1}{2\ell},1-\frac{1}{m_j}}\right) \quad (3.9)$$

The analytical results for SER are obtained using (3.8) and (3.9). These expressions are valid for an arbitrary number of antenna configurations and arbitrary fading environments. Although spatial multiplexing improves the capacity performance, error rate performance can be enhanced using appropriate detection technique. Thus, we applied the following detection techniques to improve the error rate performance.

3.5 Detection Techniques

3.5.1 Minimum Mean-Square Error-Ordered Successive Interference Cancellation (MMSE-OSIC) Detection

MMSE detection technique maximizes the post-detection signal-to-interference plus noise-ratio (SINR) due to minimized mean-square error (MSE). OSIC enhances the performance of linear detection technique by maximizing SINR, therefore, SINR based ordering is preferred. This technique requires the low hardware complexity and includes a number of linear receivers. Each receiver determines one of the parallel data streams with detected signal components those are successively canceled from the received signal at each stage [166].

The MMSE detection technique provides the 1-st estimated stream with the 1-st row vector of the MMSE weight matrix W_{MMSE} [24], expressed as

$$W_{MMSE} = (H^{\dagger}H + N_0 I)^{-1} H^{\dagger} \tag{3.10}$$

In MMSE detection, the statistical information of N_0 is essential. The i-th row vector $w_{i,MMSE}$ of W_{MMSE} is represented as

$$w_{i,MMSE} = \underset{w=(w_1, w_2, \ldots . w_{N_t})}{\arg\max} \frac{|wh_i|^2 E_s}{\sum_{j=1, j\neq i}^{N_t} E_s |wh_i|^2 + N_0 \|w\|^2} \tag{3.11}$$

where h_i is the i-th column vector of the channel matrix. Consider, the i-th order detected symbol $x_{(i)}$ which is based on the order of detection. Hence, $x_{(i)}$ can be different from the transmit signal at the i-th antenna. A sliced value of $x_{(i)}$ is represented by $\hat{x}_{(i)}$. The remaining signal is achieved by

$$\tilde{Y} = Y - \sum_{j=1}^{i-1} \hat{x}_j \, h_j \tag{3.12}$$

It is assumed that $\hat{x}_j, j = 1, 2, \ldots . , i-1$ is precisely obtained. To estimate $x_{(2)}$, the interference is canceled when $x_{(1)} = \hat{x}_{(1)}$. However, error propagation arises when $x_{(1)} \neq \hat{x}_{(1)}$. The detection order and the erroneous outcomes that arises in the previous stages affect the overall performance of OSIC detection which results error propagation.

Primarily, signals having a higher post-detection SINR are detected. The linear MMSE detection with the post-detection SINR is given as

$$\text{SINR}_i = \frac{E_s \left| w_{i,MMSE} \, h_i \right|^2}{\sum_{n\neq i} E_s \left| w_{i,MMSE} \, h_n \right| + N_0 \left\| w_{i,MMSE} \right\|^2}, \; i = 1,2, \ldots \ldots , N_t \tag{3.13}$$

Using W_{MMSE}, N_t SINR values are calculated, after that, the corresponding layer with the highest SINR is chosen. The second-detected symbol is chosen by canceling the interference due to first detected symbol from the received signals. Here, $W_{MMSE}^{(i)}, i = 1,2, \dots N_t$. If n-th symbol is canceled first, then H of (3.9) is converted into (3.13) by deleting the channel gain vector as per n-th symbol

$$H^{(n)} = [h_1\, h_2 \dots\dots h_{n-1}\, h_{n+1} \dots\dots h_{N_t}] \text{ and } W_{MMSE}^{(i)} = \left(H_i^{\dagger} H_i + N_0 I\right)^{-1} H_i^{\dagger} \tag{3.14}$$

W_{MMSE} is again computed after changing H of (3.10) by (3.14). Then, we compute $N_t - 1$ SINR values (i.e.,$(\text{SINR}_i)_{i=1, i\neq n}^{N_t}$) by selecting the symbol having highest SINR. After canceling the next symbol with the highest SINR, the same procedure is pursued with the remaining signals. Total number of calculated SINR values is given by $\sum_{j=1}^{N_t} j = N_t(N_t + 1)/2$.

The diversity order of the i-th detected stream is approximately $N_r - N_t + i, (i = 1,2, \dots, N_t)$ in MMSE-OSIC detection assuming that the accurate symbols are detected previously.

3.5.2 Maximum Likelihood (ML) Detection

ML detection computes the Euclidean distance between the received signal vectors with respect to the product of all possible transmitted signal vectors and H. The minimum distance among all the distances is computed and the estimated X with ML detection is obtained as

$$\hat{X}_{ML} = \arg \min_{X \in {C_P}^{N_t}} \|Y - HX\|^2 \tag{3.15}$$

where C_P denotes a set of symbol constellation signal points. The ML technique offers the optimal performance similar to the maximum a posteriori (MAP) detection when all the transmitted vectors are equally likely. However, its complexity increases exponentially for higher order of modulation and large N_t. Here, $|C_P|^{N_t}$ amount of ML metric calculation is required. Although, this technique gives the superior performance as compared to MMSE-OSIC, it leads to higher computational complexity as well [167].

3.5.3 Minimum Mean-Square Error-Ordered Successive Interference Cancellation with Candidates (MMSE-OSIC^2) Detection

MMSE-OSIC^2 detection selects a set of candidates at each layer. N_t stages are considered in MMSE-OSIC^2 detection like MMSE-OSIC. We select $\mathcal{M}$ candidate vectors of length N_t at N_t stages like QRM-MLD detection [71]. To facilitate the detail of this procedure, the optimal ordering of N_t is assumed. Accordingly, $\mathcal{M}$ selected candidates of matrix size $N_t \times 1$ are measured. The ordering is based on the channel matrix $\|h_k\|^2, k = i, i + 1, \dots \dots N_t$. Temporary vector $\mathcal{M} \times |C_P|$ is generated.

The $\mathcal{M}$ candidate vectors are applicable for transmit signal vectors with size $(N_t - 1) \times 1$ in $s_i{-}1$ as acquired in the $(i{-}1)$-th stage. From Y in (1.4), the interference is subtracted from each candidate vector in $\mathrm{s}_i - 1\ (j), j = 1,2..\mathcal{M}$ and similar to the first stage, every constellation point of C_P is intended to x_i by means of the MMSE-OSIC technique.

Then, $\mathcal{M} \times |C_P|$vectors of length N_t are obtained. After that, $\mathcal{M}$ candidate vector of length N_t is selected. Subsequently, truncation is obtained in $\mathcal{M}$ candidate vectors of length i. In OSIC^2 technique, unlike QRM-MLD detection, the ML metric values are used according to depth-first search to select candidate vectors. Hence, the MMSE-OSIC^2 technique is a mixture of depth-first search and breadth-first search algorithms. Unlike the QRM-MLD, the small value of $\mathcal{M}$ is chosen in MMSE-OSIC^2 detection to achieve near ML performance [75]. A near-optimal performance can be achieved with less complexity level with MMSE-OSIC^2 detection technique.

This technique is based on log likelihood ratio (LLR) computation. It is assumed that the entire transmitted symbol vectors are identical. The subset of vectors is $\mathrm{s}_{r,t} = \left[X = \mathrm{map}\left(b_{1,}b_{2\ldots\ldots}b_{N_t\log_2|C_P|}\right)\middle| X \in \mathrm{s}^{C_P}, b_r = t\right]$ and LLR computation can be expressed as

$$\mathcal{L}(b_r|Y) \approx \min_{X\in S_{r,0}}\|Y-HX\|^2 - \min_{X\in S_{r,1}}\|Y-HX\|^2 \tag{3.16}$$

The other decoding techniques hold the cases which contain $\mathrm{s}_{r,t} = \emptyset$. After the hard detection, such cases need some extra calculation or a fitting constant. In OSIC^2 detection, $s_{r,t}$ is continuously nonempty. This is due to the all possible constellation points those are likely x_i in the i-th stage. Consequently, we do not require any extra calculation to get the LLR values after a hard decision [75].

3.6 Simulation Results

Fig. 3.3 to Fig. 3.6 demonstrate the system performance with the consideration of $N_r \times N_t$ as $N_r = 1, N_t = 2,4$ for OSTBC and $N_r = 2,4, N_t = 1$ for MRC over WG fading channel to signify the suitability of proposed computation. More explicitly, in Fig. 3.3 and Fig. 3.4, SER is plotted for MIMO-OSTBC for numerous values of β and m using 16-PSK and 16-QAM respectively and it is clear that SER improves with the increase in ρ. Also, for higher values of β and m with a fixed ρ, SER performance increases. Consequently, improved SER is achieved by increasing N_t from 2 to 4. It is noted that for β=2, WG channel model approximates *K* channel model. Although, higher order modulation provides high data rate, 16-PSK and 16-QAM modulation techniques are used to analyze the system performance. The number of constellation points is same in both the modulation

techniques but 16-QAM gives improved error performance, it can be seen from Fig. 3.3 to Fig. 3.6. It is clearly depicted from the results that 16-PSK gives 3dB reduced error performance than 16-QAM. For 16-PSK, a_m =2, $b_m = 0.0381$ and for 16-QAM, $a_m = 3$, b_m= 0.1. For simulation, $\Omega = 1$ and $R_c = 1$ is considered.

Multipath is highly accountable to degrade the wireless system performance. However, the impact of shadowing also reduces the error rate performance of the wireless system. The reduced shadowing effect can be observed by high values of m. Here, four combinations of β and m are considered and SER performance is evaluated at these values. Note that the WG channel matrix H is created by the product of each entries of Weibull and gamma random variable. In Fig. 3.5 and Fig. 3.6, SER performance of MIMO-MRC system is evaluated with the same configurations and parameters as considered for OSTBC. It is analyzed from Fig. 3.3 to Fig. 3.6 that MRC ($N_r = 2,4, N_t = 1$) gives approximately 3dB enhanced SER performance than OSTBC ($N_r = 1, N_t = 2,4$). This 3dB loss is obtained due to the radiation of half energy by each transmit antenna to provide the total radiated power equivalent to one transmit antenna.

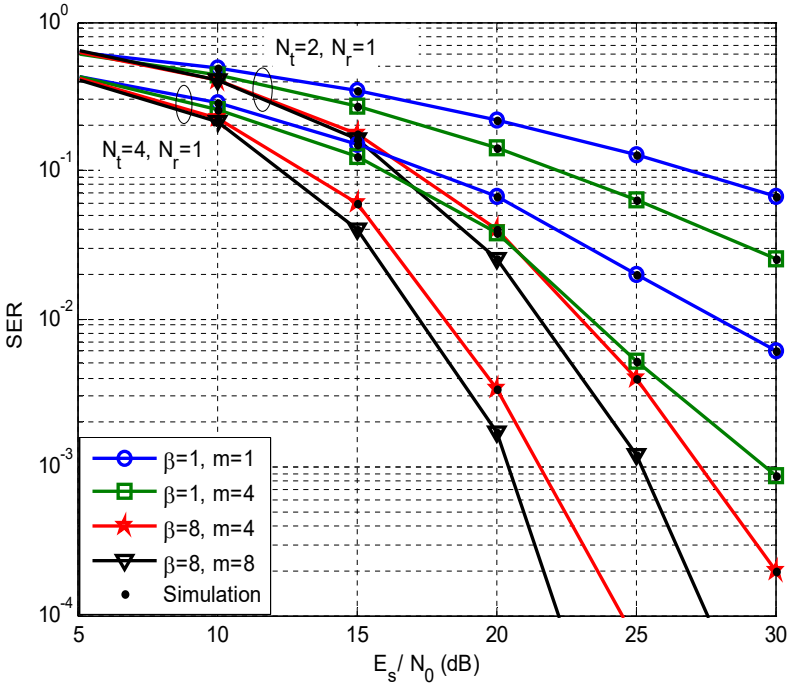

Fig. 3.3 SER for MIMO-OSTBC ($N_r = 1, N_t = 2,4$) systems using 16-PSK over WG fading channel

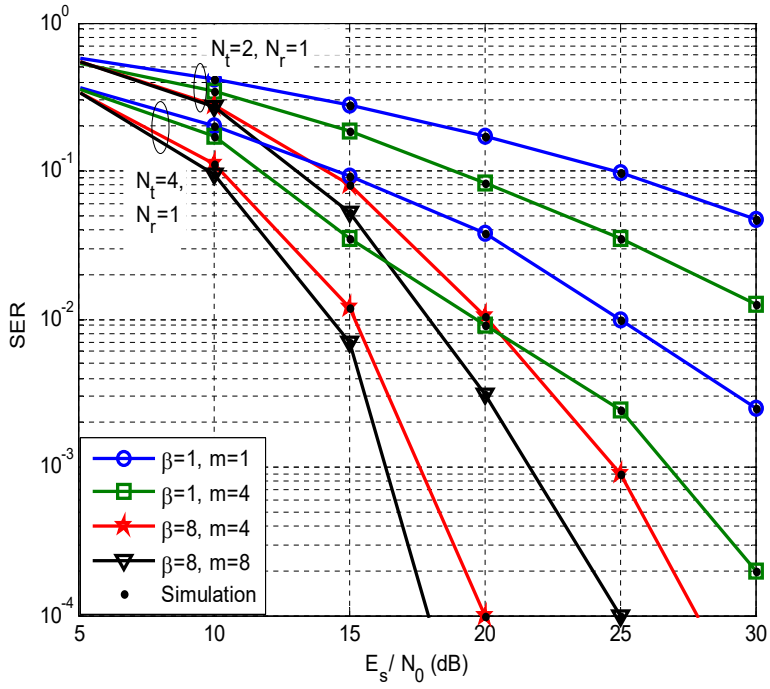

Fig. 3.4 SER for MIMO-OSTBC $(N_r = 1, N_t = 2,4)$ systems using 16-QAM over WG fading channel

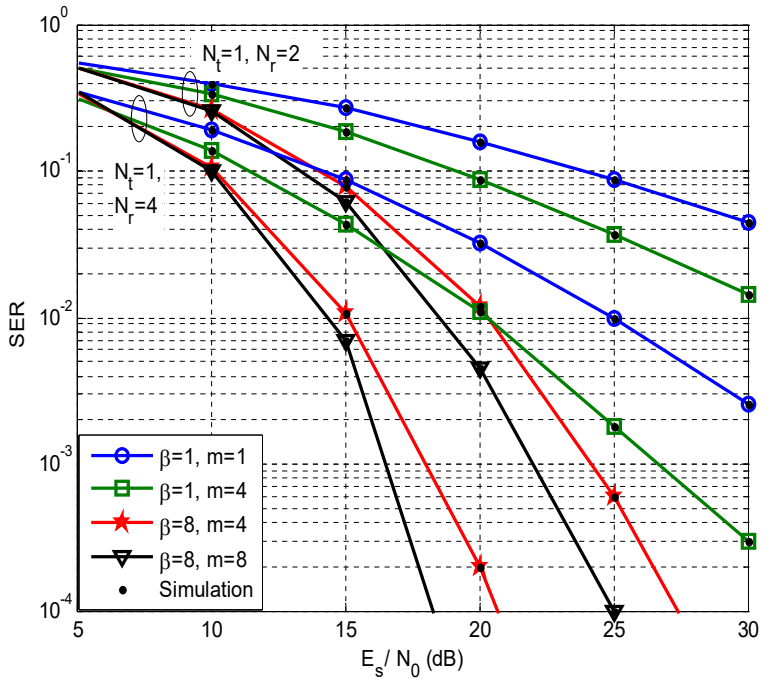

Fig. 3.5 SER for MIMO-MRC $(N_r = 2,4, N_t = 1)$ systems using 16-PSK over WG fading channel

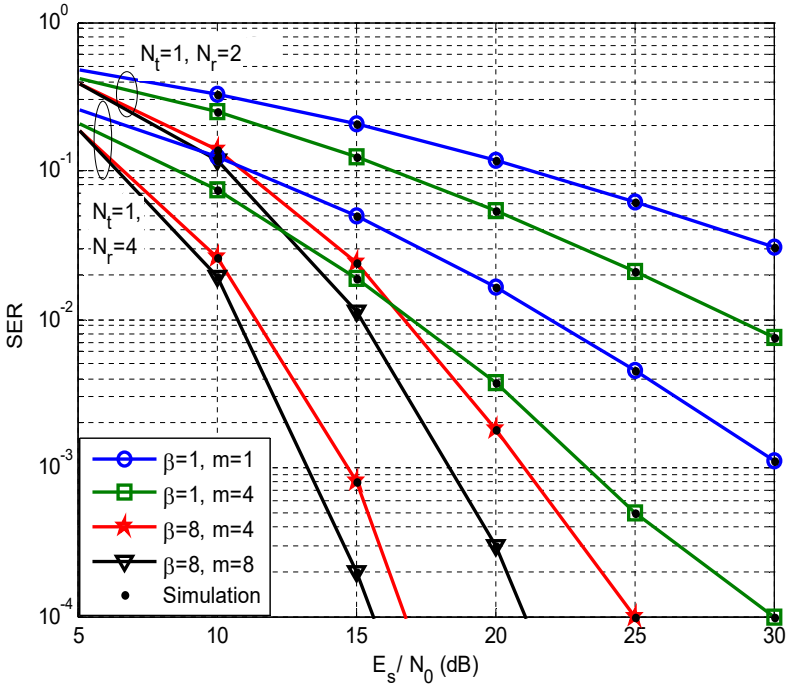

Fig. 3.6 SER for MIMO-MRC ($N_r = 2,4, N_t = 1$) systems using 16-QAM over WG fading channel

By changing the antenna configuration or increasing the number of antennas at transmitter and receiver end, SER performance can be highly improved but with the increased cost of the system.

Then, the MMSE-OSIC, ML and MMSE-OSIC^2 detection techniques are considered to improve the error performance of MIMO system. Distinct modulation techniques such as BPSK, QPSK and 16-QAM are used for performance evaluation. Fig. 3.7 shows the SER performance of the first layer ($i = 1$) with MMSE-OSIC detection which is based on SINR ordering. The SER performance is analyzed for $N_t = N_r = 2$ and 4 under WG fading scenario, where arbitrarily values of β and m are chosen. Three combinations of shape parameters ($\beta = 2, m = 1$), ($\beta = 1, m = 5$) and ($\beta = 5, m = 5$) are taken into consideration. The parameters considered for all simulation are identical. It is seen from Fig. 3.7 and Fig. 3.8 that less SNR is required in ML detection as compared to MMSE-OSIC detection. For higher values of β and m, error performance is improved. It is observed from the simulation results of Fig. 3.7, Fig. 3.8 and Fig. 3.9 that at large values of m, error performance is highly improved as compared to the large value of β. Fig. 3.7(b), Fig. 3.8(b) and Fig. 3.9(b) offer improved error rate performance due to increased number of antennas ($N_t = N_r$ =4) than Fig. 3.7(a), Fig. 3.8(a), Fig. 3.9(a) which are illustrated for $N_t = N_r$ =2.

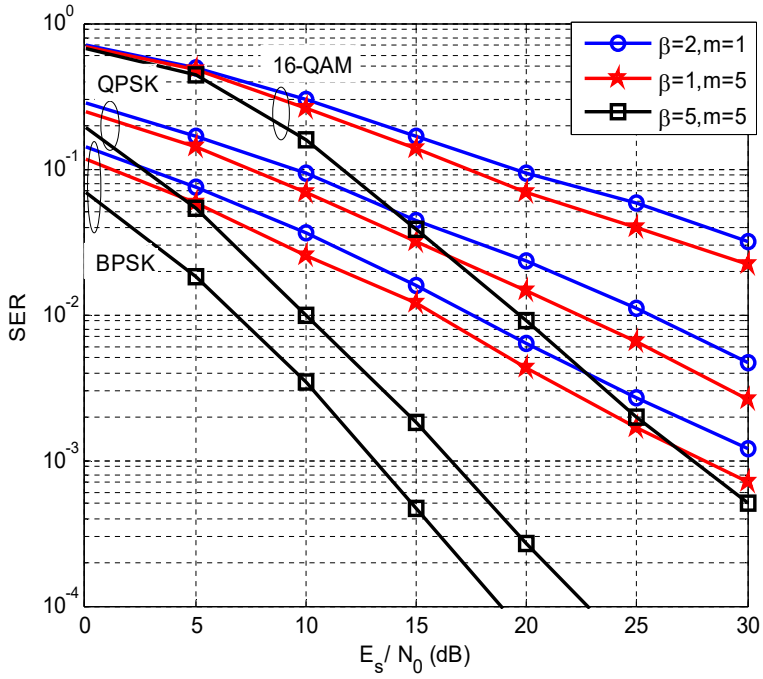

(a)

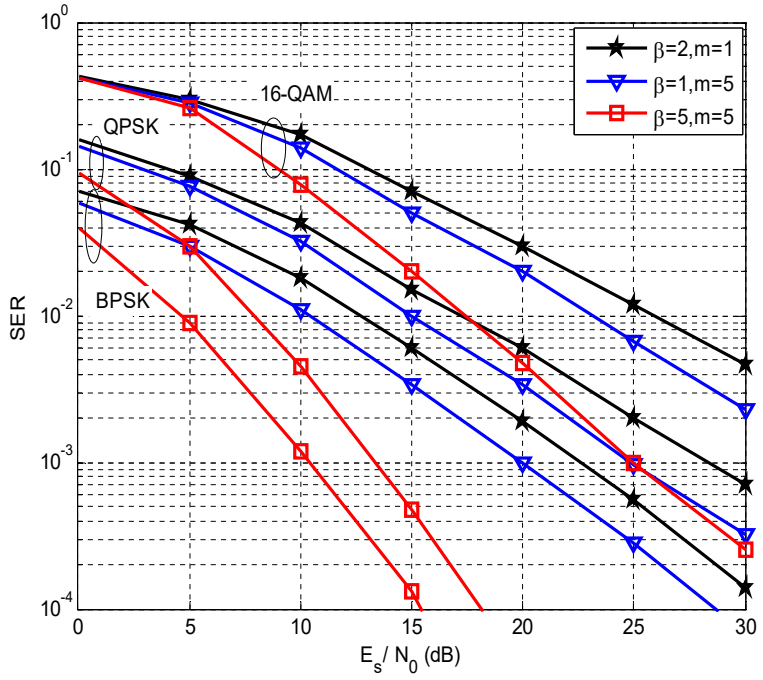

(b)

Fig. 3.7 SER of SM-MIMO system for BPSK, QPSK and 16-QAM using OSIC detection over WG fading channel when **(a)** $N_r = 2, N_t = 2$ **(b)** $N_r = 4, N_t = 4$

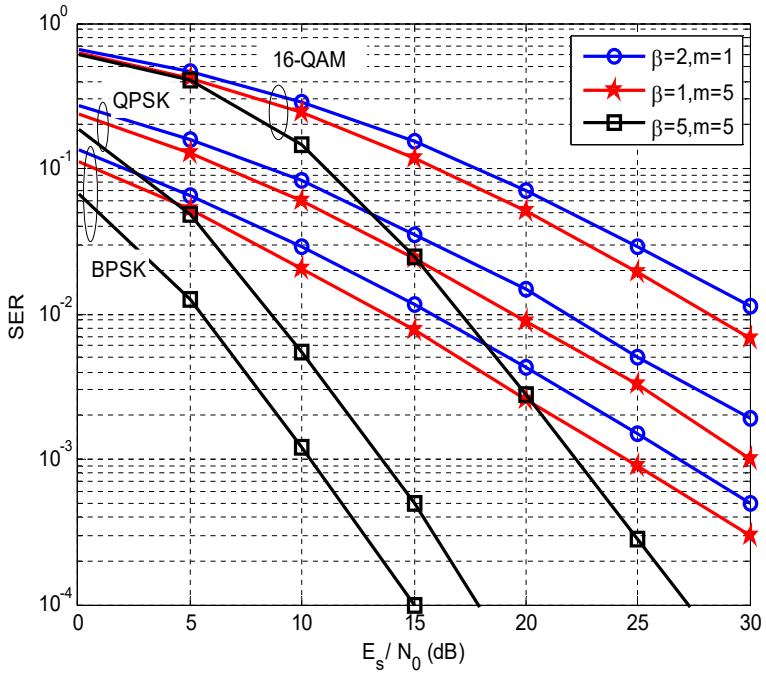

(a)

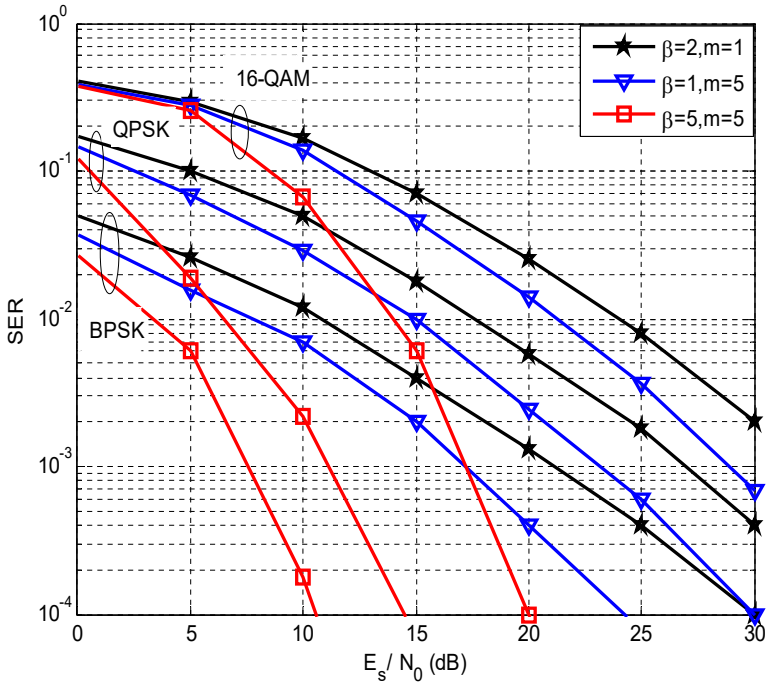

(b)

Fig. 3.8 SER of SM-MIMO system for BPSK, QPSK and 16-QAM using ML detection over WG fading channel when **(a)** $N_r = 2, N_t = 2$ **(b)** $N_r = 4, N_t = 4$

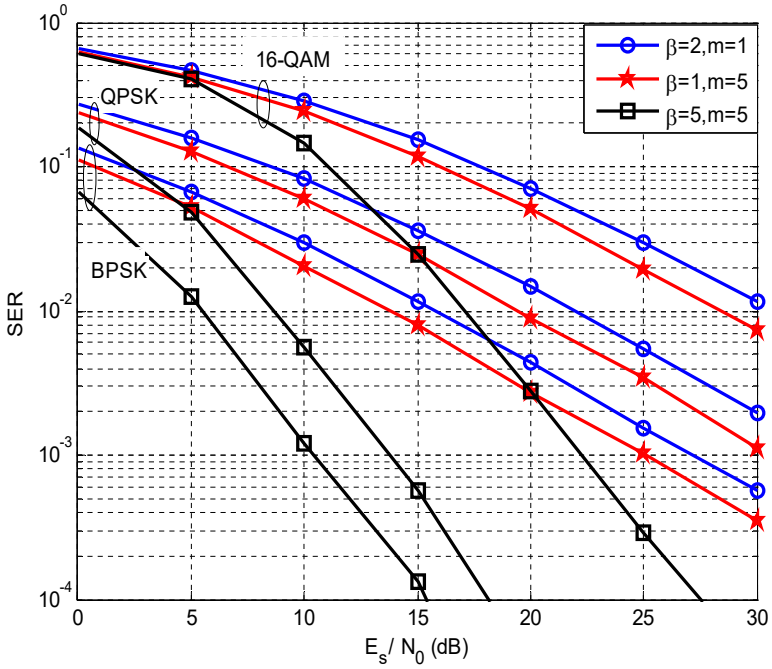

(a)

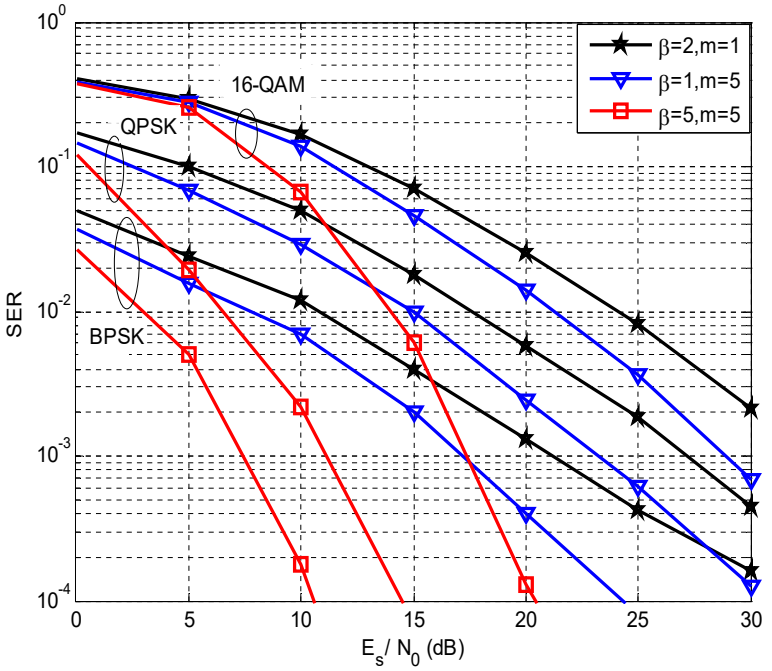

(b)

Fig. 3.9 SER of SM-MIMO system for BPSK, QPSK and 16-QAM using MMSE-OSIC[2] detection over WG fading channel for M=1 and **(a)** $N_r = 2, N_t = 2$ **(b)** $N_r = 4, N_t = 4$

In Fig. 3.9, MMSE-OSIC^2 detection is used which gives approximately same SER as ML detection for different shape parameters and modulation techniques. Only at the high SNR, SER performance is slightly reduced. In this technique, the complexity level is comparable to traditional MMSE-OSIC. Also, MMSE-OSIC^2 detection constructively generates LLR values. Therefore, this detection technique gives conformity between improved performance and an acceptable level of complexity.

All feasible constellation points are tested as x_1 in stage 1 (i = 1) of the MMSE-OSIC^2. Here, it is assumed that x_1 has the highest column norm. The layer 1 symbol can differ from x_1 and the other symbols are carried out through MMSE-OSIC. It is determined that the first layer approximates a full diversity order as ML in stage 1 (i= 1). We measured the complexity in terms of number of addition, multiplication and division operations for implementing hardware.

Ref. [75] offers the number of complex operations in MMSE-OSIC detection for 16-QAM, however, Table 3.2 gives the total number of multiplication and division operations using MMSE-OSIC detection for BPSK, QPSK and 16-QAM when N_t and N_r both vary from 2 to 4. In ML metric computation, number of required multiplication is 4 for $N_r = N_t = 2$ while a number of required multiplications are 8 for $N_r = N_t = 4$. Table 3.3 represents the measured complexity in ML detection. The number of complex operations is greatly reduced in higher order modulation i.e. 16-QAM as compared to lower order modulation i.e. BPSK. In MMSE-OSIC^2 detection, a number of complex operations for $N_r = N_t = 2$ and 4 are given in Table 3.4(a) and (b) respectively, where **MUL**= number of multiplication**, DIV**=number of division, **ITER**= Iterations.

Table 3.2 Number of complex operations in MMSE-OSIC detection

Number of Antennas	**BPSK**		**QPSK**		**16-QAM**	
	MUL	**DIV**	**MUL**	**DIV**	**MUL**	**DIV**
$N_r = N_t = 2$	26	2	53	4	367	14
$N_r = N_t = 4$	134	4	293	8	1134	28

Table 3.3 Number of complex operations in ML detection

Operation	**MUL**		
	BPSK	**QPSK**	**16-QAM**
$\lvert C_p \rvert^{N_t} \times 4 \quad (N_r = N_t = 2)$	16	64	1024
$\lvert C_p \rvert^{N_t} \times 8 \quad (N_r = N_t = 4)$	128	2048	524288

Table 3.4 Number of complex operations in MMSE-OSIC^2 detection for **(a)** $N_r = N_t = 2$ **(b)** $N_r = N_t = 4$

(a)

Operation	**BPSK**			**QPSK**			**16-QAM**		
	MUL	**DIV**	**ITER**	**MUL**	**DIV**	**ITER**	**MUL**	**DIV**	**ITER**
$\|h_i\|^2, i = 1,2$	1	0	1	2	0	1	8	0	1
$W_{MMSE}^{(i)}, i = 1,2$	4	2	1	16	2	1	151	2	1
$\|Y - HX\|^2$	2,2, $i = 1,2$	0	0	4,4 $i = 1,2$	0	2 1, $i = 1,2$	8,8, $i = 1,2$	0	8 7, $i = 1,2$
Total	10+2× $\mathcal{M}$	2		28+4× $\mathcal{M}$	2		183+8× $7 \times \mathcal{M}$	2	

(b)

Operation	**BPSK**			**QPSK**			**16-QAM**		
	MUL	**DIV**	**ITER**	**MUL**	**DIV**	**ITER**	**MUL**	**DIV**	**ITER**
$\|h_i\|^2, i = 1,2,3,4$	4	0	1	8	0	1	32	0	1
$W_{MMSE}^{(i)}, i = 1,2,3,4$	37	4	1	103	4	1	302	4	1
$\|Y - HX\|^2$	2,2,2,2 , $i = 1,2,3,4$	0	4 3, $i = 1,2,3,4$	4,4,4,4, $i = 1,2,3,4$	0	8 7, $i = 1,2,3,4$	8,8,8,8, $i = 1,2,3,4$	0	16 15, $i = 1,2,3,4$
Total	61+2× $\mathcal{M} \times 3$	4		151+4×7 $\times \mathcal{M}$	4		462+8×15 $\times \mathcal{M} \times 3$	4	

For $\mathcal{M}$=1, a number of multiplications are 239, 822 using 16-QAM for $N_r = N_t = 2$ and 4 respectively. Consequently, 32, 179 multiplications and 2, 4 divisions are required using QPSK for $N_r = N_t = 2$ and 4 respectively. For BPSK, a number of multiplications are 12, 67 and divisions are 1, 4 when $N_r = N_t = 2$ and 4 respectively.

It is observed that MMSE-OSIC technique significantly degrades the performance. Therefore, the MMSE-OSIC^2 technique ($\mathcal{M}$=1) is proposed which shows near-ML SER performance. It is illustrated that the proposed MMSE-OSIC^2 technique ($\mathcal{M}$=1) gives reduced complexity than that of

MMSE-OSIC technique. It is also determined that the proposed MMSE-OSIC^2 technique provides a most significant solution between complexity and optimal performance trade-off.

3.7 Conclusion

In this chapter, a composite WG channel model is presented to analyze the MIMO system performance. For the statistical measurement of the system, we have described PDF, CDF and AF. MIMO system is considered with OSTBC and MRC in terms of SER operating over WG fading channels. The simulation and the analytical results illustrate that 16-QAM provides decreased error rate than 16-PSK under this scenario. Also, MRC shows the better error performance than OSTBC. The mathematical and the simulation analysis provide the worth and flexibility of proposed channel model. Also, this chapter offers MMSE-OSIC, ML as well as less complex and approximate optimal detection technique i.e. MMSE-OSIC^2 for MIMO system analysis under WG fading scenario. MMSE-OSIC^2 contains a number of candidate vectors, where candidate selection depends on the ML metric values those are applied to calculate LLR values. A comparative analysis of the proposed technique is obtained with MMSE-OSIC and ML detection techniques on the basis of both computational complexity and SER performance. Simulation results showed that the MMSE-OSIC^2 signal detection technique gives a near-ML performance. Also, the complexity is comparable to the MMSE-OSIC technique. In the MMSE-OSIC^2 technique, no additional calculation is required to get LLR values for all bits. Also, small values of shape parameters result in system performance degradation. MIMO system performance improves with the increase in a number of transmit, receive antennas, fading and shadowing parameters.

CHAPTER 4

MIMO Weibull-Gamma Fading Channel Performance in Low SNR Regime

4.1 Introduction

In the previous chapters, we have analyzed the error rate performance of MIMO system by taking receiver SNR from 0dB to maximum 30dB. However, at low SNR, system performance improvement is also an issue. The application of competent detection techniques is known to improve capacity performance even below 0dB receiver SNR. As described in [131], minimization of energy per information bit (E_b) manages a trade-off between bandwidth and power of the communication channels in wideband regime which is required for efficient signal communication. Also, normalized energy per information bit to noise ratio (E_b/N_0) is preferred over per-symbol SNR to analyze MIMO system performance precisely at low SNR over distinct fading channels. In MIMO systems, figure of merit depends on E_b/N_0 instead of SNR. In low SNR regime, the channel capacity analysis as a function of per symbol gives misleading outcomes and hence it is advisable to define capacity in terms of minimum energy per information bit to noise ratio ($E_b/N_{0_{min}}$) [168, 169]. Henceforth, channel bandwidth, power, and rate transmission will be analyzed with arbitrary number of transmitting and receiving antennas by minimizing E_b [170].

In [106, 120], the ergodic capacity of SM and OSTBC MIMO system has been computed over *GK* fading channel. *GK* channel model decreases energy levels to a prominent range [171]. SM-MIMO systems with optimal, MMSE detector and OSTBC have been developed to evaluate performance at low SNR over Weibull fading channel [132], however, the shadowing effect has not been considered. Thus, a generic channel model i.e. WG which was shown to be analytically better than other composite channel models is preferred for depicting the linear approximation of the multipath and shadowing conditions [110]. $E_b/N_{0_{min}}$ and wideband slope (S_0) are significant parameters to convey any positive rate of data consistently and to analyze the capacity of MIMO system at low SNR. The benefit of SM against OSTBC in giving better capacity is established elsewhere [120]. However, SM technique is not optimum at low SNRs and apart from eigen statistics, it permits to work with channel matrix trace [168]. Optimal detectors offer the maximum capacity of MIMO system, MMSE detectors are less complex than optimal detectors and offer

improved capacity performance. Moreover, OSTBC is diversity oriented technique. Thus, we have explored these three techniques in WG fading scenario. We have evaluated the capacity of MIMO system at low SNR under WG fading channel.

The rest of the chapter is organized as follows. In Section 4.2, we present MIMO system models used in this work. We evaluate the closed form expressions for capacity analysis of MIMO systems in low SNR regime using three models, namely, SM with the optimal detector, SM with the MMSE detector and OSTBC, in Section 4.3. Section 4.4 presents the simulation results. Section 4.5 concludes the chapter.

4.2 MIMO Signal Models

The $N_r \times N_t$ channel matrix H is assumed to be perfectly known at the receiver but unknown to the transmitter, and normalized to satisfy

$$E_H\left[\text{trace}\left(HH^{\dagger}\right)\right]=N_r N_t \tag{4.1}$$

Although the PDF of Weibull and gamma random variable is given in chapter 1 by (1.33) and (1.35), the first and second moment of gamma random variable are computed as

$$E[g] = \Omega \quad \text{and} \quad E[g^2] = \Omega^2\left(1+\frac{1}{m}\right) \tag{4.2}$$

Similarly, the n-th moment is also calculated for Weibull random variables [170] and given by

$$E(x^n) = \varphi^n \Gamma(1 + n/\beta) \tag{4.3}$$

where $\text{trace}\left(H^{\dagger}H\right) = \|H\|^2 = g\ \text{trace}({H_w}^{\dagger}H_w)$.

4.2.1 Optimal Detection for SM MIMO System

The optimal detectors are used to minimize the probability of error when all the data vectors are identical. Nevertheless, the implementation complexity is very high, power distribution is uniform across the transmit antennas with an average SNR (ρ).

When we take $\Re_{xx} = 1$ in (1.19), the SNR and ergodic capacity [172] are given respectively as

$$\gamma_{optimal} = \frac{\rho}{N_t}\left[\text{trace}\left(H^{\dagger}H\right)\right] \tag{4.4}$$

$$C_{ergodic}(\rho) \triangleq E_H\left[\log_2\left\{\det\left(I_{N_t} + \gamma_{optimal}\right)\right\}\right] \tag{4.5}$$

4.2.2 MMSE Signal Detection for SM MIMO System

Optimal detectors are complex in nature which makes them unemployable in low-cost communication systems. Therefore, linear detectors like MMSE detectors are designed to reduce computational complexity [54, 173]. In MMSE detection, W_{MMSE} in (3.10) is selected to minimize the mean-square error cost function. The solution to this optimization problem has been well defined (see, e.g., [174]), and is given by

$$W_{MMSE} = \sqrt{\frac{N_t}{E_s}} H^{\dagger} \left[HH^{\dagger} + \frac{N_t}{\rho} I_{N_r} \right]^{-1}$$
$$= \sqrt{\frac{N_t}{E_s}} \left[H^{\dagger}H + \frac{N_t}{\rho} I_{N_t} \right]^{-1} H^{\dagger} \quad (4.6)$$

where the second line is due to the matrix inversion lemma. At the k^{th} receiver output, the post-processing SNR when $N_r \geq N_t$, is represented as

$$\gamma_k^{MMSE} \triangleq \frac{1}{\left[\left(\mathrm{I}_{N_t} + \frac{\rho}{N_t} (H^{\dagger}H) \right)^{-1} \right]_{k,k}} - 1, \quad k = 1,2, \ldots N_t \quad (4.7)$$

where $[.]_{k,k}$ returns the k^{th} diagonal element of a matrix. The achievable sum rate can be determined by assuming the independent decoding at the receiver side, which is given by

$$\mathcal{R}^{MMSE}(\rho) \triangleq \sum_{k=1}^{N_t} E_{\gamma_k^{MMSE}} \left[\log_2 \left(1 + \gamma_k^{MMSE} \right) \right] \quad (4.8)$$

4.2.3 OSTBC MIMO System

OSTBC technique is preferred due to its simplicity and reliability. It is used to achieve the maximum diversity order of $N_t N_r$ and is computationally efficient for per symbol detection. MIMO channel can be converted into identical scalar channel by taking the response similar to that of Frobenius norm of channel matrix [175]. For the OSTBC MIMO systems, the SNR and the Shannon's capacity with rate R_c can be expressed respectively as

$$\gamma_{OSTBC} = \frac{\rho}{R_c N_t} \left[\mathrm{trace} \left(H^{\dagger}H \right) \right] \quad (4.9)$$

$$C_{STBC}(\rho) \triangleq R_c E_H [\log_2 (1 + \gamma_{OSTBC})] \quad (4.10)$$

4.3 Low SNR Analysis

According to [106], minimization of E_b governs a trade-off between bandwidth and power of the communication channels in wideband regime which is desirable for efficient signal communication.

Also, E_b/N_0 is preferred over per-symbol SNR in the measurement of MIMO system performance precisely at low SNR over distinct fading channels. It is obtained from $C(\rho)$ by

$$C\left(\frac{E_b}{N_0}\right) = C(\rho) \tag{4.11}$$

Also,

$$\frac{E_b}{N_0} = \frac{\rho}{C(\rho)} \tag{4.12}$$

It is noted that $\frac{E_b}{N_0}$ is related to the normalized *received* energy per information bit, $\frac{E_b^{Rx}}{N_0}$, by

$$\frac{E_b^{Rx}}{N_0} = N_r \frac{E_b}{N_0} \tag{4.13}$$

Closed-form expressions for (4.11) are not forthcoming, however, this representation is well approximated by [168] at low levels. Therefore, the capacity C can be characterized as

$$C\left(\frac{E_b}{N_0}\right) \approx S_0 \log_2\left(\frac{\frac{E_b}{N_0}}{\frac{E_b}{N_{0_{min}}}}\right) \tag{4.14}$$

where the parameters $E_b/N_{0_{min}}$ and S_0 prompt the low SNR nature desired for efficient transmission of positive rate and wideband slope. Also, $E_b/N_{0_{min}}$ represents minimum E_b/N_0 desired for reliable communication and S_0 expresses the slope of spectral efficiency in b/s/Hz/3dB at the point $E_b/N_{0_{min}}$. First order derivative $C'(.)$ and second order derivative $C"(.)$ of ergodic capacity are derived from (4.5) at ρ=0. They are used to determine following two figures of merits

$$\frac{E_b}{N_{0_{min}}} = \frac{1}{C\prime(0)}\,, S_0 = -2\ln 2 \frac{(C\prime(0))^2}{C"(0)} \tag{4.15}$$

The following properties (4.13), (4.16) and (4.17) are represented by $N_t \times N_r$ MIMO systems over i.i.d. WG fading channels in low SNR regime

$$E[\text{trace}(H^\dagger H)] = \frac{\Omega \varphi^2 N_t N_r}{d^v} \Gamma(1 + 2/\beta) \tag{4.16}$$

It depends on the moments of WG variates, which can be evaluated by combining (4.2) -(4.3). Firstly, i-th (i= 1, 2…..N_t) diagonal element of $(H^\dagger H)^2$ is augmented, which is computed by

$$\left[(H^\dagger H)^2\right]_{i,i} = \left(\sum_{i=1}^{N_r} \left|h_{k,i}\right|^2\right) + \sum_{n=1, n\neq i}^{N_t} \left(\sum_{k=1}^{N_r} h_{k,i} h_{k,n}^*\right)\left(\sum_{k=1}^{N_r} h_{k,i}^* h_{k,n}\right) \tag{4.17}$$

After some simple algebraic computation, the expected value of (4.17) is obtained as

$$E\left(\left[(H^{\dagger}H)^2\right]_{i,i}\right) = \frac{\Omega^2\varphi^4 N_r}{d^{2\upsilon}}\left[\left(1+\frac{1}{m}\right)\Gamma(1+4/\beta) + (N_t+N_r-2)\Gamma\left(1+\frac{2}{\beta}\right)^2\right] \tag{4.18}$$

All diagonal elements of (4.18) are summed up to get (4.19).

$$E[\text{trace}((H^{\dagger}H)^2)] = \frac{\Omega^2\varphi^4 N_t N_r}{d^{2\upsilon}}\left[\left(1+\frac{1}{m}\right)\Gamma\left(1+\frac{4}{\beta}\right) + (N_t+N_r-2)\Gamma\left(1+\frac{2}{\beta}\right)^2\right] \tag{4.19}$$

Note that all the elements of H are i.i.d. random variables, to obtain

$$E[(\text{trace}(H^{\dagger}H))^2] = N_t N_r E\left(|h_{11}|^4\right) + N_t N_r (N_t N_r - 1)\left(E\left(|h_{11}|^2\right)\right)^2 \tag{4.20}$$

Equation (4.21) is obtained by employing (4.2) and (4.3) in (4.20) after some simplifications.

$$E[(\text{trace}(H^{\dagger}H))^2] = \frac{\Omega^2\varphi^4 N_t N_r}{d^{2\upsilon}}\left[\left(1+\frac{1}{m}\right)\Gamma\left(1+\frac{4}{\beta}\right) + (N_t N_r-1)\Gamma\left(1+\frac{2}{\beta}\right)^2\right] \tag{4.21}$$

Using (4.14), we evaluated the capacity performance of SM MIMO with the optimal detector, SM MIMO with the MMSE detector and OSTBC MIMO systems at low SNR.

Proposition 1: The respective $E_b/N_{0_{min}}$ and S_0 for SM MIMO systems with optimal detector using $N_t \times N_r$ antennas are represented as

$$\frac{E_b^{optimal}}{N_{0_{min}}} = \frac{d^{\upsilon}\ln 2}{\Omega\varphi^2 N_r \Gamma(1+2/\beta)} \tag{4.22}$$

$$S_0^{optimal} = \frac{2N_t N_r}{\left(1+\frac{1}{m}\right)\Phi(\beta)+(N_t+N_r-2)} \tag{4.23}$$

where $\Phi(\beta) = \frac{\Gamma(1+4/\beta)}{\Gamma(1+2/\beta)^2}$ (4.24)

Proof: In [131], the matrices for low SNR are rearranged to form

$$\frac{E_b}{N_{0_{min}}} = \frac{N_t \ln 2}{E\{\text{trace}(H^{\dagger}H)\}} \tag{4.25}$$

$$S_0 = \frac{(E[\text{trace}(H^{\dagger}H)])^2}{E[\text{trace}((H^{\dagger}H)^2)]} \tag{4.26}$$

Substituting (4.16)-(4.19) into (4.25)-(4.26), we get (4.22) and (4.23) using simple mathematical formulation. Equation (4.22) is the increasing function of β and the decreasing function of φ. As $\Phi(\beta)$ is a function of β in (4.24), $S_0^{optimal}$ increases with the increase in β. In (4.22), $E_b^{optimal}/N_{0_{min}}$ do not depend on m and β. When extra receive antennas get additional power, $E_b/N_{0_{min}}$ decreases monotonically with the increase in N_r [106, 120]. Equation (4.22)

remains unchanged with the increase in N_t, however, capacity increases due to higher value of $S_0^{optimal}$. The wideband slope $S_0^{optimal}$ is lower bounded ($\beta \to 0$) and upper bounded ($\beta \to \infty$) as

$$0 \leq S_0^{optimal} \leq \frac{2N_tN_r}{N_t+N_r-1} \tag{4.27}$$

Nevertheless, $E_b/N_{0_{min}}$ is reduced by increasing N_r because higher number of receive antennas need more power as mentioned in [106] and [131]. The parameters chosen for *K* fading, and Rayleigh fading are $\Omega = \beta = 2, \varphi = 1$ and $\Omega = \beta = 2, \varphi = 1, m \to \infty$ respectively. Equations (4.22)-(4.23) are simplified to form Rayleigh fading as

$$\frac{E_b^{optimal}}{N_{0_{min}}} = \frac{\ln 2}{N_r\Omega},\ S_0^{optimal} = \frac{2N_tN_r}{N_t+N_r} \tag{4.28}$$

Proposition 2: $E_b/N_{0_{min}}$ and S_0 for SM MIMO systems with MMSE detector using $N_t \times N_r$, ($N_r \geq N_t$) are given by

$$\frac{E_b^{MMSE}}{N_{0_{min}}} = \frac{d^{\upsilon}\ln 2}{\Omega\varphi^2 N_r\Gamma(1+2/\beta)} \tag{4.29}$$

$$S_0^{MMSE} = \frac{2N_tN_r}{\left(1+\frac{1}{m}\right)\Phi(\beta)+(2N_t+N_r-3)} \tag{4.30}$$

Proof: In [173], the following expressions are provided for the above derivatives

$$\mathcal{R}'^{MMSE}(0) = \frac{1}{\ln 2}\left(E_H[\mathrm{trace}(H^{\dagger}H)] - \frac{1}{N_t}\sum_{k=1}^{N_t} E_H\left[\mathrm{trace}\left(H_k^{\dagger}H_k\right)\right]\right)$$

$$= \frac{\Omega\varphi^2 N_r\Gamma\left(1+\frac{2}{\beta}\right)}{d^{\upsilon}\ln 2} \tag{4.31}$$

$$\mathcal{R}''^{MMSE}(0) = -\frac{1}{{N_t}^2\ln 2}\left(N_tE_H[\mathrm{trace}((H^{\dagger}H)^2)] - \sum_{k=1}^{N_t} E_H[\mathrm{trace}(\left(H_k^{\dagger}H_k\right)^2)]\right)$$

$$= -\frac{\Omega^2\varphi^4}{d^{2\upsilon}N_t\ln 2}\left[N_r\left(1+\frac{1}{m}\right)\Gamma\left(1+\frac{4}{\beta}\right) + \Gamma\left(1+\frac{2}{\beta}\right)^2(2N_tN_r + {N_r}^2 - 3N_r)\right] \tag{4.32}$$

H is replaced by H_k after removal of k-th column. The elements of H follow i.i.d WG fading. Using (4.16)-(4.19), the expectations in (4.31)-(4.32) can be evaluated. The desired results are obtained using (4.15). It is observed that (4.22) and (4.29) represent the same mathematical expression.

Therefore, due to $E_b/N_{0_{min}}$, optimal detection is realizable through MMSE detectors and S_0 gives suboptimal detection. It can be shown that

$$\frac{S_0^{optimal}}{S_0^{MMSE}} = 1 + \frac{(N_t-1)}{\left(1+\frac{1}{m}\right)\Phi(\beta)+N_t+N_r-2} \tag{4.33}$$

The above ratio $\left(\text{i.e.}, \frac{S_0^{optimal}}{S_0^{MMSE}}\right)$ decreases with the increase in N_r and increases with the increase in N_t. Subsequently, MMSE detector has degraded interference cancellation capability for larger N_t that increases number of data streams. In case $N_t = 1$, then $S_0^{optimal} = S_0^{MMSE}$ and therefore, interfering data streams cancellation is not possible. For Rayleigh fading conditions, (4.29)-(4.30) are simplified and resembles [173, Equations (33) and (52)] which is given by

$$\frac{E_b^{MMSE}}{N_{0_{min}}} = \frac{\ln 2}{N_r\Omega},\ S_0^{MMSE} = \frac{2N_tN_r}{2N_t+N_r-1} \tag{4.34}$$

Proposition 3: The respective $E_b/N_{0_{min}}$ and S_0 for OSTBC MIMO systems using $N_t \times N_r$ are expressed as

$$\frac{E_b^{STBC}}{N_{0_{min}}} = \frac{d^{\upsilon}\ln 2}{\Omega\varphi^2 N_r\Gamma(1+2/\beta)} \tag{4.35}$$

$$S_0^{STBC} = \frac{2R_cN_tN_r}{\left(1+\frac{1}{m}\right)\Phi(\beta)+(N_tN_r-1)} \tag{4.36}$$

Proof: It can be seen from (4.10) that

$$C'_{STBC}(0) = \frac{E[\text{trace}(H^{\dagger}H)]}{N_t\ln 2} \tag{4.37}$$

$$C''_{STBC}(0) = -\frac{E[(\text{trace}(H^{\dagger}H))^2]}{R_c{N_t}^2\ln 2} \tag{4.38}$$

If we combine (4.16) and (4.21) with (4.37)-(4.38) and then substituting into (4.15), desired results (4.35)-(4.36) are obtained after some simple algebraic calculation.

$$\frac{S_0^{optimum}}{S_0^{STBC}} = \frac{\left(1+\frac{1}{m}\right)\Phi(\beta)+(N_tN_r-1)}{\left[R_c\left(1+\frac{1}{m}\right)\Phi(\beta)+(N_t+N_r-2)\right]} \tag{4.39}$$

$$\frac{S_0^{MMSE}}{S_0^{STBC}} = \frac{\left(1+\frac{1}{m}\right)\Phi(\beta)+(N_tN_r-1)}{\left[R_c\left(1+\frac{1}{m}\right)\Phi(\beta)+(2N_t+N_r-3)\right]} \tag{4.40}$$

Since $(N_t N_r - 1) \geq (N_t + N_r - 2)$, $(N_t N_r - 1) \geq (2N_t + N_r - 3)$ and $R_c \leq 1$.

Therefore, $S_0^{optimum} \geq S_0^{MMSE} \geq S_0^{STBC}$, it shows that SM MIMO systems with optimal/MMSE detector have higher wideband slope than OSTBC system. For i.i.d. Rayleigh fading conditions, (4.35)-(4.36) simplify as

$$\frac{E_b^{STBC}}{N_{0_{min}}} = \frac{\ln 2}{N_r \Omega}, \quad S_0^{STBC} = \frac{2R_c N_t N_r}{N_t N_r + 1} \tag{4.41}$$

4.4 Simulation Results

This section presents the capacity performance analysis in low SNR regime using optimal, MMSE detectors and OSTBCs. In Fig. 4.1, the capacity results are evaluated at $\varphi = 1$. In this case, the effects of low and high multipath fading are considered for $\beta = 20$ and 2 respectively in the presence of light shadowing (m =70) and heavy shadowing ($m = 1$). In light shadowing environment, i.e. for $\beta = 2$, Rayleigh fading is observed. In addition, the capacity for the special cases (i.e.,≈Rayleigh and *K*-fading) of *GK* fading in [106] approaches both the special cases of WG fading. Thus, it is observed that WG is an alternative to *GK* fading channel. The range of low SNR is taken numerically negative values from -8dB to -1dB.

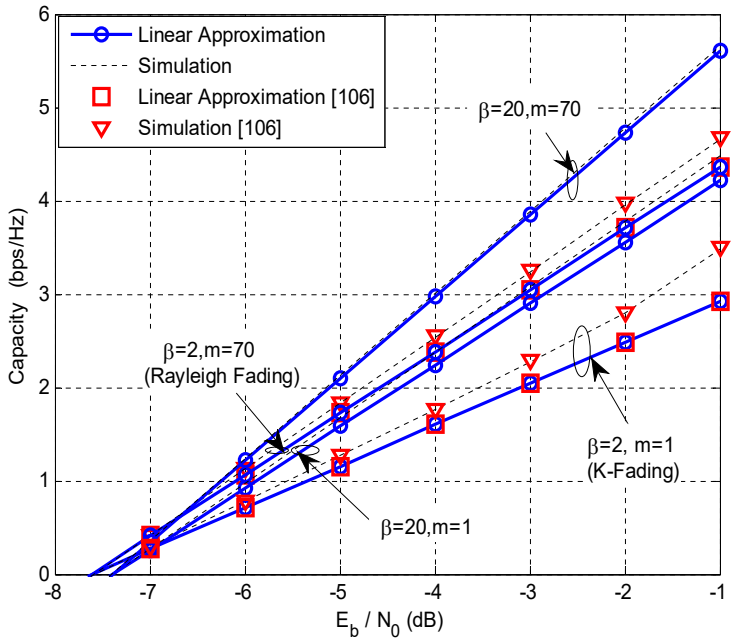

Fig. 4.1 Capacity of SM MIMO system with optimal detector over WG fading channels for different *m* and β when $N_t = N_r = 2$.

Simulation results illustrates that capacity increases in low multipath and light shadowing environment. As $1+1/m \approx 1$ for light shadowing (when m is large), the impact of shadowing on wideband slope is negligible. The generation of WG MIMO fading channels occurs as the product of a gamma random variable and H_w with i.i.d. Weibull entries. Moreover, the simulation results of capacity at low SNR for SM MIMO systems with optimal detectors follow analytical approximations of Proposition 1. Also, S_0 decreases consistently due to the influence of shadowing on wideband slope, which reflects the divergence from small scale fading. Here, m = 1 shows the severe shadowing effect and consequent reduction in S_0 which is depicted in Fig. 4.2.

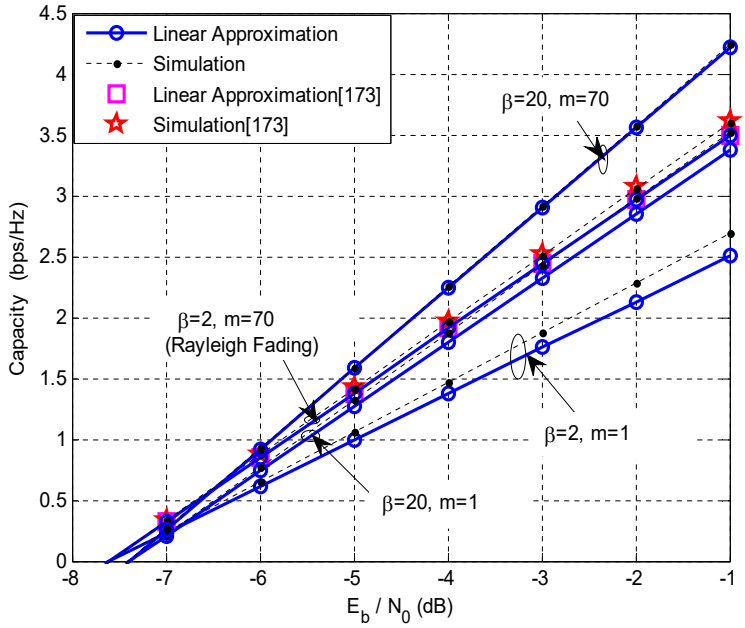

Fig. 4.2 Capacity of SM MIMO system with MMSE detector over WG fading channels for different m and β when $N_t = N_r = 2$.

For a fair assessment, we have compared our result with the results of [173] for a special case (i.e., Rayleigh fading) of WG fading. SM MMSE gives a performance with a high data rate keeping the complexity low. However, it is disadvantageous to system reliability. Therefore, we have considered OSTBC in Proposition 3.

In Proposition 3, it is discussed that $E_b/N_{0_{min}}$ is affected by code rate, transmission distance, and average channel gains. In Fig. 4.3, spectral efficiency of OSTBC systems in MIMO WG fading channels for β=2, 20 and m=1, 70 is shown for N_t= N_r= 2, $\lambda = 1$ and $R_c = 1$ bps. It is shown that,

S_0 is reduced by 50% when $m = 1$ instead of $m = 70$. $E_b/N_{0_{min}}$ increases with the increase in fading parameter β, and an elevated wideband slope is observed which compensate the increased maximum energy per bit. OSTBC diversity leads to a reduction in capacity, which we examined by comparing it with the average capacity obtained from i.i.d. Gaussian inputs and by assigning equal transmits power.

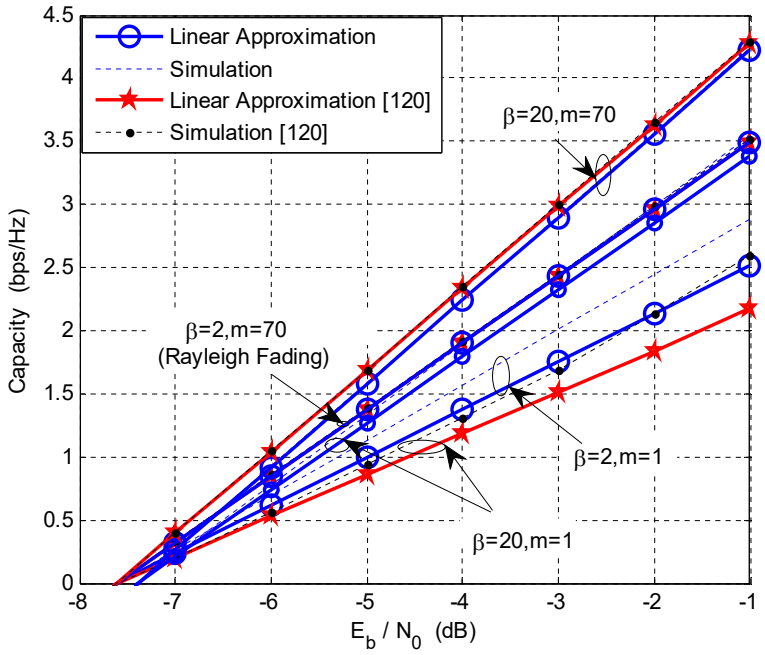

Fig. 4.3 Capacity of OSTBC MIMO system over WG fading channels for different *m* and β when $N_t = N_r = 2$. (m and β are shadowing and fading parameter for both WG and *GK* Fading [120])

After some simple mathematical formulation, it is observed that $E_b/N_{0_{min}}$ for all three configurations is identical, while S_0 is different. We have determined that the approximations are precise for the proposed cases at adequately low SNR values, particularly for high values of fading parameters. However, they become inappropriate for small values of β and m ($0 \leq \beta \leq 1.5$, $0 \leq m \leq 1$) due to the unreliable nature of $\Phi(\beta)$. As shown in Fig. 4.3, the capacity does not show significant improvement for less fading and high shadowing under *GK* fading [120] compared to WG fading condition. In addition, for $\beta = 20, m = 1$, MIMO system can achieve more capacity in WG fading than that of *GK* fading, however, WG fading degrades the capacity at high values of both the parameters. Our results are approximately same as obtained and compared in [15] for

special cases such as Rayleigh and Weibull fading. Also, analytical results are well suited to simulation results.

Fig. 4.4 shows the comparison of optimal and MMSE detection with OSTBC diversity technique on the basis of capacity performance. At -3dB SNR, nearly 0.5 bps/Hz and 0.24 bps/Hz improved capacity is achieved using optimal and MMSE detection respectively than that of OSTBC for $m = 1, \beta = 2$. However, MMSE detector reduces 0.25 bps/Hz capacity compared to that of optimal detector for the same parameters. It is noted that optimal detector experiences more computation complexity than MMSE detector.

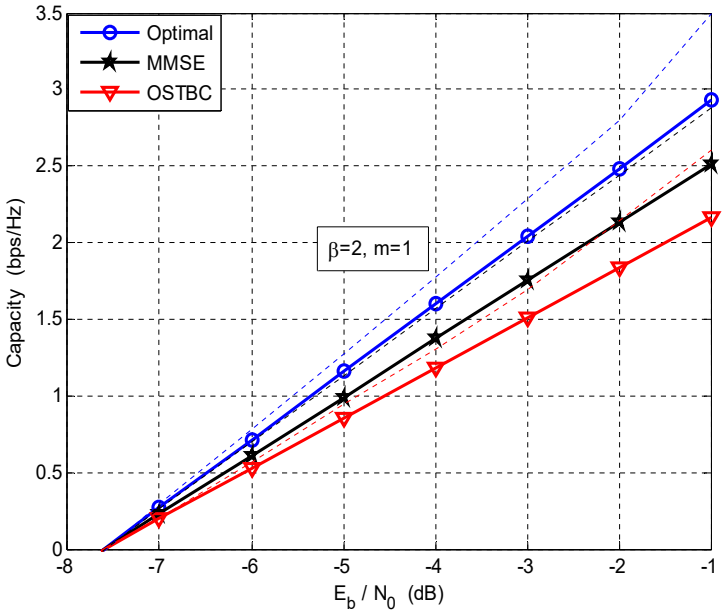

Fig. 4.4 Capacity comparison of Optimal and MMSE detection with OSTBC over WG fading channel for $m = 1, \beta = 2$ when $N_t = N_r = 2$ (Dotted lines illustrate simulation results using optimal, MMSE and OSTBC techniques)

4.5 Conclusion

In this chapter, we presented that the WG fading model shows a wide range of agreement with measured data in several environment conditions. The performance evaluation of MIMO systems in WG fading channels is restricted, generally due to the problem to deal with the non-Gaussian behaviour of the fading coefficients. We used AF to evaluate different channel conditions. A comprehensive low SNR analysis of different MIMO systems operating in WG fading channels is presented in this chapter. Novel tractable expressions for $E_b/N_{0_{min}}$ and S_0 are deduced. These

expressions were verified by previous results of Rayleigh and *K/GK*-fading. The proposed analysis of MIMO system deals with three techniques namely SM with optimal detection, SM with MMSE detection and OSTBC. The average capacity of OSTBC systems is usually subsidiary to that of capacity-oriented SM MIMO techniques, whereas OSTBC system is a diversity-oriented technique. Further, this work can be extended using the same channel model with other performance measures.

CHAPTER 5

Antenna Selection for MIMO Weibull-Gamma Fading Channel

5.1 Introduction

In the previous chapters, we showed that MIMO offers superior performance than SISO system with no extra bandwidth or transmit power extensively. Although spatial diversity and spatial multiplexing are two main benefits of MIMO systems, however, the problem arises when we require expensive RF modules due to multiple antennas [176]. Earlier, we assumed that CSI was known to the receiver only. The availability of CSI (partial or perfect knowledge of channel) at receiver has a potential to solve this problem. Also, it improves the capacity and error rate performance of MIMO system by reducing complexity [177, 178]. The best possible way to decrease the cost of multiple RF modules is to use antenna selection (AS) techniques. Authors [76, 179] used the selection diversity followed by AS algorithms at the transmitter and receiver sides using a generic channel model but without considering shadowing effects. Although in the past, different multipath fading models have been taken into account for system performance evaluation, but for this work we have considered WG fading scenario. In [24, 180], authors demonstrate the capacity and BER performance of MIMO system using AS techniques over Rayleigh and Nakagami-*m* fading channel, however, the shadowing effect has not been taken into account.

This chapter describes the optimal and sub-optimal AS techniques to evaluate the capacity performance of MIMO system in WG fading environment. For the analysis, we also used AS to evaluate BER performance using OSTBC for M-QAM over same WG fading channel [181].

5.2 System and Channel Model

Consider a MIMO system with $N_r \times N_t$ antennas and complex channel matrix H. Each element h_{ij} of H is identical and independently distributed Gaussian random variable represented as channel gain from i^{th} transmit antenna to j^{th} receive antenna with zero mean and N_0 variance. The effective channel is considered by L columns after selecting L antennas from N_t transmit antennas of $H \in \mathbb{C}^{N_r \times N_t}$.

Fig. 5.1 demonstrates the end-to-end arrangement of the antenna selection which considers only L RF modules to support N_t transmit antennas $L < N_t$. It is noted that L RF modules are selectively mapped to L of N_t transmit antennas.

The index $\mathcal{J}_k$ is considered for the k-th selected column, $k = 1, 2 \ldots . L$. The consequent effective channel is modeled as $H_{(\mathcal{J}_1,\mathcal{J}_2,\ldots.\mathcal{J}_L)} \in \mathbb{C}^{N_r \times L}$. The mapping of spatially-multiplexed or space-time coded stream into L selected antennas is specified as $x \in \mathbb{C}^{L \times 1}$.

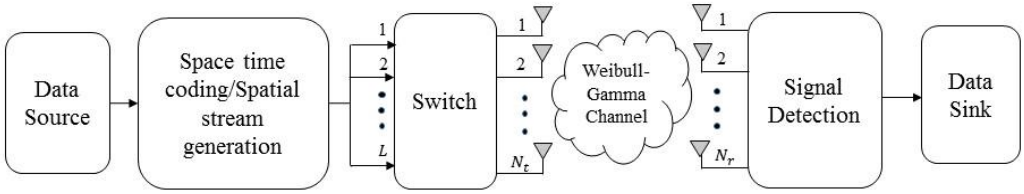

Fig. 5.1 Antenna selections with L RF modules and N_t transmit antennas ($L < N_t$)

The received signal Y is given by

$$Y = \sqrt{\frac{E_S}{L}} H_{(\mathcal{J}_1,\mathcal{J}_2,\ldots.\mathcal{J}_L)} X + \mathcal{N} \tag{5.1}$$

where H represents WG fading channel and its PDF in terms of amplitude and SNR is given in (3.2) and (3.3) respectively.

5.3 Average Capacity Analysis

The AS techniques are applied to enhance the system capacity performance. In (5.1), the channel capacity of the system relies upon the selected transmit antennas. In this section, optimal and sub-optimal AS techniques are given for capacity analysis of MIMO systems.

5.3.1 Optimal Antenna Selection Technique

Out of N_t transmit antennas, L antennas are chosen to increase the capacity. The system channel capacity with L chosen transmit antennas is represented in [24] as

$$C_{(\mathcal{J}_1,\mathcal{J}_2,\ldots.\mathcal{J}_L)} \triangleq \log_2 \det\left(I_{N_r} + \frac{E_S}{LN_0} H_{(\mathcal{J}_1,\mathcal{J}_2,\ldots.\mathcal{J}_L)} H^{\dagger}_{(\mathcal{J}_1,\mathcal{J}_2,\ldots.\mathcal{J}_L)}\right) \tag{5.2}$$

The antenna having maximum capacity is chosen to maximize the system capacity and given as

$$\left(\mathcal{J}_1{}^o, \mathcal{J}_2{}^0, \ldots . \mathcal{J}_L{}^0\right) = \underset{(\mathcal{J}_1,\mathcal{J}_2,\ldots.\mathcal{J}_L)\in A_L}{\arg\max} C_{(\mathcal{J}_1,\mathcal{J}_2,\ldots.\mathcal{J}_L)} \tag{5.3}$$

where A_L is a set of all promising antenna arrangements with L selected antennas. However, it consists the huge complexity, mostly when N_t is very large.

5.3.2 Sub-optimal Antenna Selection Technique

To reduce the complexity arises due to optimal AS technique, sub-optimal AS technique is used [24]. In this technique, firstly one antenna with the highest capacity is chosen as

$$\begin{aligned} \mathcal{J}_1^{so} &= \arg_{\mathcal{J}_1} \max C_{(\mathcal{J}_1)} \\ &= \arg_{\mathcal{J}_1} \max \log_2 \det\left(I_{N_r} + \frac{E_s}{LN_0} H_{(\mathcal{J}_1)} H_{(\mathcal{J}_1)}^{\dagger}\right) \end{aligned} \tag{5.4}$$

We chose the second antenna while considering first chosen antenna so as to maximize the capacity, i.e.,

$$\begin{aligned} \mathcal{J}_2^{so} &= \arg\max_{\mathcal{J}_2 \neq \mathcal{J}_1^{so}} C_{(\mathcal{J}_1^{so}, \mathcal{J}_2)} \\ &= \arg\max_{\mathcal{J}_2 \neq \mathcal{J}_1^{so}} \log_2 \det\left[I_{N_r} + \frac{E_s}{LN_0} H_{(\mathcal{J}_1^{so}, \mathcal{J}_2)} H_{(\mathcal{J}_1^{so}, \mathcal{J}_2)}^{\dagger}\right] \end{aligned} \tag{5.5}$$

After completing n iterations ($\mathcal{J}_1^{so}, \mathcal{J}_2^{so}, \ldots\ldots\ldots \mathcal{J}_n^{so}$), the updated capacity with an extra antenna q is given as

$$\begin{aligned} C_q &= \log_2 \det\left[I_{N_r} + \frac{E_s}{LN_0}\left\{H_{(\mathcal{J}_1^{so}, \mathcal{J}_2^{so}, \ldots, \mathcal{J}_n^{so})} H_{(\mathcal{J}_1^{so}, \mathcal{J}_2^{so}, \ldots, \mathcal{J}_n^{so})}^{\dagger} + H_{(q)} H_{(q)}^{\dagger}\right\}\right] \\ &= \log_2 \det\left[I_{N_r} + \frac{E_s}{LN_0} H_{(\mathcal{J}_1^{so}, \mathcal{J}_2^{so}, \ldots, \mathcal{J}_n^{so})} H_{(\mathcal{J}_1^{so}, \mathcal{J}_2^{so}, \ldots, \mathcal{J}_n^{so})}^{\dagger}\right] \\ &\quad + \log_2\left[1 + \frac{E_s}{LN_0} H_{(q)}\left\{H_{(\mathcal{J}_1^{so}, \mathcal{J}_2^{so}, \ldots, \mathcal{J}_n^{so})} H_{(\mathcal{J}_1^{so}, \mathcal{J}_2^{so}, \ldots, \mathcal{J}_n^{so})}^{\dagger}\right\}^{-1} H_{(q)}^{\dagger}\right] \end{aligned} \tag{5.6}$$

We derived it using following identities,

$$\begin{aligned} \det(\mathrm{U} + \mathrm{VW}^{\dagger}) &= (1 + \mathrm{W}^{\dagger}\mathrm{U}^{-1}\mathrm{V})\det(\mathrm{U}) \\ \log_2 \det(\mathrm{U} + \mathrm{VW}^{\dagger}) &= \log_2(1 + \mathrm{W}^{\dagger}\mathrm{U}^{-1}\mathrm{V}) \det(\mathrm{U}) \\ &= \log_2 \det(\mathrm{U}) + \log_2(1 + \mathrm{W}^{\dagger}\mathrm{U}^{-1}\mathrm{V}) \end{aligned} \tag{5.7}$$

where $\mathrm{U} = I_{N_r} + \frac{E_s}{LN_0} H_{(\mathcal{J}_1^{so}, \mathcal{J}_2^{so}, \ldots, \mathcal{J}_n^{so})} H_{(\mathcal{J}_1^{so}, \mathcal{J}_2^{so}, \ldots, \mathcal{J}_n^{so})}^{\dagger}$ and $\mathrm{V} = \mathrm{W} = \sqrt{\frac{E_s}{LN_0}} H_{(\mathcal{J}_q)}$

After that, the additional $(n+1)$-th antenna is chosen to enhance the capacity, given as,

$$\mathcal{J}_{n+1}^{so} = \underset{q \notin (\mathcal{J}_1^{so}, \mathcal{J}_2^{so}, \ldots, \mathcal{J}_n^{so})}{\arg\max} C_q$$

$$= \underset{q \notin (\mathcal{J}_1^{so}, \mathcal{J}_2^{so}, \ldots, \mathcal{J}_n^{so})}{\arg\max} H_{(q)} \left[\frac{LN_0}{E_s} I_{N_r} + H_{(\mathcal{J}_1^{so}, \mathcal{J}_2^{so}, \ldots, \mathcal{J}_n^{so})} H_{(\mathcal{J}_1^{so}, \mathcal{J}_2^{so}, \ldots, \mathcal{J}_n^{so})}^{\dagger} \right]^{-1} H_{(q)}^{\dagger} \tag{5.8}$$

This procedure keeps on until all L antennas are selected. Only one matrix inversion is essential in the way of selection practice. The similar procedure can be applied by removing the antenna in decreasing order of reduced channel capacity. Then, we select a set of antenna indices $\mathbb{i}_n$ in the n-th iteration. Initially, all the antennas are considered ($\mathbb{i}_1 = 1,2, \ldots N_t$) and the antenna that gives smallest capacity is selected, i.e.,

$$\mathcal{J}_1^{remove} = \underset{\mathcal{J}_1 \in \mathbb{i}_1}{\arg\max} \log_2 \det \left(I_{N_r} + \frac{E_s}{LN_0} H_{\mathbb{i}_1 - (\mathcal{J}_1)} H_{\mathbb{i}_1 - (\mathcal{J}_1)}^{\dagger} \right) \tag{5.9}$$

The antenna selected from (5.9) is then removed from the antenna index set, and the updated antenna set is $\mathbb{i}_2 = \mathbb{i}_1 - (\mathcal{J}_1^{remove})$. When $|\mathbb{i}_2| = N_t - 1 > L$, one more antenna is selected to remove which gives least to the capacity. Consequently, it is given for the antenna index set $\mathbb{i}_2$ as

$$\mathcal{J}_2^{remove} = \underset{\mathcal{J}_2 \in \alpha_2}{\arg\max} \log_2 \det \left(I_{N_r} + \frac{E_s}{LN_0} H_{\mathbb{i}_2 - (\mathcal{J}_2)} H_{\mathbb{i}_2 - (\mathcal{J}_2)}^{\dagger} \right) \tag{5.10}$$

Again, we update the rest of the antenna index set to $\mathbb{i}_3 = \mathbb{i}_2 - (\mathcal{J}_2^{remove})$. This procedure continues up to all L AS ($|\mathbb{i}_n| = L$).

5.4 Error Rate Analysis for OSTBC

BER is an important measure to evaluate MIMO-OSTBC system performance. Therefore, transmit antennas selected to reduce the error probability. For $H_{(\mathcal{J}_1, \mathcal{J}_2, \ldots \mathcal{J}_L)}$ with L columns of H chosen, an upper bounded pairwise error probability for OSTBC is represented by [24]

$$P_e\left(d_i \to d_j \middle| H_{(\mathcal{J}_1, \mathcal{J}_2, \ldots \mathcal{J}_L)}\right) = L \left[\sqrt{\frac{\rho \left\| H_{(\mathcal{J}_1, \mathcal{J}_2, \ldots \mathcal{J}_L)} \varepsilon_{ij} \right\|^2}{2N_t}} \right] \leq \exp \left[- \frac{\rho \left\| H_{(\mathcal{J}_1, \mathcal{J}_2, \ldots \mathcal{J}_L)} \varepsilon_{ij} \right\|^2}{4N_t} \right] \tag{5.11}$$

Then, L transmit antennas are selected to minimize the upper bound in (5.11)

$$\left(\mathcal{J}_1{}^{o}, \mathcal{J}_2{}^{0}, \ldots . \mathcal{J}_L{}^{0} \right) = \underset{(\mathcal{J}_1, \mathcal{J}_2, \ldots . \mathcal{J}_L) \in A_L}{\arg\max} \left\| H_{(\mathcal{J}_1, \mathcal{J}_2, \ldots \mathcal{J}_L)} \mathcal{E}_{ij} \right\|^2$$

$$= \underset{(\mathcal{J}_1, \mathcal{J}_2, \ldots . \mathcal{J}_L) \in A_L}{\arg\max} \text{Trace}\left(H_{(\mathcal{J}_1,\mathcal{J}_2,\ldots.\mathcal{J}_L)} \mathcal{E}_{ij} \mathcal{E}_{ij}^{\dagger} H_{(\mathcal{J}_1,\mathcal{J}_2,\ldots.\mathcal{J}_L)}^{\dagger}\right)$$

$$= \underset{(\mathcal{J}_1, \mathcal{J}_2, \ldots . \mathcal{J}_L) \in A_L}{\arg\max} \text{Trace}\left(H_{(\mathcal{J}_1,\mathcal{J}_2,\ldots.\mathcal{J}_L)} H_{(\mathcal{J}_1,\mathcal{J}_2,\ldots.\mathcal{J}_L)}^{\dagger}\right) \tag{5.12}$$

$$= \underset{(\mathcal{J}_1, \mathcal{J}_2, \ldots . \mathcal{J}_L) \in A_L}{\arg\max} \left\| H_{(\mathcal{J}_1,\mathcal{J}_2,\ldots.\mathcal{J}_L)} \right\|^2$$

Equation (5.12) has been derived using the fact that the error matrix $\mathcal{E}_{ij}$ has the property $\mathcal{E}_{ij}\mathcal{E}_{ij}^{\dagger} = \alpha I$ with constant α. The antennas subsequent to high column norms are chosen to reduce the error rate. The average received SNR with L selected antennas of $(\mathcal{J}_k)_{k=1}^{L}$ is denoted as

$$\gamma_{(\mathcal{J}_1,\mathcal{J}_2,\ldots.\mathcal{J}_L)} = \frac{\rho}{L} \left\| H_{(\mathcal{J}_1,\mathcal{J}_2,\ldots.\mathcal{J}_L)} \right\|^2 \tag{5.13}$$

It is recommended in (5.12) and (5.13) that the antennas with the maximum received SNR are chosen. The indices $\left(\mathcal{J}_1{}^{o}, \mathcal{J}_2{}^{0}, \ldots . \mathcal{J}_L{}^{0}\right)$ with the maximum L column norms of selection are given by following inequality

$$\frac{\left\| H_{\left(\mathcal{J}_1{}^{o}, \mathcal{J}_2{}^{0}, \ldots . \mathcal{J}_L{}^{0}\right)} \right\|^2}{L} \geq \frac{\|H\|^2}{N_t} \tag{5.14}$$

For $L \leq N_t$, we also considered following inequality

$$\left\| H_{\left(\mathcal{J}_1{}^{o}, \mathcal{J}_2{}^{0}, \ldots . \mathcal{J}_L{}^{0}\right)} \right\|^2 = \left\| H_{\left(\mathcal{J}_1{}^{o}\right)} \right\|^2 + \left\| H_{\left(\mathcal{J}_2{}^{0}\right)} \right\|^2 + \ldots . + \left\| H_{\left(\mathcal{J}_L{}^{0}\right)} \right\|^2$$

$$\leq \left\| H_{(1)} \right\|^2 + \left\| H_{(2)} \right\|^2 + \ldots . + \left\| H_{(N_t)} \right\|^2 = \|H\|^2 \tag{5.15}$$

where $H_{(k)}$is the k-th column norm of H. Using (5.14) and (5.15), the following range for the average SNR on the receiver side is given for the optimal selection of antennas

$$\frac{\rho}{L}\|H\|^2 \geq \gamma_{\left(\mathcal{J}_1{}^{o}, \mathcal{J}_2{}^{0}, \ldots . \mathcal{J}_L{}^{0}\right)} \geq \frac{\rho}{N_t}\|H\|^2 \tag{5.16}$$

It is clear from (5.16) that the upper and lower bound are the function of $\|H\|^2$ and hence diversity order $N_t N_r$ is achieved with optimal AS in (5.3), when all the entries of H are i.i.d. Gaussian distributed.

5.5 Simulation Results

We illustrate the channel capacity with AS in Fig. 5.2, for $N_t = N_r = 4$ and L varies from 2 to 4. It is clearly depicted that the channel capacity increases with L. It is also illustrated in Fig. 5.2 that the

impact of shadowing is diminished for $\beta = 2, m = 70$ and hence capacity of MIMO system under this scenario approaches the MIMO system capacity under Rayleigh fading [24].

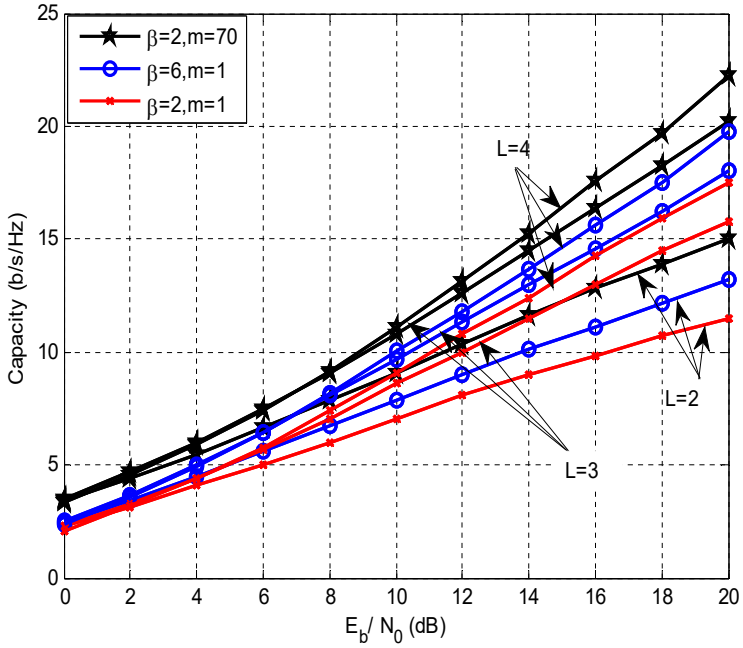

Fig. 5.2 Capacity of MIMO system for $N_t = N_r = 4$ and $L = 2,3,4$ using optimal antenna selection

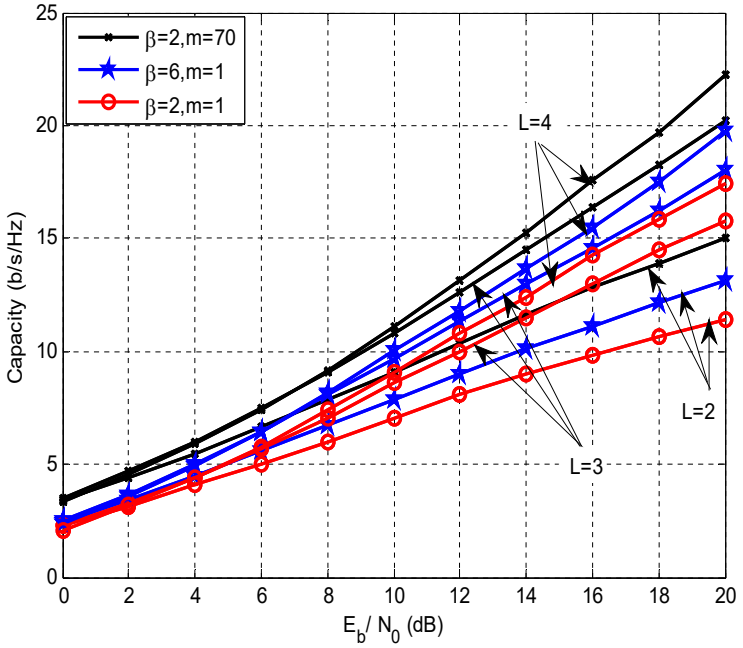

Fig. 5.3 Capacity of MIMO system for $N_t = N_r = 4$ and $L = 2,3,4$ using Sub-optimal antenna selection (descending order)

Then, the dominating effect of shadowing ($m = 1$) is taken into account which degrades the capacity performance even if β is high ($\beta = 6$). Consequently, for less than 10dB SNR, three selected antennas are sufficient to permit the channel capacity nearly the use of four antennas. For less values of β and m (severe fading and shadowing) channel capacity decreases, which is illustrated in Fig. 5.2. Also, at very less SNR, capacity performance is almost same by selecting three out of four transmit antennas. It is noted that WG MIMO channel is produced by the product of Weibull and Gamma random variables.

Fig. 5.3 shows that for the same simulation parameters as Fig. 5.2, the capacity for different selected antennas in descending order using sub-optimal AS technique approaches the capacity of optimal AS technique with reduced complexity. For simulation, the selection made in ascending/descending order is given by 0/1. The selection complexity in descending order is greater than that of ascending order. Nevertheless, the selection process in descending order gives better performance compared to that of ascending order ($1 < L < N_t$). There are two special cases. First, when $L = N_t - 1$, the selection process in descending order generates the same antenna index set as the optimal AS technique generates in (5.12). Second, when $L = 1$, the selection technique in ascending order generates the same antenna index as the optimal AS technique in (5.12) and offers superior performance compared to other selection approaches [24].

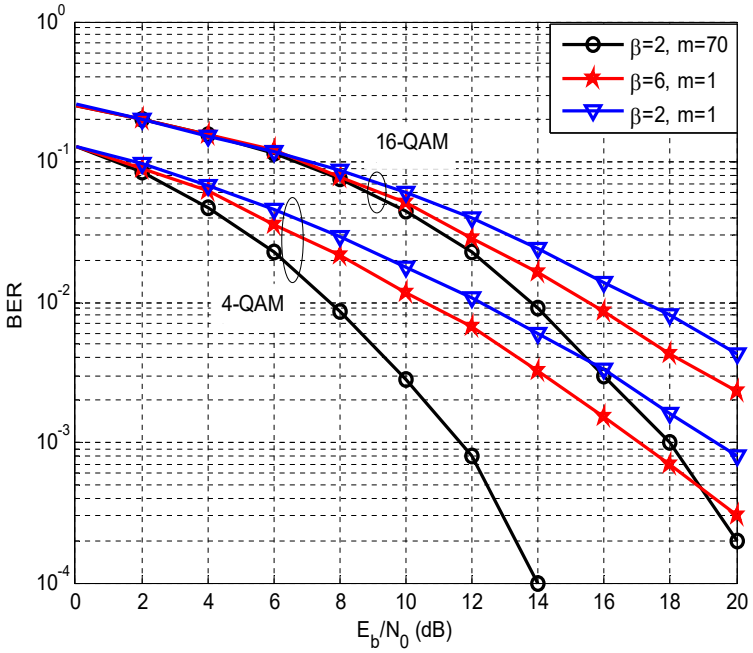

Fig. 5.4 BER of OSTBC-MIMO system with antenna selection $L = 2$ and $N_t = 4$

It is shown in Fig. 5.4 that 4-QAM outperforms that of 16-QAM by selecting 2 out of 4 transmit antennas. For low values of SNR, 16-QAM gives improved BER performance even in the severely faded environment ($\beta = 2, m = 1$). By increasing β from 2 to 6 approximately 5dB less SNR is required for 4-QAM compared to 16-QAM. At $\beta = 2, m = 70$, BER performance approximates the BER performance in Rayleigh fading [24]. Consequently, system performance improves with the increase in β and m.

5.6 Conclusion

In this chapter, the capacity performance of MIMO system is evaluated using optimal and sub-optimal AS techniques. We concluded from the simulation results that sub-optimal AS approaches the optimal performance with reduced complexity and cost. OSTBC-MIMO system gives reduced error rate using 2 out of 4 transmit antenna with 4-QAM compared to 16-QAM. Consequently, higher modulation order and less value of shape parameters degrade the system performance.

CHAPTER 6

MIMO Weibull-Gamma Fading Channel Subject to AWGGN

6.1 Introduction

In the previous chapters, we analyzed MIMO system performance in AWGN noise scenario. In [133-135], wireless system performance has been analyzed over multipath fading channel in the presence of AWGN. However, the actual noise can deviate from AWGN which demands the requirement of a generic noise model and hence, we require a generalized noise distribution. In this chapter, we consider a generalized noise model for analyzing the MIMO system performance over WG fading channel using appropriate detection techniques.

We have used a simple detection i.e. OSIC with MMSE for the error rate performance improvement in a composite fading scenario in the presence of generalized noise [182]. Among all the detection ordering (SNR based, column norm based and SINR based) SINR based ordering gives enhanced error rate performance. Thus, we used it in our analysis. We have seen that post detection SINR based ordering offers the best performance among all three ordering techniques [24]. Therefore, MMSC-OSIC detection is prefereed to achieve the improved error rate performance with acceptable complexity level under composite fading. Maximum likelihood detection is used at the expense of system complexity to achieve the optimal error rate performance. Later on, MMSE-OSIC with candidates (MMSE-OSIC^2) [75] technique is proposed which gives a near ML performance with a complexity level comparable to that of traditional MMSE-OSIC and effectively generates the LLR values. Therefore, to improve the error performance of MIMO system, this technique is considered in this chapter.

The generalized Gaussian distribution (GGD) is considered to be a developing research area to model different noise effects. This generic noise model reflects various forms of noise such as impulsive, gamma, Gaussian, Laplacian [140, 183, 184]. Authors [185], have analyzed the performance over multipath fading channel in AWGGN scenario. The average symbol error probability (ASEP) has been computed for rectangular-QAM using Gaussian Q-function in composite fading scenario disturbed by additive white generalized Gaussian noise (AWGGN) [145], where, rectangular-QAM is generated by combining in-phase and quadrature-phase pulse amplitude modulation (PAM) signals.

This chapter evaluates the MIMO system performance over composite WG fading channel with the exixtence of generalized noise. SM is preferred to improve the MIMO system performance with simple detection i.e. MMSE-OSIC, optimal detection i.e. ML and an efficient detection i.e. MMSE-OSIC^2. The resulting expressions of ASEP in [145] are evaluated again which were earlier restricted to SISO system. The higher order modulation is preferred to attain the high data rate of the wireless link, although, they provide less flexibility to noise and interference. We computed exact analytical expressions in terms of Fox-H function (FHF) [186] for 16-QAM in MIMO WG fading perturbed by AWGGN. Two special cases of AWGGN namely AWGN and Laplacian noise are taken into account considering later's ability to model impulsive noise with significant accuracy. We have also demonstrated the variations of fading and shadowing parameters.

The remainder of the chapter is arranged as follows. Section 6.2 provides the system and channel model. ASEP for M-QAM is described in Section 6.3. In Section 6.4, we provided simulation results and analysis for ASEP of SM-MIMO in WG fading along with generic noise using specified detection technique. Finally, Section 6.5 concludes the chapter.

6.2 System and Channel Model

In a MIMO system, transmit signal X is modulated by 16-QAM and X is multiplied by a composite flat fading channel envelope H. Earlier, we have considered AWGN noise to evaluate system performance. Nevertheless, this section undertakes $\mathcal{N}$ as an AWGGN noise in (1.4) instead of AWGN with zero mean and $N_0/2$ variance.

AWGGN noise PDF is presented in [187, Equation (6.2)] over $n \in \mathbb{R}$ as

$$p_{\mathcal{N}}(n|m_n,\sigma,\eta) = \frac{\eta\,\psi}{2\Gamma(1/\eta)}\exp(-\psi^{\eta}|n-m_n|^{\eta}) \tag{6.1}$$

where η and m_n represent shaping parameter of $\mathcal{N}$ and mean respectively ($\eta \in \mathbb{R}^+, m_n \in \mathbb{R}^+$). Besides, we can define the coefficient ψ by normalizing the noise power and coefficient ψ_0 relating to η as

$$\psi = \frac{\psi_0}{\sigma} = \sqrt{\frac{2\Gamma(3/\eta)}{N_0\Gamma(1/\eta)}} \tag{6.2}$$

where $\psi_0 = \sqrt{\frac{\Gamma(3/\eta)}{\Gamma(1/\eta)}}$ and parameter $\sigma^2 = E[\mathcal{N}^2] - {m_n}^2 = N_0/2$ implies the AWGGN variance.

The random variable of AWGGN distribution strictly dependent on its shaping parameter η. This distribution provides a superior fitting to the measured noise statistics with the varying physical

channel environments and creates different noise categories as special cases of AWGGN. When η = 2, η = 1, $\eta = 0.5$ and $\eta = 0$, it exemplifies the Gaussian, Laplacian, gamma and impulsive noise respectively as shown in Table 6.1. Subsequently, statistical properties and accurate simulation technique have been established for $\eta = 1/2$ and $\eta = 1/3$ in the existence of AWGGN [188].

Table 6.1 Type of noise and its noise parameter

Noise shaping parameter	Type of Noise
η = 2	Gaussian
η = 1	Laplacian
$\eta = 0.5$	Gamma
$\eta = 0$	Impulsive

WG distribution is formed by simplifying the PDF of the received signal envelope Y given in [189] defined over $y \in (0, \infty)$ and expressed as

$$p_Y(y) = \frac{2}{\Gamma m}\left[\frac{(m+1)\Gamma\left(1+\frac{1}{\kappa}\right)}{\Omega}\right]^m y^{2m-1}\,\Gamma\left[\left(1-\frac{m}{\kappa}\right), 0, \left(\frac{(m+1)\Gamma\left(1+\frac{1}{\kappa}\right)}{\Omega}\right)^m y^2, 1/\kappa\right] \tag{6.3}$$

where $\Gamma(.,.,.,.)$ denotes extended incomplete gamma function, represented as $\Gamma(\xi, s, a, \mu) = \int_s^\infty y^{\xi-1}\exp(-y - ay^{-\mu})\,dy$, $(x \in \mathbb{R}^+)$, $(\xi, a, \mu) \in \mathbb{C}$ [187, Equation (6.2)]. κ and m are fading figure (diversity severity/order) and shadowing shaping parameter respectively, where $0.5 \leq \kappa < \infty, 0 \leq m < \infty$. Here, $\Omega = E[Y^2]$ $(0 \leq \Omega < \infty)$ denotes the average power of the received signal envelope.

The SNR γ for received symbols subjected to AWGGN follows WG PDF, characterized over $\gamma \in (0, \infty)$. The average SNR per symbol is denoted as $\bar{\gamma} = E[\gamma] = E[Y^2]E_s/N_0$. PDF is simplified in the form of SNR by exchanging variables and given as

$$p_\gamma(\gamma) = \frac{1}{\Gamma m}\left[\frac{(m+1)\Gamma\left(1+\frac{1}{\kappa}\right)}{\bar{\gamma}}\right]^m \gamma^{m-1}\,\Gamma\left[\left(1-\frac{m}{\kappa}\right), 0, \left(\frac{(m+1)\Gamma\left(1+\frac{1}{\kappa}\right)}{\bar{\gamma}}\right)^m \gamma, 1/\kappa\right] \tag{6.4}$$

Equation (6.4) is represented in the form of FHF applying [187, Equation (6.22), 190, Equations (2.1.4), (2.1.5) and (2.1.11)] and simplifying [191, Equation 8] as

$$p_\gamma(\gamma) = \frac{1}{\Gamma m\,\gamma} H_{0,2}^{2,0}\left[\frac{(m+1)\Gamma\left(1+\frac{1}{\kappa}\right)\gamma}{\bar{\gamma}}\middle|_{\left(1,\frac{1}{\kappa}\right),(m,1)}^{-}\right] \tag{6.5}$$

where $H_{p,q}^{m,n}\left[z\middle|\begin{matrix}(a_j,A_j)_{1,p}\\(b_k,B_k)_{1,q}\end{matrix}\right]=\frac{1}{2\pi i}\int_c^{-}\frac{\prod_{k=1}^{m}\Gamma(b_k,B_k s)\prod_{j=1}^{n}\Gamma(1-a_j,A_j s)}{\prod_{k=n+1}^{p}\Gamma(a_j,A_j s)\prod_{k=m+1}^{q}\Gamma(1-b_k,B_k s)}z^{-s}ds$, $H_{p,q}^{m,n}(.)$ is FHF defined in [190, Equation (1.1.1), 192] and c represents Mellin-Barnes contour.

6.3 Average Symbol Error Probability for *M*-QAM

The symbol error probability is given in [133, Equation (10)] for QAM in the presence of AWGN. M-QAM signal constellation is given by two independent in-phase and quadrature M-ary PAM signals, where M_I-ary PAM and M_Q-ary PAM are in-phase and quadrature signals respectively and $M=M_I M_Q$. Given that, GGD and Gaussian distribution demonstrate the identical symmetry properties. According to [145], the identical symmetry properties can be used to define SEP of M-QAM, given as

$$p(SEP)=2\left(1-\frac{1}{M_I}\right)\mathcal{Q}_\eta\left(\mathcal{A}_I\right)+2\left(1-\frac{1}{M_Q}\right)\mathcal{Q}_\eta\left(\mathcal{A}_Q\right)-4\left(1-\frac{1}{M_I}\right)\left(1-\frac{1}{M_Q}\right)\mathcal{Q}_\eta(\mathcal{A}_I)\mathcal{Q}_\eta(\mathcal{A}_Q) \tag{6.6}$$

where $\mathcal{A}_I=\frac{\mathcal{D}_I}{\sigma},\mathcal{A}_Q=\frac{\mathcal{D}_Q}{\sigma}$, $\mathcal{D}_I$ and $\mathcal{D}_Q$ denote the decision distances for in-phase and quadrature phase components respectively. $\mathcal{Q}_\eta(.)$ is generalized-$\mathcal{Q}$ function for $x\geq 0$ defined in [191] as

$$\mathcal{Q}_\eta(x)=\frac{\eta\,\psi_0}{2\Gamma(1/\eta)}\int_x^\infty e^{-\psi_0{}^\eta t^\eta}\,dt \tag{6.7}$$

In [191, (A.5)], the representation of (6.7) in the form of FHF using [192, Equation (8.3.2/21), (A.4)] is given as

$$\mathcal{Q}_\eta(x)=\frac{1}{2\Gamma(1/\eta)}H_{1,2}^{2,0}\left[\psi_0{}^\eta|x|^\eta\middle|\begin{matrix}(1,1)\\(1/\eta,1),(0,1)\end{matrix}\right] \tag{6.8}$$

The ASEP is obtained by averaging the conditional SEPs in (6.6) under slow fading conditions over the PDF of γ. Then, $p_\gamma(\gamma)$ is represented by

$$pr(S_e)=2\left(1-\frac{1}{M_I}\right)\mathfrak{T}(\mathcal{A}_I)+2\left(1-\frac{1}{M_Q}\right)\mathfrak{T}\left(\mathcal{A}_Q\right)-4\left(1-\frac{1}{M_I}\right)\left(1-\frac{1}{M_Q}\right)\mathfrak{J} \tag{6.9}$$

$$\text{where } \mathfrak{T}(x)=\int_0^\infty\mathcal{Q}_\eta\left(\sqrt{\gamma}x\right)p_\gamma(\gamma)d\gamma \tag{6.10}$$

$$\mathfrak{J}=\int_0^\infty\mathcal{Q}_\eta\left(\sqrt{\gamma}\mathcal{A}_I\right)\mathcal{Q}_\eta\left(\sqrt{\gamma}\mathcal{A}_Q\right)p_\gamma(\gamma)d\gamma \tag{6.11}$$

It is difficult to formulate $\mathfrak{T}(.)$ and $\mathfrak{J}$ using the conventional expressions of WG distribution and GGD. Therefore, alternative expressions (6.5) and (6.8) are used to compute simplified analytical expressions for $\mathfrak{T}(.)$and $\mathfrak{J}$ and then resulting expression for the ASEP. In (6.10), $\mathfrak{T}(x)$ consists of

an integral including the product of two FHFs which is comparable to that of [191] considering the normalized value of fading shaping factor and severity of shadowing. Unlike [191], we prefer an efficient SINR based ordering for MMSE detection to enhance the error rate performance of MIMO system. Using [145] and [190, Equation (1.1.1)], $\mathfrak{T}(x)$ can be represented in the form of FHF by a closed form expression given as

$$\mathfrak{T}(x) = \frac{1}{\eta\Gamma(1/\eta)\Gamma m} H_{2,3}^{2,2}\left[\frac{(m+1)\Gamma\left(1+\frac{1}{\kappa}\right)}{x^2{\psi_0}^2\bar{\gamma}}\middle|\begin{matrix}\left(1-\frac{1}{\eta},\frac{2}{\eta}\right),\left(1,\frac{2}{\eta}\right)\\ (1,1/\kappa),(m,1),(0,2/\eta)\end{matrix}\right] \tag{6.12}$$

$$\mathfrak{J} = \frac{1}{2\eta\Gamma(1/\eta^2)\Gamma m} H_{2,1;0,2;1,2}^{0,2;2,0;2,0}\left[\frac{(m+1)\Gamma\left(1+\frac{1}{\kappa}\right)}{\mathcal{A}_I{}^2{\psi_0}^2\bar{\gamma}}, \left(\frac{\mathcal{A}_Q}{\mathcal{A}_I}\right)^{\eta}\middle|\begin{matrix}\left(1-\frac{1}{\eta},\frac{2}{\eta},1\right),\left(1;\frac{2}{\eta},1\right),\left(0;\frac{2}{\eta},1\right)\\ \left(1,\frac{1}{\kappa}\right),(m,1),(1,1),\left(\frac{1}{\eta},1\right),(0,1)\end{matrix}\right] \tag{6.13}$$

Substituting (6.5) and (6.8) in (6.11), an integral which includes the product of three FHFs is used to describe (6.13). Then, using [193, Equation (2.3)], $\mathfrak{J}$ is represented in terms of the FHF of two variables identified as the Bivariate Fox H-function (BFHF).

Substituting (6.12) and (6.13) in (6.9), we computed the ASEP of M-QAM. This ASEP expression is given for rectangular ($M_I \neq M_Q$), square ($M_I = M_Q$) QAM in arbitrary WG fading with AWGGN. Consequently, it maintains substantial range of noise and fading parameters. The commonly considered noise cases of AWGGN in composite fading scenario are as follows

Case 1: WG Fading with Laplacian Noise

The first special case of AWGGN occurs when η = 1, and the noise is considered as Laplacian. Taking η = 1, $\mathfrak{T}(x)$ is represented as

$$\mathfrak{T}(x) = \frac{1}{\Gamma m} H_{2,3}^{2,2}\left[\frac{(m+1)\Gamma\left(1+\frac{1}{\kappa}\right)}{2x^2\bar{\gamma}}\middle|\begin{matrix}(0,2),(1,2)\\ (1,1/\kappa),(m,1),(0,2)\end{matrix}\right] \tag{6.14}$$

Using [190, 193], FHF and BFHF functions are well explored and utilized to make a simplified form of (6.14) by reducing number of terms in $H_{\cdot,\cdot}^{\cdot,\cdot}(.)$ as

$$\mathfrak{T}(x) = \frac{1}{\Gamma m} H_{1,2}^{2,1}\left[\frac{(m+1)\Gamma\left(1+\frac{1}{\kappa}\right)}{2x^2\bar{\gamma}}\middle|\begin{matrix}(1,2)\\ (1,1/\kappa),(m,1)\end{matrix}\right] \tag{6.15}$$

Similarly, $\mathfrak{J}$ can be written as

$$\Im = \frac{1}{2\Gamma m} H_{2,1;0,2;1,2}^{0,2;2,0;2,0}\left[\frac{(m+1)\Gamma\left(1+\frac{1}{\kappa}\right)}{2\mathcal{A}_I{}^2\bar{\gamma}}, \left(\frac{\mathcal{A}_Q}{\mathcal{A}_I}\right)\middle|\begin{matrix}(0;2,1),(1;2,1),(0;2,1)\\ \left(1,\frac{1}{\kappa}\right),(m,1),(1,1),(1,1),(0,1)\end{matrix}\right] \tag{6.16}$$

Using [193, Equation (1.1)], for the description of BHFH and [187, Equations (6.29) and (6.42)], $\Im$ is represented as

$$\Im = \frac{1}{2\Gamma m} H_{1,2}^{2,1}\left[\frac{(m+1)\Gamma\left(1+\frac{1}{\kappa}\right)}{2(\mathcal{A}_I{}^2+\mathcal{A}_Q{}^2)\,\bar{\gamma}}\middle|\begin{matrix}(1,2)\\ \left(1,\frac{1}{\kappa}\right),(m,1)\end{matrix}\right] \tag{6.17}$$

Equations (6.15) and (6.17) are used to calculate ASEP when Laplacian noise is present.

Case 2: WG Fading with AWGN

For $\eta = 2$, (6.12) and (6.13) can be re-arranged to find the ASEP in AWGN environment. Again, the expressions for $\mathfrak{T}(x)$ and $\Im$ are reduced as

$$\mathfrak{T}(x) = \frac{1}{2\sqrt{\pi}\,\Gamma m} H_{2,3}^{2,2}\left[\frac{(m+1)\Gamma\left(1+\frac{1}{\kappa}\right)}{2x^2\bar{\gamma}}\middle|\begin{matrix}\left(\frac{1}{2},1\right)(1,1)\\ \left(1,\frac{1}{\kappa}\right),(m,1),(0,1)\end{matrix}\right] \tag{6.18}$$

$$\Im = \frac{1}{14.5\,\Gamma m} H_{2,1;0,2;1,2}^{0,2;2,0;2,0}\left[\frac{(m+1)\Gamma\left(1+\frac{1}{\kappa}\right)}{2\,\mathcal{A}_I{}^2\bar{\gamma}}, \left(\frac{\mathcal{A}_Q}{\mathcal{A}_I}\right)^2\middle|\begin{matrix}\left(\frac{1}{2},1,1\right),(1;1,1),(0;1,1)\\ \left(1,\frac{1}{\kappa}\right),(m,1),(1,1),\left(\frac{1}{2},1\right),(0,1)\end{matrix}\right] \tag{6.19}$$

Here, $m \to \infty$ eliminates the effect of shadowing. For $m \to \infty$, WG approximates Weibull distribution and $m \to \infty, \kappa = 1$ converts WG distribution into Rayleigh distribution [189, Table 1]. Thus, the fading scenario can be changed by setting the parameters m and κ.

Initially, we considered OSIC technique that offers diversity order greater than $N_r - N_t + 1$ for all symbols. Following the ordering approach, the diversity order of the first detected symbol is also greater than $N_r - N_t + 1$. Nevertheless, the diversity order of remaining symbols depends on either the formerly detected symbols are exact or not. Suppose, all the symbols are exact, then, the diversity order of the i-th detected symbol is $N_r - N_t + i$. The i-th detected symbol is different from the one transmitted from the i-th transmit antenna. Since, the ordering is based on SINR for MMSE detection, therefore, (3.13) is used to improve the ASEP performance. Then, we used ML detection and compared the ASEP performance with the efficient MMSE-OSIC^2. We considered γ and $\bar{\gamma}$ according to MMSE-OSIC, ML and MMSE-OSIC^2 which is given in chapter 3. Taking $\mathcal{M}$=1 in MMSE-OSIC^2 detection, the required number of multiplications, divisions and iterations are same

as given in Table 3.3(a). It has been observed that less number of mathematical operations are required in MMSE-OSIC^2 than ML. We proposed the following algorithm for the error rate using MMSE-OSIC^2 in AWGGN scenario.

Algorithm: Error rate calculation using MMSE-OSIC^2 detection with AWGGN

Input (N_t, N_r, *X, g, s*, m, Ω, κ, $\mathcal{N}$)
Output (H, S_M, *nErr*, S_p)
BEGIN
Step 1: Variable declaration
N_t: *Number of transmit antenna*
N_r: *Number of receive antenna*
g: *gamma random variable*
s: *Weibull random variable*
m: *shadowing parameter*
Ω: *average power*
κ: *fading figure*
$\mathcal{N}$: *AWGGN*
H: *WG channel*
S_M:*16-QAM Modulated symbol*
nErr: Number of errors count
S_p= *Symbol error probability*
n =*noise distance*
$Q_n(\sqrt{X})$: *Generalized Q-function*
$\mathcal{M}$ = *number of candidate vectors*
C_P= *signal constellation*
Step 2: Data Transmission
for *ii* ← *1: length (SNR)*
S_M *generation*
Step 3: Channel generation and AWGGN noise addition
$H \leftarrow g * s$, $\{g \sim gamma\ (m, \Omega, N_r, N_t)$ *and* $s \sim Weibull\ (\kappa, N_r, N_t)\}$
Squeeze (Sum (H.S_M,2)) + 10^(-$E_b N_0$(ii)/20) * $\mathcal{N}$, {$\mathcal{N} \sim Q_n(\sqrt{X})$}*
if $n \leftarrow 0$
Impulsive noise
elseif $n \leftarrow 0.5$
Gamma noise
elseif $n \leftarrow 1$
Laplacian noise
elseif $n \leftarrow 2$
Gaussian noise
elseif $n \leftarrow \infty$
Uniform noise
end
end
end
end
end
Step 4: Detection using MMSE-OSIC^2 technique
$|h_k|^2$, *k=i,i+1....N_t, (i=1, first stage) based ordering*
Temporary vector generation $\mathcal{M} \times |C_P|$ *of length* N_t,
Selection of $\mathcal{M}$ *candidate vector of length* N_t

Selected $\mathcal{M}$ candidate vectors of length N_t ***then***
Truncated and stored as x_i

Step 5: Reception
Received data
nErr=(modulated symols- demodulated symbols) ***then***
S_p=nErr/Total no. of symbols

end
END

6.4 Simulation Results

We used 16-QAM modulation to evaluate the MIMO system performance, as a function of SNR for the generalized case of noise. Therefore, distinct values of η and arbitrarily values of m and κ are taken into consideration. The in-phase-to-quadrature phase decision distance ratio is represented as $R_{ddr} = \frac{\mathcal{D}_Q}{\mathcal{D}_I} = \frac{\mathcal{A}_Q}{\mathcal{A}_I}$. For this case, the average total energy per symbol $\mathrm{E_T}$ is given as $\mathrm{E_T} = 10.5\bar{\gamma}\,{\mathcal{D}_I}^2 + 2.5\bar{\gamma}\,{\mathcal{D}_Q}^2 = 0.5\left(21 + 5{R_{ddr}}^2\right)\bar{\gamma}\,{\mathcal{D}_I}^2$ and hence $\mathrm{E_T}/\sigma^2 = 0.5\left(21 + 5{R_{ddr}}^2\right)\bar{\gamma}\,{\mathcal{A}_I}^2$ [145]. Taking a fixed $R_{ddr} = (10.5)^{1/2}$, the identical average energies of the in-phase and quadrature signals are obtained.

The R_{ddr} provides a way to assess system performance. When $R_{ddr} = 1$, the most favorable case occurs, this implies that the in-phase and quadrature distance are identical for both the Laplacian and Gaussian noise. For $R_{ddr} = (10.5)^{1/2}$, same energy is obtained between the in-phase and quadrature signal thus the system performance is reduced with a small amount i.e. approximately 1dB SNR reduction for large SNRs. When the quadrature signal contains 10.5 times the average energy of the in-phase signal, for this instant loss is more essential as it gets approximately 4dB SNR loss for large SNRs, comparative to the aforementioned case, where $R_{ddr} = 1$.

Firstly, we considered the composite WG fading in Laplacian noise scenario. The parameters are setted to $m \to \infty$ and $m \to \infty, \kappa = 1$ to obtain Weibull and Rayleigh fading respectively. Fig. 6.1 and Fig. 6.4 depict the ASEP as a function of average SNR per symbol $\mathrm{E_T}/\sigma^2$ for both Gaussian and Laplacian cases of noise. In addition, distinct values of m and κ are chosen to determine the severity of fading. Analytical results are presented by (6.12) and (6.13) demonstrate the perfect match of the simulation results. The performance of the system is improved with increased values of both the parameters m and κ. Results shown in Fig. 6.1 and Fig. 6.4 show that the ASEP performance in Laplacian noise is superior than that of Gaussian noise for lower SNR or less than 15dB SNR. However, for high SNR, less fading ($\kappa \geq 2$), the situation is reversed, and ASEP

performance improves in the Gaussian noise than Laplacian noise. For severe fading (m = 0.5), Laplacian noise offers better results than Gaussian noise. We used three detection techniques namely MMSE-OSIC, ML and MMSE-OSIC^2 for error rate performance improvement of system. Although a comparison between Fig. 6.1 and Fig. 6.4 illustrates that by taking κ =5, m =5 at 10^{-4} ASEP, ML and OSIC^2 required approximately 3dB and 4dB less SNR than OSIC technique in Gaussian noise and Laplacian noise scenario respectively.

Afterward, the special cases of WG fading i.e, Weibull and Rayleigh fading are considered. In Fig. 6.2 and Fig. 6.5, Rayleigh fading case is taken into account. In this case, the system gives a superior performance by diminishing η, which validates the previous result in which the Laplacian noise gives better performance than the Gaussian noise in severe fading. It was previously mentioned that large fading parameter refers to less fading. In Fig. 6.3 and Fig. 6.6, the ASEP is demonstrated as a function of the SNR per QAM symbol in Weibull fading environment (κ=5) with AWGGN for which $\eta = 8, 2, 0.5, 0.25$. In this case, when the less fading condition occurs, the different two regions are investigated. At low SNR, the ASEP degrades with the increased values of η and at high SNR it improves by increasing η.

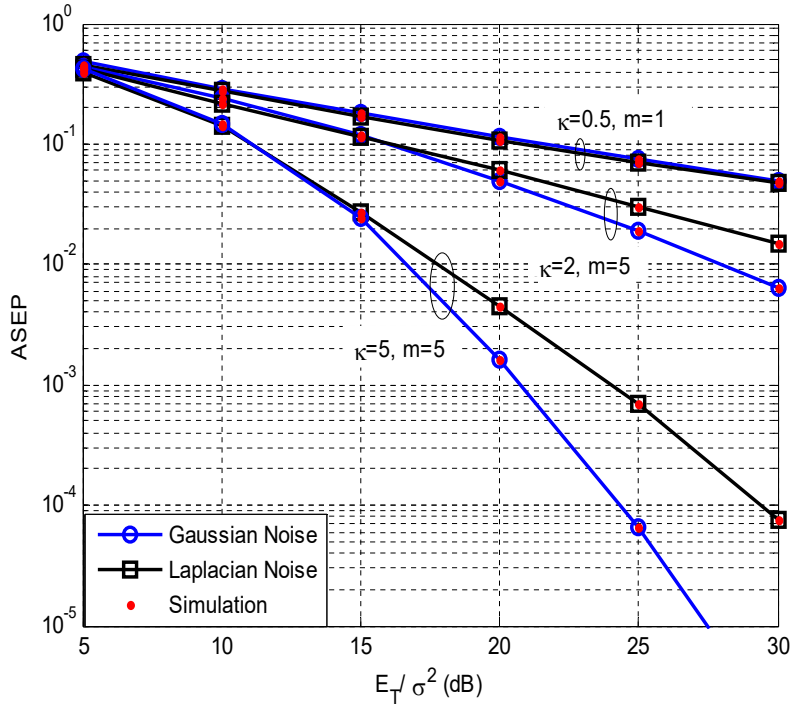

Fig. 6.1 ASEP of MIMO system for 16-QAM using MMSE-OSIC detection over WG fading channel subject to Laplacian and Gaussian noise when $N_t = N_r = 2$

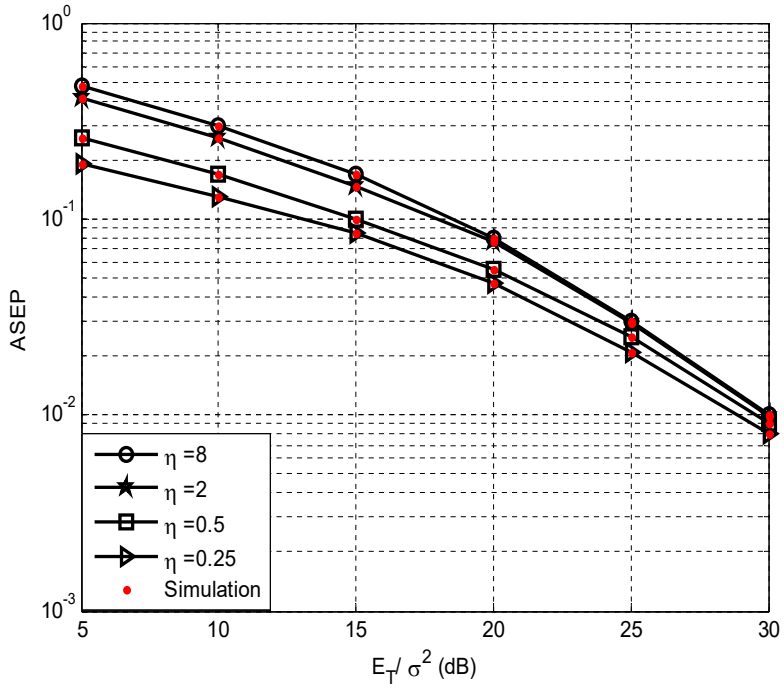

Fig. 6.2 ASEP of MIMO system for 16-QAM using MMSE-OSIC over Rayleigh fading channel with arbitrarily values of η when $N_t = N_r = 2$

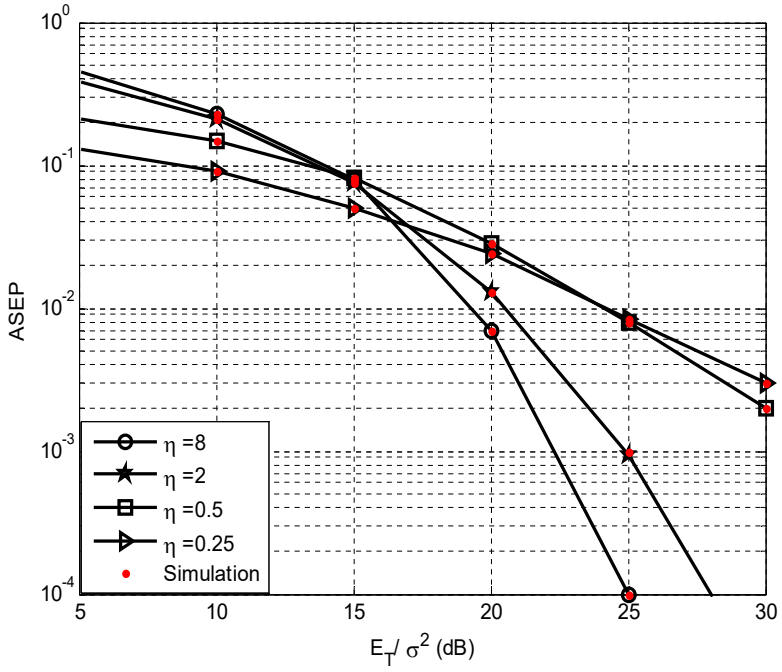

Fig. 6.3 ASEP of MIMO system for 16-QAM using MMSE-OSIC detection over Weibull fading channel ($\kappa = 5$) with arbitrarily values of η when $N_t = N_r = 2$

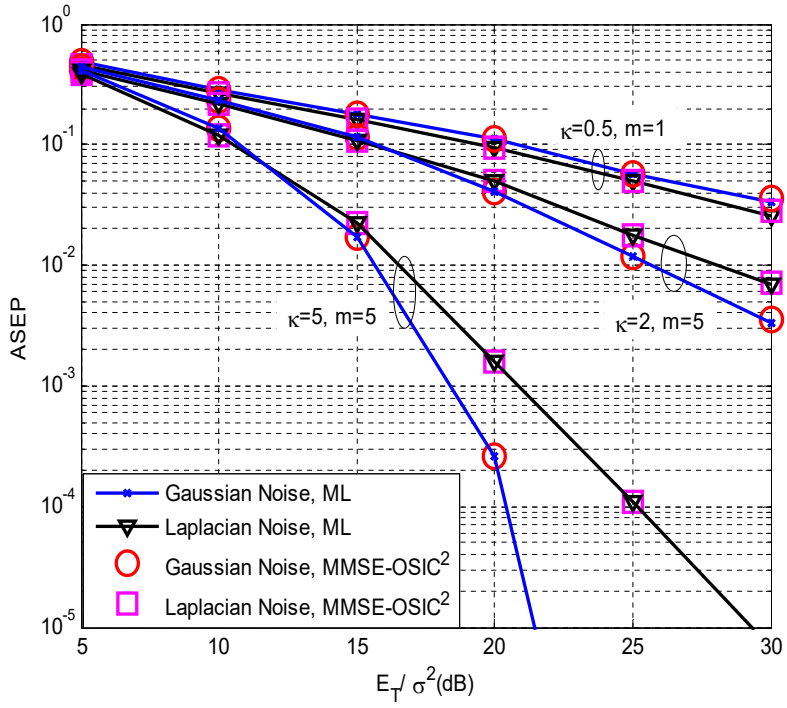

Fig. 6.4 ASEP of MIMO system using ML and MMSE-OSIC^2 detection ($\mathcal{M}$=1) over WG fading channel subject to Laplacian and Gaussian noise when $N_t = N_r = 2$

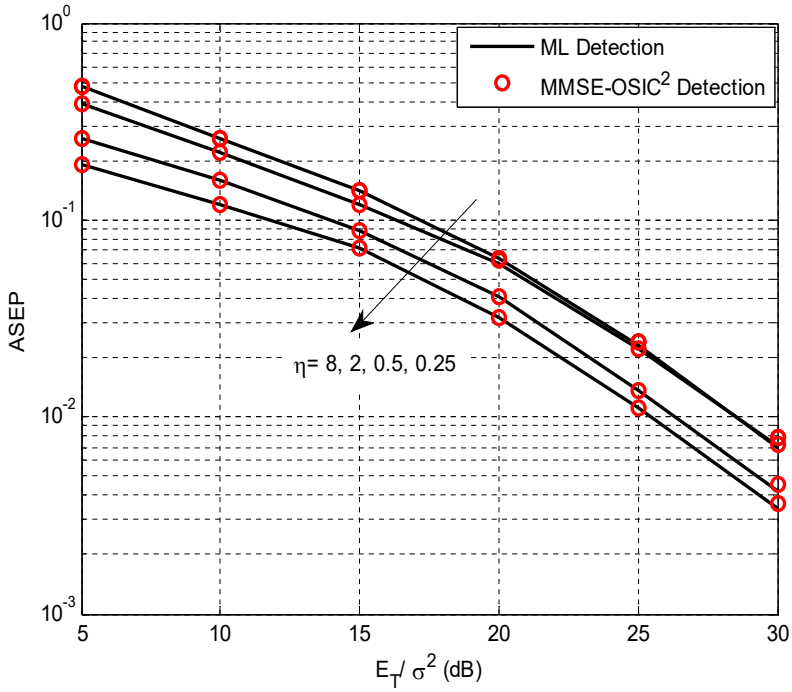

Fig. 6.5 ASEP of MIMO system for 16-QAM using ML and MMSE-OSIC^2 ($\mathcal{M}$=1) over Rayleigh fading channel with arbitrarily values of η when $N_t = N_r = 2$

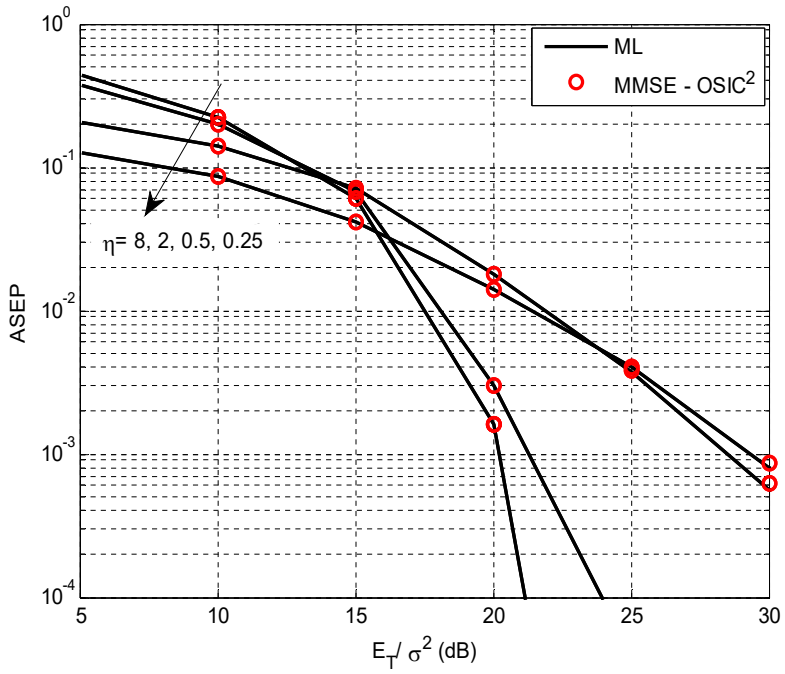

Fig. 6.6 ASEP of MIMO system for 16-QAM using ML and MMSE-OSIC^2 detection ($\mathcal{M}$=1) over Weibull fading channel ($\kappa = 5$) with arbitrarily values of η when $N_t = N_r = 2$

In MMSE-OSIC^2, ASEP performance is slightly reduced at the high SNR than ML. Also, the complexity level is comparable to traditional MMSE-OSIC. Also, MMSE-OSIC^2 detection constructively generates LLR values. Therefore, this detection technique gives conformity between improved performance and an acceptable level of complexity. Comparing all three-detection technique, MMSE-OSIC^2 delivers the superior performance by managing the complexity issue with improved performance. It can be seen from Fig. 6.1 to Fig. 6.6 that MMSE-OSIC^2 illustrates the decreasing error rate at high SNRs while at low SNR slight improvement in the error rate performance can be seen.

6.5 Conclusion

This chapter evaluates the ASEP performance of MIMO system in composite WG fading environment subject to AWGGN. MMSE-OSIC, ML and MMSE-OSIC^2 detection are used to analyze the MIMO system performance. In which, MMSE-OSIC offers simplicity at the cost of below optimal performance. Thus, MMSE-OSIC^2 is proposed to achieve the optimal performance like ML with reduced number of complex operations. Simulation results illustrate that ASEP performance is highly improved at high SNR compared to low SNR in ML followed by MMSE-OSIC^2. Analytical expressions for ASEP are derived using 16-QAM containing two independent in-

phase and quadrature signals of PAM. The MMSE-OSIC detection is for improving the error rate performance of MIMO system. We conclude from the results that the ASEP performance in Laplacian noise is better than that of Gaussian noise for low SNR. However, in less fading, performance is degraded for high SNR, and improved error performance is obtained in Gaussian noise than Laplacian noise. In severe fading, improved error rate performance is achieved in the presence Laplacian noise than Gaussian noise. In Rayleigh fading case, the system offers superior performance for low noise shaping parameter η. This result again proves that the Laplacian noise gives the better performance than the Gaussian noise in severe fading. In Weibull fading, the different two regions are inspected for less amount of fading or large fading parameter. Moreover, the ASEP reduces with η at low SNR and it increases by η at high SNR.

CHAPTER 7

Conclusion and Future Scope

In this work, we used OSTBC to achieve transmit diversity and MRC to support receiver diversity separately for analyzing error rate performance of MIMO system under different multipath fading such as Rayleigh, Rician, Nakagami-*m* and Weibull. We have demonstrated that MRC with lower modulation order always leads to the low error rate. Consequently, for the same SER, less SNR is required for BPSK and QPSK than 16-QAM. Thus, diversity techniques with suitable digital modulation using multiple antenna systems has a potential to increase the reliability and throughput. Then, the effects of double Weibull fading which shows the cascaded nature of channel has also been presented which depicts that degraded performance is obtained in double-Weibull fading environment compared to single-Weibull fading. As the fading parameter increases for any modulation technique, the required SNR gap between single and double-Weibull fading decreases.

After multipath fading models and cascaded channel model (i.e., double-Weibull), a composite Weibull-gamma (WG) channel model is used that considers multipath fading along with shadowing. The performance evaluation of MIMO systems in WG fading channels is limited, generally due to the difficulty to deal with the non-Gaussian nature of the fading coefficients. Thus, we used AF to evaluate different channel conditions. Furthermore, we analyzed the error rate performance using the same diversity techniques (i.e., OSTBC and MRC) and different competent detection techniques. We clearly showed that from the results that MRC provides 3dB error performance gain compared to OSTBC in less fading and severe fading environment, however, OSTBC offers a better computational complexity. For the statistical measurement of the system, we have also described PDF, CDF and AF. The mathematical and the simulation analysis provide the worth and flexibility of proposed channel model. We offered MMSE-OSIC, ML as well as less complex and approximate optimal detection technique i.e. MMSE-OSIC^2 for MIMO system analysis under WG fading scenario. MMSE-OSIC^2 contains a number of candidate vectors where candidate selection depends on the ML metric values those are applicable to calculate LLR values. A comparative analysis of the proposed technique is obtained with MMSE-OSIC and ML detection techniques on the basis of both computational complexity and error rate performance. In the MMSE-OSIC^2 technique, no additional calculation is required to get LLR values for all bits. Thus, simulation results illustrate that MMSE-OSIC^2 signal detection technique gives a near-ML performance. Consequently, the

complexity is comparable to MMSE-OSIC technique. Also, small values of shape parameters produce system performance degradation. MIMO system performance improves with the increase in a number of transmit/receive antennas, fading and shadowing parameters.

Then, we evaluated the system performance considering the same scenario in low SNR regime. We showed that the WG fading model illustrates a broad range of agreement with measured data for several environment conditions. A comprehensive low SNR analysis of MIMO system with suitable detection and diversity is presented in WG fading scenario. Novel maganeable expressions for $E_b/N_{0_{min}}$ and S_0 are deduced. The proposed analysis of MIMO system deals with three techniques, namely, SM with the optimal detection, SM with the MMSE detection and OSTBC. The average capacity of OSTBC systems is usually subsidiary to that of capacity-oriented SM MIMO techniques, whereas OSTBC system is a diversity-oriented technique.

Antenna selection analyzes further improvement in the system performance. Thus, we preferred optimal and sub-optimal detection techniques to evaluate the capacity. In which, less complex sub-optimal detection is preferably used in WG fading scenario. The capacity for different selected antennas in descending order using sub-optimal AS technique approaches the capacity of optimal AS technique with reduced complexity. However, the selection complexity in descending order is greater than that of ascending order. Consequently, OSTBC-MIMO system gives reduced error rate using 2 out of 4 transmit antenna with 4-QAM compared to 16-QAM.

In next step, we evaluated the ASEP performance of MIMO system in composite WG fading environment subject to AWGGN using MMSE-OSIC, ML and MMSE-OSIC^2. We concluded that the ASEP performance in Laplacian noise is better compared to that of Gaussian noise for low SNR. However, in less fading, system performance is degraded for high SNR, and improved error performance is obtained in Gaussian noise than Laplacian noise. In severe fading, improved error rate performance is achieved in the presence of Laplacian noise than Gaussian noise. In Rayleigh fading case, the system offers superior performance for small noise shaping parameter η. This result again proves that the Laplacian noise gives the better performance than the Gaussian noise in severe fading. In Weibull fading case, the different two regions are inspected for less amount of fading or large fading parameter. Moreover, the ASEP reduces with η at low SNR and it increases by η at high SNR.

To make this work feasible and employable for more practical design of wireless system, we implant number of antennas at the base station to avoid the bulkiness of mobile units. However, the

overall improved system performance can be achieved at the expense of increased complexity or cost. Consequently, we consider all possible fading, shadowing and noise scenario using a composite channel model.

Cooperative networking has appeared as a prime segment of future wireless networks since it delivers high data rate communication over vast geographical areas. In this condition, distributed-MIMO (D-MIMO) arises as a promising tool for achieving substantial performance improvements in wireless systems, identical to those given by conventional MIMO in a point-to-point wireless radio channel. Therefore, the work proposed in this thesis can be extended by using antenna selection with transmit antenna selection (TAS)/MRC and D-MIMO system. Also, the AWGGN noise scenario can be considered using OSTBC/MRC in the same composite fading scenario. Furthermore, multi-user MIMO and fifth generation (5G) evolutionary massive MIMO system performance can be analyzed in such scenario for further performance enhancement by computing capacity and error rate.

REFERENCES

[1] G. J. Foschini, "Layered space-time architecture for wireless communication in a fading environment when using multi-element antennas," Bell labs technical journal, vol. 1, pp. 41-59, 1996.

[2] E. Telatar, "Capacity of Multi-antenna Gaussian Channels," European transactions on telecommunications, vol. 10, pp. 585-595, 1999.

[3] S. M. Alamouti, "A simple transmit diversity technique for wireless communications," IEEE Journal on selected areas in communications, vol. 16, pp. 1451-1458, 1998.

[4] V. Tarokh, H. Jafarkhani, and A. R. Calderbank, "Space-time block codes from orthogonal designs," IEEE Transactions on Information theory, vol. 45, pp. 1456-1467, 1999.

[5] V. Tarokh, H. Jafarkhani, and A. R. Calderbank, "Space-time block coding for wireless communications: performance results," IEEE Journal on selected areas in communications, vol. 17, pp. 451-460, 1999.

[6] K. Y. Jo, Satellite communications network design and analysis: Artech house, 2011.

[7] A. Paulraj, R. Nabar, and D. Gore, Introduction to space-time wireless communications: Cambridge university press, 2003.

[8] J. Ventura-Traveset, G. Caire, E. Biglieri, and G. Taricco, "Impact of diversity reception on fading channels with coded modulation. I. Coherent detection," IEEE Transactions on Communications, vol. 45, pp. 563-572, 1997.

[9] V. Tarokh, N. Seshadri, and A. R. Calderbank, "Space-time codes for high data rate wireless communication: Performance criterion and code construction," IEEE Transactions on Information theory, vol. 44, pp. 744-765, 1998.

[10] M. Jankiraman, Space-time codes and MIMO systems: Artech House, 2004.

[11] T. S. Rappaport, Wireless communications: principles and practice vol. 2: Prentice Hall PTR New Jersey, 1996.

[12] B. L. Hughes, "Differential space-time modulation," IEEE Transactions on Information theory, vol. 46, pp. 2567-2578, 2000.

[13] B. M. Hochwald and W. Sweldens, "Differential unitary space-time modulation," IEEE Transactions on Communications, vol. 48, pp. 2041-2052, 2000.

[14] S. Sandhu, R. Nabar, D. Gore, and A. Paulraj, "Introduction to Space-Time codes," Applications of Space-Time Adaptive Processing, IEE Publishers http://www. stanford. edu/group/sarg/sandhu062503. pdf (Accessed on 18/07/2015), 2003.

[15] E. Biglieri, R. Calderbank, A. Constantinides, A. Goldsmith, A. Paulraj, and H. V. Poor, MIMO wireless communications: Cambridge university press, 2007.

[16] G. Tsoulos, MIMO system technology for wireless communications: CRC press, 2006.

[17] L. M. Cortes-Pena, "MIMO Space-Time Block Coding (STBC): Simulations and Results," Design Project: Personal and Mobile Communications, p. 8, 2009.

[18] C. E. Shannon, "Communication in the presence of noise," Proceedings of the IRE, vol. 37, pp. 10-21, 1949.

[19] M. K. Simon and M.-S. Alouini, Digital communication over fading channels vol. 95: John Wiley & Sons, 2005.

[20] M.-S. Alouini and M. K. Simon, "An MGF-based performance analysis of generalized selection combining over Rayleigh fading channels," IEEE Transactions on Communications, vol. 48, pp. 401-415, 2000.
[21] A. Goldsmith, Wireless communications: Cambridge university press, 2005.
[22] M. H. Vu, "Exploiting transmit channel side information in MIMO wireless systems," Stanford University, 2006.
[23] B. Sklar, Digital communications vol. 2: Prentice Hall NJ, 2001.
[24] Y. S. Cho, J. Kim, W. Y. Yang, and C. G. Kang, MIMO-OFDM wireless communications with MATLAB: John Wiley & Sons, 2010.
[25] G. J. Foschini and M. J. Gans, "On limits of wireless communications in a fading environment when using multiple antennas," Wireless personal communications, vol. 6, pp. 311-335, 1998.
[26] K. S. Ahn, "Performance analysis of MIMO-MRC system in the presence of multiple interferers and noise over Rayleigh fading channels," IEEE Transactions on Wireless Communications, vol. 8, pp. 3727-3735, 2009.
[27] T. Kaiser, Smart Antennas: State of the Art vol. 3: Hindawi Publishing Corporation, 2005.
[28] N. C. Sagias and G. K. Karagiannidis, "Gaussian class multivariate Weibull distributions: theory and applications in fading channels," IEEE Transactions on Information theory, vol. 51, pp. 3608-3619, 2005.
[29] N. C. Sagias and G. S. Tombras, "On the cascaded Weibull fading channel model," Journal of the Franklin Institute, vol. 344, pp. 1-11, 2007.
[30] A. Papoulis and S. U. Pillai, Probability, random variables, and stochastic processes: Tata McGraw-Hill Education, 2002.
[31] I. Kostic, "Analytical approach to performance analysis for channel subject to shadowing and fading," IEE Proceedings-Communications, vol. 152, pp. 821-827, 2005.
[32] S. L. Cotton and W. G. Scanlon, "Higher order statistics for lognormal small-scale fading in mobile radio channels," IEEE Antennas and Wireless Propagation Letters, vol. 6, pp. 540-543, 2007.
[33] M. Pätzold, Mobile radio channels: John Wiley & Sons, 2011.
[34] P. M. Shankar, Fading and shadowing in wireless systems: Springer Science & Business Media, 2011.
[35] A. Abdi and M. Kaveh, "On the utility of gamma PDF in modeling shadow fading (slow fading)," in Vehicular Technology Conference, 1999 IEEE 49th, 1999, pp. 2308-2312.
[36] S. Atapattu, C. Tellambura, and H. Jiang, "Representation of composite fading and shadowing distributions by using mixtures of gamma distributions," in 2010 IEEE Wireless Communication and Networking Conference, 2010, pp. 1-5.
[37] I. Al Falujah and V. K. Prabhu, "Error rates of DPSK systems with MIMO EGC diversity reception over Rayleigh fading channels," IEEE Transactions on Communications, vol. 56, pp. 897-903, 2008.
[38] R. M. Radaydeh and M. M. Matalgah, "Compact formulas for the average error performance of noncoherent m-ary orthogonal signals over generalized Rician, Nakagami-m, and

Nakagami-q fading channels with diversity reception," IEEE Transactions on Communications, vol. 56, pp. 32-38, 2008.

[39] C.-H. Tse, K.-W. Yip, and T.-S. Ng, "Performance tradeoffs between maximum ratio transmission and switched-transmit diversity," in Personal, Indoor and Mobile Radio Communications, 2000. PIMRC 2000. The 11th IEEE International Symposium on, 2000, pp. 1485-1489.

[40] M. Li, M. Lin, Z. Gong, J. Yu, Z. Zhang, R. Peng, et al., "Performance analysis of MIMO MRC systems," Electronics Letters, vol. 43, pp. 1-2, 2007.

[41] J. M. Romero-Jerez and J. P. Pena-Martin, "ASER of rectangular MQAM in noise-limited and interference-limited MIMO MRC systems," IEEE Wireless Communications Letters, vol. 1, pp. 18-21, 2012.

[42] P. A. Dighe, R. K. Mallik, and S. S. Jamuar, "Analysis of transmit-receive diversity in Rayleigh fading," IEEE Transactions on Communications, vol. 51, pp. 694-703, 2003.

[43] Y. Wu, R. H. Louie, and M. R. McKay, "Asymptotic Outage Probability of MIMO-MRC Systems in Double-Correlated Rician Environments," IEEE Transactions on Wireless Communications, vol. 15, pp. 367-376, 2016.

[44] M. Li, M. Lin, W.-P. Zhu, Y. Huang, A. Nallanathan, and Q. Yu, "Performance Analysis of MIMO MRC Systems With Feedback Delay and Channel Estimation Error," IEEE Transactions on Vehicular Technology, vol. 65, pp. 707-717, 2016.

[45] W. Zhang, X.-G. Xia, and K. B. Letaief, "Space-time/frequency coding for MIMO-OFDM in next generation broadband wireless systems," IEEE Wireless Communications, vol. 14, pp. 32-43, 2007.

[46] S. N. Diggavi, N. Al-Dhahir, A. Stamoulis, and A. Calderbank, "Great expectations: The value of spatial diversity in wireless networks," Proceedings of the IEEE, vol. 92, pp. 219-270, 2004.

[47] H. Wang and X.-G. Xia, "Upper bounds of rates of complex orthogonal space-time block codes," IEEE Transactions on Information theory, vol. 49, pp. 2788-2796, 2003.

[48] T. Hashem and M. I. Islam, "Performance analysis of MIMO link under fading channels," in Computer and Information Technology (ICCIT), 2014 17th International Conference on, 2014, pp. 498-503.

[49] W. Li and N. C. Beaulieu, "Effects of channel-estimation errors on receiver selection-combining schemes for Alamouti MIMO systems with BPSK," IEEE Transactions on Communications, vol. 54, pp. 169-178, 2006.

[50] G. A. Ropokis, A. A. Rontogiannis, P. T. Mathiopoulos, and K. Berberidis, "An exact performance analysis of MRC/OSTBC over generalized fading channels," IEEE Transactions on Communications, vol. 58, pp. 2486-2492, 2010.

[51] D. N. C. Tse, P. Viswanath, and L. Zheng, "Diversity-multiplexing tradeoff in multiple-access channels," IEEE Transactions on Information Theory, vol. 50, pp. 1859-1874, 2004.

[52] Y. Lee, H.-C. Shih, C.-S. Huang, and J.-Y. Li, "Low-complexity MIMO detection: a mixture of ZF, ML and SIC," in 2014 19th International Conference on Digital Signal Processing, 2014, pp. 263-268.

[53] C. Siriteanu, S. D. Blostein, A. Takemura, H. Shin, S. Yousefi, and S. Kuriki, "Exact MIMO zero-forcing detection analysis for transmit-correlated Rician fading," IEEE Transactions on Wireless Communications, vol. 13, pp. 1514-1527, 2014.

[54] Y. Jiang, M. K. Varanasi, and J. Li, "Performance analysis of ZF and MMSE equalizers for MIMO systems: an in-depth study of the high SNR regime," IEEE Transactions on Information theory, vol. 57, pp. 2008-2026, 2011.

[55] H. Zhang, H. Dai, and B. L. Hughes, "Analysis on the diversity-multiplexing tradeoff for ordered MIMO SIC receivers," IEEE Transactions on Communications, vol. 57, pp. 125-133, 2009.

[56] T.-H. Liu, "Some results for the fast MMSE-SIC detection in spatially multiplexed MIMO systems," IEEE Transactions on Wireless Communications, vol. 8, pp. 5443-5448, 2009.

[57] Y. Song, C. Liu, and F. Lu, "Lattice reduction-ordered successive interference cancellation detection algorithm for multiple-input–multiple-output system," IET Signal Processing, vol. 9, pp. 553-561, 2015.

[58] S. Yunchao, L. Chen, and L. Feng, "The optimal MMSE-based OSIC detector for MIMO system," IEICE Transactions on Communications, vol. 99, pp. 232-239, 2016.

[59] Y. Bae and J. Lee, "Low complexity antenna selection for V-BLAST systems with OSIC detection," EURASIP Journal on Wireless Communications and Networking, vol. 2011, p. 1, 2011.

[60] H. Liu, "Error performance of MIMO systems in frequency selective Rayleigh fading channels," in Global Telecommunications Conference, 2003. GLOBECOM'03. IEEE, 2003, pp. 2104-2108.

[61] J. Xu, X. Tao, and P. Zhang, "Analytical SER performance bound of M-QAM MIMO system with ZF-SIC receiver," in 2008 IEEE International Conference on Communications, 2008, pp. 5103-5107.

[62] M. Vehkapera and M. Juntti, "On the performance of space-time coded and spatially multiplexed MIMO systems with linear receivers," IEEE Transactions on Communications, vol. 58, pp. 642-651, 2010.

[63] T.-H. Liu, J.-Y. Jiang, and Y.-S. Chu, "A low-cost MMSE-SIC detector for the MIMO system: algorithm and hardware implementation," IEEE Transactions on Circuits and Systems II: Express Briefs, vol. 58, pp. 56-61, 2011.

[64] T.-h. Liu and Y.-L. Y. Liu, "Modified fast recursive algorithm for efficient MMSE-SIC detection of the V-BLAST system," IEEE Transactions on Wireless Communications, vol. 7, pp. 3713-3717, 2008.

[65] R. P. F. Hoefel, "IEEE 802.11 n: On performance with MMSE and OSIC spatial division multiplexing transceivers," in 2012 International Symposium on Wireless Communication Systems (ISWCS), 2012, pp. 376-380.

[66] R. Narasimhan, "Error propagation analysis of V-BLAST with channel-estimation errors," IEEE Transactions on Communications, vol. 53, pp. 27-31, 2005.

[67] Y. A. Eldemerdash, O. A. Dobre, and M. Oner, "Signal Identification for Multiple-Antenna Wireless Systems: Achievements and Challenges."

[68] K. Punia, E. M. George, K. V. Babu, and G. R. Reddy, "Signal detection for Spatially Multiplexed multi input multi output (MIMO) systems," in Communications and Signal Processing (ICCSP), 2014 International Conference on, 2014, pp. 612-616.

[69] Y. Dai, S. Sun, and Z. Lei, "A comparative study of QRD-M detection and sphere decoding for MIMO-OFDM systems," in 2005 IEEE 16th International Symposium on Personal, Indoor and Mobile Radio Communications, 2005, pp. 186-190.

[70] W. Shin, H. Kim, M.-h. Son, and H. Park, "An improved LLR computation for QRM-MLD in coded MIMO systems," in 2007 IEEE 66th Vehicular Technology Conference, 2007, pp. 447-451.

[71] H. Kawai, K. Higuchi, N. Maeda, and M. Sawahashi, "Adaptive control of surviving symbol replica candidates in QRM-MLD for OFDM MIMO multiplexing," IEEE Journal on selected areas in communications, vol. 24, pp. 1130-1140, 2006.

[72] I. H. Kurniawan, J.-H. Yoon, J.-K. Kim, and J. Park, "Low-Power Channel-Adaptive Reconfigurable 4× 4 QRM-MLD MIMO Detector," ETRI Journal, vol. 38, pp. 100-111, 2016.

[73] A. Balatsoukas-Stimming, M. B. Parizi, and A. Burg, "LLR-based successive cancellation list decoding of polar codes," IEEE Transactions on Signal Processing, vol. 63, pp. 5165-5179, 2015.

[74] H. Yuan and P.-Y. Kam, "On the LLR Metrics for DPSK Modulations Over Two-Symbol Observation Intervals for the Flat Rician Fading Channel," IEEE Transactions on Communications, vol. 63, pp. 4950-4963, 2015.

[75] T.-H. Im, J. Kim, J.-H. Yi, S. Yun, and Y.-S. Cho, "MMSE-OSIC² Signal Detection for Spatially Multiplexed MIMO Systems," in Vehicular Technology Conference, 2008. VTC Spring 2008. IEEE, 2008, pp. 1468-1472.

[76] S. Sanayei and A. Nosratinia, "Antenna selection in MIMO systems," IEEE Communications Magazine, vol. 42, pp. 68-73, 2004.

[77] J. Jeganathan, A. Ghrayeb, L. Szczecinski, and A. Ceron, "Space shift keying modulation for MIMO channels," IEEE Transactions on Wireless Communications, vol. 8, pp. 3692-3703, 2009.

[78] T. K. Lyu and X. Wang, "Capacity of precoding for MU-MIMO systems," in Information and Communication Technology Convergence (ICTC), 2015 International Conference on, 2015, pp. 405-407.

[79] M. R. Bhatnagar, A. Hjorungnes, and L. Song, "Precoded differential orthogonal space-time modulation over correlated Ricean MIMO channels," IEEE Journal of Selected Topics in Signal Processing, vol. 2, pp. 124-134, 2008.

[80] J. M. Hamamreh, E. Guvenkaya, T. Baykas, and H. Arslan, "A practical physical-layer security method for precoded OSTBC-based systems," in Wireless Communications and Networking Conference (WCNC), 2016 IEEE, 2016, pp. 1-6.

[81] C.-T. Lin and W.-R. Wu, "QRD-based antenna selection for ML detection of spatial multiplexing MIMO systems: algorithms and applications," IEEE Transactions on Vehicular Technology, vol. 60, pp. 3178-3191, 2011.

[82] J. Li, Y. Zheng, J. Ge, C. Zhang, and X. Yu, "Simplified relay antenna selection with source beamforming for MIMO two-way relaying networks," Science China Information Sciences, vol. 60, p. 022310, 2017.

[83] X. Zhou, B. Bai, and W. Chen, "Invited Paper: Antenna selection in energy efficient MIMO systems: A survey," China Communications, vol. 12, pp. 162-173, 2015.

[84] M. Kulkarni, L. Choudhary, B. Kumbhani, and R. S. Kshetrimayum, "Performance analysis comparison of transmit antenna selection with maximal ratio combining and orthogonal space time block codes in equicorrelated Rayleigh fading multiple input multiple output channels," IET Communications, vol. 8, pp. 1850-1858, 2014.

[85] X. Yu, W. Tan, Y. Wang, X. Liu, Y. Rui, and M. Chen, "Performance Analysis of Distributed Antenna Systems with Antenna Selection over MIMO Rayleigh Fading Channel," TIIS, vol. 8, pp. 3016-3033, 2014.

[86] H. Zhang and T. A. Gulliver, "Capacity and error probability analysis for orthogonal space-time block codes over fading channels," IEEE Transactions on Wireless Communications, vol. 4, pp. 808-819, 2005.

[87] J. Wang, Q. Zhou, J. Dou, and L. Qiu, "On the Channel Capacity of MIMO Systems under Correlated Rayleigh Fading," in 2007 International Conference on Wireless Communications, Networking and Mobile Computing, 2007, pp. 134-136.

[88] C.-K. Wen, S. Jin, and K.-K. Wong, "On the sum-rate of multiuser MIMO uplink channels with jointly-correlated Rician fading," IEEE Transactions on Communications, vol. 59, pp. 2883-2895, 2011.

[89] C. Zhong, K.-K. Wong, and S. Jin, "Capacity bounds for MIMO Nakagami-fading channels," IEEE Transactions on Signal Processing, vol. 57, pp. 3613-3623, 2009.

[90] J. Cheng, C. Tellambura, and N. C. Beaulieu, "Performance analysis of digital modulations on Weibull fading channels," in Vehicular Technology Conference, 2003. VTC 2003-Fall. 2003 IEEE 58th, 2003, pp. 236-240.

[91] G. K. Karagiannidis, D. A. Zogas, N. C. Sagias, S. A. Kotsopoulos, and G. S. Tombras, "Equal-gain and maximal-ratio combining over nonidentical Weibull fading channels," IEEE Transactions on Wireless Communications, vol. 4, pp. 841-846, 2005.

[92] A. Bessate and F. El Bouanani, "A new performances analysis for MRC receiver over correlated Weibull multipath fading channels," in Codes, Cryptography and Communication Systems (WCCCS), 2014 5th Workshop on, 2014, pp. 157-160.

[93] M. Lupupa and M. E. Dlodlo, "Performance of MIMO system in Weibull fading channel-Channel capacity analysis," in EUROCON 2009, EUROCON'09. IEEE, 2009, pp. 1735-1740.

[94] M. Cheng, L. Guo, Y. Zhang, and J. Li, "Selection combining optimization for FSO links over exponentiated Weibull fading channels," in Wireless and Optical Communication Conference (WOCC), 2016 25th, 2016, pp. 1-4.

[95] R. Kwan and C. Leung, "General order selection combining for Nakagami and Weibull fading channels," IEEE Transactions on Wireless Communications, vol. 6, pp. 2027-2032, 2007.

[96] M. You, H. Sun, J. Jiang, and J. Zhang, "Effective Rate Analysis in Weibull Fading Channels," 2016.
[97] J. B. Andersen, "Statistical distributions in mobile communications using multiple scattering," in Proc. 27th URSI General Assembly, 2002.
[98] J. Salo, H. M. El-Sallabi, and P. Vainikainen, "Impact of double-Rayleigh fading on system performance," in Proc. 1st IEEE Int. Symp. on Wireless Pervasive Computing, ISWPC 2006, 2006.
[99] D. Chizhik, G. Foschini, M. Gans, and R. Valenzuela, "Propagation and capacities of multi-element transmit and receive antennas," in Antennas and Propagation Society International Symposium, 2001. IEEE, 2001, pp. 438-441.
[100] H. Shin and J. H. Lee, "Performance analysis of space-time block codes over keyhole Nakagami-m fading channels," IEEE Transactions on Vehicular Technology, vol. 53, pp. 351-362, 2004.
[101] F. Benkhelifa, Z. Rezki, and M.-S. Alouini, "The capacity of the cascaded fading channel in the low power regime," in 2014 IEEE Wireless Communications and Networking Conference (WCNC), 2014, pp. 154-159.
[102] Z. Zheng, "Statistical Analysis of Cascaded Multipath Fading Channels," 2015.
[103] P. C. Sofotasios, L. Mohjazi, S. Muhaidat, M. Al-Qutayri, and G. K. Karagiannidis, "Energy detection of unknown signals over cascaded fading channels," IEEE Antennas and Wireless Propagation Letters, vol. 15, pp. 135-138, 2016.
[104] Z. Motamedi and M. R. Soleymani, "For better or worse: The impact of shadow fading on the capacity of large MIMO networks," in IEEE GLOBECOM 2007-IEEE Global Telecommunications Conference, 2007, pp. 3200-3204.
[105] A. Abdi and M. Kaveh, "K distribution: an appropriate substitute for Rayleigh-lognormal distribution in fading-shadowing wireless channels," Electronics Letters, vol. 34, pp. 851-851, 1998.
[106] M. Matthaiou, N. D. Chatzidiamantis, G. K. Karagiannidis, and J. A. Nossek, "On the capacity of generalized-K fading MIMO channels," IEEE Transactions on Signal Processing, vol. 58, pp. 5939-5944, 2010.
[107] M. R. Bhatnagar and M. Arti, "On the closed-form performance analysis of maximal ratio combining in Shadowed-Rician fading LMS channels," IEEE Communications Letters, vol. 18, pp. 54-57, 2014.
[108] M. R. Bhatnagar and M. Arti, "Performance analysis of AF based hybrid satellite-terrestrial cooperative network over generalized fading channels," IEEE Communications Letters, vol. 17, pp. 1912-1915, 2013.
[109] P. S. Bithas, "Weibull-gamma composite distribution: alternative multipath/shadowing fading model," Electronics Letters, vol. 45, pp. 749-751, 2009.
[110] K. Tiwari, D. S. Saini, and S. V. Bhooshan, "On the Capacity of MIMO Weibull-Gamma Fading Channels in Low SNR Regime," Journal of Electrical and Computer Engineering, vol. 2016, 2016.
[111] H. Suzuki, "A statistical model for urban radio propogation," IEEE Transactions on Communications, vol. 25, pp. 673-680, 1977.

[112] M. Patzold, U. Killat, and F. Laue, "An extended Suzuki model for land mobile satellite channels and its statistical properties," IEEE Transactions on Vehicular Technology, vol. 47, pp. 617-630, 1998.
[113] P. Karadimas and S. A. Kotsopoulos, "A generalized modified Suzuki model with sectored and inhomogeneous diffuse scattering component," Wireless personal communications, vol. 47, pp. 449-469, 2008.
[114] A. Abdi and M. Kaveh, "Comparison of DPSK and MSK bit error rates for K and Rayleigh-lognormal fading distributions," IEEE Communications Letters, vol. 4, pp. 122-124, 2000.
[115] P. M. Shankar, "Error rates in generalized shadowed fading channels," Wireless Personal Communications, vol. 28, pp. 233-238, 2004.
[116] S. Gonzalez-Aurioles, J. F. Valenzuela-Valdés, J. L. Padilla, P. Padilla, and F. Luna-Valero, "Capacity in weibull fading with shadowing for MIMO distributed system," Wireless personal communications, vol. 80, pp. 1625-1633, 2015.
[117] P. Karadimas and S. A. Kotsopoulos, "The Weibull–lognormal fading channel: analysis, simulation, and validation," IEEE Transactions on Vehicular Technology, vol. 58, pp. 3808-3813, 2009.
[118] J. Reig and L. Rubio, "Estimation of the composite fast fading and shadowing distribution using the log-moments in wireless communications," IEEE Transactions on Wireless Communications, vol. 12, pp. 3672-3681, 2013.
[119] A. M. Mitic and M. M. Jakovljevic, "Second-Order Statistics in Weibull-Lognormal Fading Channels," in 2007 8th International Conference on Telecommunications in Modern Satellite, Cable and Broadcasting Services, 2007.
[120] J. Xue, C. Zhong, and T. Ratnarajah, "Performance analysis of orthogonal STBC in generalized-K fading MIMO channels," IEEE Transactions on Vehicular Technology, vol. 61, pp. 1473-1479, 2012.
[121] A. Kaur, "Performance Analysis of Multihop Wireless Communication Using Generalized-K Fading Model," Wireless Personal Communications, pp. 1-14.
[122] F. Yilmaz and M.-S. Alouini, "Extended Generalized-K (EGK): A New Simple and General Model for Composite Fading Channels," arXiv preprint arXiv:1012.2598, 2010.
[123] M. S. Aloqlah and F. A. Nawafleh, "Performance study of decode and forward based multi-hop relaying in wireless networks over extended generalized-K fading channels," in 2016 International Conference on Computing, Networking and Communications (ICNC), 2016, pp. 1-5.
[124] S. P. Singh and S. Kumar, "Closed form expressions for ABER and capacity over EGK fading channel in presence of CCI," International Journal of Electronics, vol. 104, pp. 513-527, 2017.
[125] I. S. Ansari and M.-S. Alouini, "On the Performance Analysis of Digital Communications over Weibull-Gamma Channels," in 2015 IEEE 81st Vehicular Technology Conference (VTC Spring), 2015, pp. 1-7.
[126] J. Anastasov, G. Djordjevic, and M. Stefanovic, "Outage probability of interference-limited system over Weibull-gamma fading channel," Electronics Letters, vol. 48, pp. 408-410, 2012.

[127] G. Molenberghs and G. Verbeke, "On the Weibull-Gamma frailty model, its infinite moments, and its connection to generalized log-logistic, logistic, Cauchy, and extreme-value distributions," Journal of Statistical Planning and Inference, vol. 141, pp. 861-868, 2011.
[128] S. Nadarajah and S. Kotz, "A class of generalized models for shadowed fading channels," Wireless personal communications, vol. 43, pp. 1113-1120, 2007.
[129] T. S. B. Reddy, R. Subadar, and P. Sahu, "Outage probability of selection combiner over exponentially correlated Weibull-gamma fading channels for arbitrary number of branches," in Communications (NCC), 2010 National Conference on, 2010, pp. 1-5.
[130] Z. Ni, X. Zhang, X. Liu, and D. Yang, "Bivariate Weibull-gamma composite distribution with arbitrary fading parameters," Electronics Letters, vol. 48, p. 1, 2012.
[131] P. Bender, P. Black, M. Grob, R. Padovani, N. Sindhushyana, and S. Viterbi, "CDMA/HDR: a bandwidth efficient high speed wireless data service for nomadic users," IEEE Communications Magazine, vol. 38, pp. 70-77, 2000.
[132] M. Matthaiou and C. Zhong, "Low-SNR analysis of MIMO Weibull fading channels," IEEE Communications Letters, vol. 16, pp. 694-697, 2012.
[133] N. C. Beaulieu, "A useful integral for wireless communication theory and its application to rectangular signaling constellation error rates," IEEE Transactions on Communications, vol. 54, pp. 802-805, 2006.
[134] G. K. Karagiannidis, "On the symbol error probability of general order rectangular QAM in Nakagami-m fading," IEEE Communications Letters, vol. 10, pp. 745-747, 2006.
[135] H. A. Suraweera and J. Armstrong, "A simple and accurate approximation to the SEP of rectangular QAM in arbitrary Nakagami-m fading channels," IEEE Communications Letters, vol. 11, pp. 426-428, 2007.
[136] M. Zimmermann and K. Dostert, "Analysis and modeling of impulsive noise in broad-band powerline communications," IEEE transactions on Electromagnetic compatibility, vol. 44, pp. 249-258, 2002.
[137] L. Di Bert, P. Caldera, D. Schwingshackl, and A. M. Tonello, "On noise modeling for power line communications," in Power Line Communications and Its Applications (ISPLC), 2011 IEEE International Symposium on, 2011, pp. 283-288.
[138] A. Mathur and M. R. Bhatnagar, "PLC Performance Analysis Assuming BPSK Modulation Over Nakagami-Additive Noise," IEEE Communications Letters, vol. 18, pp. 909-912, 2014.
[139] A. Mathur, M. R. Bhatnagar, and B. K. Panigrahi, "Performance evaluation of PLC under the combined effect of background and impulsive noises," IEEE Communications Letters, vol. 19, pp. 1117-1120, 2015.
[140] R. Viswanathan and A. Ansari, "Distributed detection of a signal in generalized Gaussian noise," IEEE Transactions on Acoustics, Speech, and Signal Processing, vol. 37, pp. 775-778, 1989.
[141] E. Salahat and H. Saleh, "Novel average bit error rate analysis of generalized fading channels subject to additive white generalized Gaussian noise," in Signal and Information Processing (GlobalSIP), 2014 IEEE Global Conference on, 2014, pp. 1107-1111.

[142] S. A. Kassam, Signal detection in non-Gaussian noise: Springer Science & Business Media, 2012.
[143] E. Salahat and H. Saleh, "Novel Unified Analysis of Orthogonal Space-Time Block Codes over Generalized-K and AWGGN MIMO Networks," in 2015 IEEE 81st Vehicular Technology Conference (VTC Spring), 2015, pp. 1-4.
[144] O. S. Badarneh and F. S. Almehmadi, "Performance of Multihop Wireless Networks in-Fading Channels Perturbed by an Additive Generalized Gaussian Noise," IEEE Communications Letters, vol. 20, pp. 986-989, 2016.
[145] H. Soury, F. Yilmaz, and M.-S. Alouini, "Error rates of M-PAM and M-QAM in generalized fading and generalized gaussian noise environments," IEEE Communications Letters, vol. 17, pp. 1932-1935, 2013.
[146] F. Yilmaz, A. Yilmaz, M.-S. Alouini, and O. Kucur, "Transmit antenna selection based on shadowing side information," in Vehicular Technology Conference (VTC Spring), 2011 IEEE 73rd, 2011, pp. 1-5.
[147] B. Clerckx and C. Oestges, MIMO wireless networks: Channels, techniques and standards for multi-antenna, multi-user and multi-cell systems: Academic Press, 2013.
[148] A. Garg and M. R. Bhatnagar, "Performance analysis of diagonal precoding for alamouti STBC over Nakagami-m fading channels," in Vehicular Technology Conference (VTC Spring), 2016 IEEE 83rd, 2016, pp. 1-5.
[149] I. Khan, N. Rajatheva, S. Tanoli, and S. Jan, "Performance analysis of cooperative network over Nakagami and Rician fading channels," International Journal of Communication Systems, vol. 27, pp. 2703-2722, 2014.
[150] Q. Wang, D. Wu, and P. Fan, "Effective capacity of a correlated Rayleigh fading channel," Wireless Communications and Mobile Computing, vol. 11, pp. 1485-1494, 2011.
[151] A. Bessate and F. El Bouanani, "A very tight approximate results of MRC receivers over independent Weibull fading channels," Physical Communication, vol. 21, pp. 30-40, 2016.
[152] K. Tiwari and D. S. Saini, "BER Performance comparison of MIMO system with STBC and MRC over different fading channels," in High Performance Computing and Applications (ICHPCA), 2014 International Conference on, 2014, pp. 1-6.
[153] N. D. Chatzidiamantis, H. G. Sandalidis, G. K. Karagiannidis, S. A. Kotsopoulos, and M. Matthaiou, "New results on turbulence modeling for free-space optical systems," in Telecommunications (ICT), 2010 IEEE 17th International Conference on, 2010, pp. 487-492.
[154] K. Tiwari, D. S. Saini, and S. V. Bhooshan, "Performance improvement in spatially multiplexed MIMO systems over Weibull-Gamma fading channel," Frequenz, vol. 70, pp. 547-553, 2016.
[155] G. K. Karagiannidis, T. A. Tsiftsis, and N. C. Sagias, "A closed-form upper-bound for the distribution of the weighted sum of Rayleigh variates," IEEE Communications Letters, vol. 9, pp. 589-591, 2005.
[156] V. Adamchik and O. Marichev, "The algorithm for calculating integrals of hypergeometric type functions and its realization in REDUCE system," in Proceedings of the international symposium on Symbolic and algebraic computation, 1990, pp. 212-224.

[157] I. Korn and L. Hii, "Relation between bit and symbol error probabilities for DPSK and FSK with differential phase detection," IEEE Transactions on Communications, vol. 42, pp. 2778-2780, 1994.
[158] G. John, "Proakis, Digital Communications," Beijing, China: Publishing House of Electronic Industry, 2001.
[159] L. Zheng and D. N. C. Tse, "Diversity and multiplexing: A fundamental tradeoff in multiple-antenna channels," IEEE Transactions on information theory, vol. 49, pp. 1073-1096, 2003.
[160] B. Holter and G. Oien, "On the amount of fading in MIMO diversity systems," IEEE Transactions on Wireless Communications, vol. 4, pp. 2498-2507, 2005.
[161] G. Mohamed and S. El-Rabaie, "Signal detection enhancement in LTE-A downlink physical layer using OSIC-based K-Best algorithm," Physical Communication, vol. 14, pp. 24-31, 2015.
[162] I. S. Gradshteyn and I. M. Ryzhik, Table of integrals, series, and products: Academic press, 2014.
[163] H. El-Sallabi, K. Qaraqe, and E. Serpedin, "Some Insights on the Amount of Fading in Radio Channels," in Proc. PIERS, 2013.
[164] P. S. Bithas, N. C. Sagias, P. T. Mathiopoulos, G. K. Karagiannidis, and A. Rontogiannis, "Digital communications over generalized-K fading channels," in 2005 2nd International Symposium on Wireless Communication Systems, 2005, pp. 684-687.
[165] K. Tiwari and D. S. Saini, "SER improvisation of MIMO-MRC system over Weibull-Gamma fading channel," in Signal Processing and Communication (ICSC), 2015 International Conference on, 2015, pp. 70-73.
[166] G. Golden, C. Foschini, R. Valenzuela, and P. Wolniansky, "Detection algorithm and initial laboratory results using V-BLAST space-time communication architecture," Electronics letters, vol. 35, pp. 14-16, 1999.
[167] K. T. Tasneem, "Reduced Complexity Detection Techniques for Multi-Antenna Communication Systems," 2013.
[168] S. Verdú, "Spectral efficiency in the wideband regime," IEEE Transactions on Information Theory, vol. 48, pp. 1319-1343, 2002.
[169] X. Wu and R. Srikant, "MIMO channels in the low-SNR regime: Communication rate, error exponent, and signal peakiness," IEEE transactions on information theory, vol. 53, pp. 1290-1309, 2007.
[170] A. Lozano, A. M. Tulino, and S. Verdú, "Multiple-antenna capacity in the low-power regime," IEEE Transactions on Information Theory, vol. 49, pp. 2527-2544, 2003.
[171] N. Bahl, A. K. Sharma, and H. K. Verma, "On the energy utilization for WSN based on BPSK over the Generalized-K shadowed fading channel," Wireless Networks, vol. 20, pp. 2385-2393, 2014.
[172] U. Charash, "Reception through Nakagami fading multipath channels with random delays," IEEE Transactions on Communications, vol. 27, pp. 657-670, 1979.

[173] M. R. McKay, I. B. Collings, and A. M. Tulino, "Achievable sum rate of MIMO MMSE receivers: A general analytic framework," IEEE transactions on information theory, vol. 56, pp. 396-410, 2010.
[174] R. N. McDonough and A. D. Whalen, Detection of signals in noise: Academic Press, 1995.
[175] X. Li, T. Luo, G. Yue, and C. Yin, "A squaring method to simplify the decoding of orthogonal space-time block codes," IEEE Transactions on Communications, vol. 49, pp. 1700-1703, 2001.
[176] S. Chen and J. Zhao, "The requirements, challenges, and technologies for 5G of terrestrial mobile telecommunication," IEEE Communications Magazine, vol. 52, pp. 36-43, 2014.
[177] V. Mai-hong, "Exploiting Transmit Channel Side Information in MIMO Wireless Systems," Stanford: Stanford University, 2005.
[178] H. Ilhan, "The performance of MIMO system using MRT scheme in vehicular systems," International Journal of Communication Systems, 2016.
[179] B. Kumbhani, "Performance Analysis of MIMO Systems: Transmit Antenna Selection, Cooperative Communications and Spatial Modulation," Indian Institute of Technology Guwahati, 2015.
[180] S. Meraji, "Performance analysis of transmit antenna selection in Nakagami-m fading channels," Wireless Personal Communications, vol. 43, pp. 327-333, 2007.
[181] K. Tiwari, D. S. Saini, and S. V. Bhooshan, "Antenna selection for MIMO systems over Weibull–Gamma fading channel," Perspectives in Science, vol. 8, pp. 475-478, 2016.
[182] K. Tiwari, D. S. Saini, and S. V. Bhooshan, "ASEP of MIMO System with MMSE-OSIC Detection over Weibull-Gamma Fading Channel Subject to AWGGN," Journal of Computer Networks and Communications, vol. 2016, 2016.
[183] J.-M. Guo, H. Prasetyo, M. E. Farfoura, and H. Lee, "Vehicle verification using features from curvelet transform and generalized Gaussian distribution modeling," IEEE Transactions on Intelligent Transportation Systems, vol. 16, pp. 1989-1998, 2015.
[184] S. Yu, A. Zhang, and H. Li, "A review of estimating the shape parameter of generalized Gaussian distribution," J. Comput. Inf. Syst, vol. 8, pp. 9055-9064, 2012.
[185] E. Salahat, D. Shehada, and C. Y. Yeun, "Novel Performance Analysis of Multi-Access MIMO Relay Cooperative RM-DCSK over Nakagami-m Fading Subject to AWGGN," in Vehicular Technology Conference (VTC Fall), 2015 IEEE 82nd, 2015, pp. 1-5.
[186] H. Soury and M.-S. Alouini, "New results on the sum of two generalized Gaussian random variables," in 2015 IEEE Global Conference on Signal and Information Processing (GlobalSIP), 2015, pp. 1017-1021.
[187] M. A. Chaudhry and S. M. Zubair, On a class of incomplete gamma functions with applications: CRC press, 2001.
[188] M. Nardon and P. Pianca, "Simulation techniques for generalized Gaussian densities," Journal of Statistical Computation and Simulation, vol. 79, pp. 1317-1329, 2009.
[189] F. Yilmaz and M.-S. Alouini, "A new simple model for composite fading channels: Second order statistics and channel capacity," in Wireless Communication Systems (ISWCS), 2010 7th International Symposium on, 2010, pp. 676-680.
[190] A. A. Kilbas, H-transforms: Theory and Applications: CRC Press, 2004.

[191] H. Soury, F. Yilmaz, and M.-S. Alouini, "Average bit error probability of binary coherent signaling over generalized fading channels subject to additive generalized Gaussian noise," IEEE Communications Letters, vol. 16, pp. 785-788, 2012.
[192] A. Prudnikov, O. Marichev, and A. Brychkov Yu, "Integrals and Series, Vol. 3: More Special Functions (Newark, NJ: Gordon and Breach)," 1990.
[193] P. Mittal and K. Gupta, "An integral involving generalized function of two variables," in Proceedings of the Indian Academy of Sciences-Section A, 1972, pp. 117-123.

LIST OF PUBLICATIONS

JOURNALS

[1] Keerti Tiwari, Davinder S. Saini and Sunil V. Bhooshan, "Efficient Detection for Improving ASEP Performance of MIMO Composite Fading Channel with Generalized Noise," Wireless Personal Communication (Springer), pp. 1-11, Oct. 2017. http://dx.doi.org/10.1007/s11277-017-5007-4

[2] Keerti Tiwari, Davinder S. Saini and Sunil V. Bhooshan, "On the Capacity of MIMO Weibull-Gamma Fading Channels in Low SNR Regime," Journal of Electrical and Computer Engineering (Hindawi), vol. 2016, Article ID 9304597, 8 pages, Nov. 2016. http://dx.doi.org/10.1155/2016/9304597

[3] Keerti Tiwari, Davinder S. Saini and Sunil V. Bhooshan, "Performance Improvement in Spatially Multiplexed MIMO Systems over Weibull-Gamma Fading Channel", Frequenz: Journal of RF-engineering and telecommunications (De-Gruyter), vol. 70, issue 11-12, pp. 547-553, Aug. 2016. http://dx.doi.org/10.1515/freq-2016-0034

[4] Keerti Tiwari, Davinder S. Saini and Sunil V. Bhooshan, "Antenna Selection for MIMO Systems over Weibull-Gamma Fading Channel", Perspectives in Science (Elsevier), vol. 8, pp. 475-478, June 2016. http://dx.doi.org/10.1016/j.pisc.2016.06.004

[5] Keerti Tiwari, Davinder S. Saini and Sunil V. Bhooshan, "ASEP of MIMO System with MMSE-OSIC Detection over Weibull-Gamma Fading Channel Subject to AWGGN", Journal of Computer Networks and Communications (Hindawi), vol. 2016, Article ID 7918456, 7 pages, Feb. 2016. http://dx.doi.org/10.1155/2016/7918456

[6] Keerti Tiwari, Davinder S. Saini and Sunil V. Bhooshan, "Error Rate Analysis of MIMO System with OSTBC and MRC in Composite Weibull-Gamma Fading," International Journal on Electrical Engineering and Informatics, Aug. 2017 (Revision incorporated).

[7] Keerti Tiwari, Davinder S. Saini and Sunil V. Bhooshan, "Symbol Error Rate of MIMO Single and Double-Weibull Fading Channels with OSTBC and MRC," World Journal of Engineering, Nov. 2017 (Revision incorporated).

INTERNATIONAL CONFERENCES

[8] Keerti Tiwari and Davinder S. Saini, "SER Improvisation of MIMO-MRC System over Weibull-Gamma Fading Channel," Proc. of the IEEE International conference on Signal Processing and Communication (ICSC 2015), Noida, India, 16-18 March, 2015, pp. 70-73. http://dx.doi.org/10.1109/ICSPCom.2015.7150622.

[9] Keerti Tiwari and Davinder S. Saini, "BER Performance Comparison of MIMO System with STBC and MRC over Different Fading Channels," Proc. of the IEEE International conference on High Performance Computing and Application (ICHPCA 2014), Bhubaneswar, India, 22-24 Dec., 2014, pp. 1-6. http://dx.doi/10.1109/ICHPCA.2014.704530.